

Summer 2014

Analysis of a mathematical model for the heave motion of a micro aerial vehicle with flexible wings having non-local damping effects

Jonathan B. Walters

Follow this and additional works at: <https://digitalcommons.latech.edu/dissertations>

 Part of the [Applied Mathematics Commons](#)

**ANALYSIS OF A MATHEMATICAL MODEL FOR THE HEAVE
MOTION OF A MICRO AERIAL VEHICLE WITH FLEXIBLE
WINGS HAVING NON-LOCAL DAMPING EFFECTS**

by

Jonathan B. Walters, B.S. M.S.

A Dissertation Presented in Partial Fulfillment
of the Requirements for the Degree
Doctor of Philosophy

COLLEGE OF ENGINEERING AND SCIENCE
LOUISIANA TECH UNIVERSITY

August 2014

UMI Number: 3662461

All rights reserved

INFORMATION TO ALL USERS

The quality of this reproduction is dependent upon the quality of the copy submitted.

In the unlikely event that the author did not send a complete manuscript and there are missing pages, these will be noted. Also, if material had to be removed, a note will indicate the deletion.

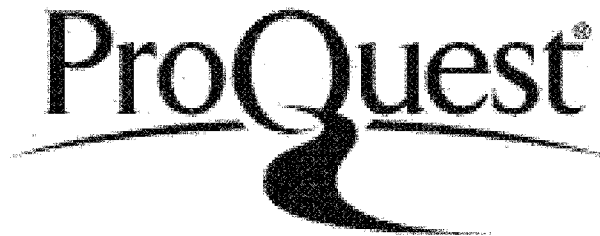


UMI 3662461

Published by ProQuest LLC 2015. Copyright in the Dissertation held by the Author.

Microform Edition © ProQuest LLC.

All rights reserved. This work is protected against unauthorized copying under Title 17, United States Code.



ProQuest LLC
789 East Eisenhower Parkway
P.O. Box 1346
Ann Arbor, MI 48106-1346

LOUISIANA TECH UNIVERSITY

THE GRADUATE SCHOOL

6-9-14
Date

We hereby recommend that the dissertation prepared under our supervision
by Jonathan Bruce Walters

entitled Analysis of a Mathematical Model for the Heave Motion of a Micro Aerial
Vehicle with Flexible Wings Having Non-Local Damping Effects

be accepted in partial fulfillment of the requirements for the Degree of
Doctor of Philosophy

KA A. Gwan

Supervisor of Dissertation Research

Head of Department

Head of Department

Mathematics and Statistics
Department

Recommendation concurred in:

Animesh Chakravarty by Kae
(present electronically)

Tom Ah

Steph Wells

Advisory Committee

Head of Department

Approved:

[Signature]
Director of Graduate Studies

Approved:

Sheryl S. Sheemaker
Dean of the Graduate School

Rish Hegab/SOP
Dean of the College

ABSTRACT

In this work we analyze a one dimensional model for a flexible wing micro aerial vehicle which can undergo heaving motion. The vehicle is modeled with a non-local type of internal damping known as spatial hysteresis as well as viscous external damping. We present a rigorous theoretical analysis of the model proving that the linearly approximated system is well-posed and the first order feedback system operators generate exponentially stable C_0 -semigroups.

Furthermore, we present numerical simulations of control designs used on the linearly approximated model to control the associated nonlinear model in two different strategies. The first strategy used to control the system is a target tracking strategy. The second strategy used in this work is morphing the system to a target state over time. The controllers used in this work include Linear Quadratic Regulator, Linear Quadratic Gaussian, and central control.

In light of the theory of this work we have incorporated the appropriate Riccati equation solutions into the control design for a system with a mode problem (i.e. zero eigenvalue for stiffness operator). This work remains consistent with the literature that concerns multiple component structures with a mode problem.

APPROVAL FOR SCHOLARLY DISSEMINATION

The author grants to the Prescott Memorial Library of Louisiana Tech University the right to reproduce, by appropriate methods, upon request, any or all portions of this Dissertation. It is understood that "proper request" consists of the agreement, on the part of the requesting party, that said reproduction is for his personal use and that subsequent reproduction will not occur without written approval of the author of this Dissertation. Further, any portions of the Dissertation used in books, papers, and other works must be appropriately referenced to this Dissertation.

Finally, the author of this Dissertation reserves the right to publish freely, in the literature, at any time, any or all portions of this Dissertation.

Author Jonathan B. Wilton

Date July 29, 2014

DEDICATION

To Cathy.

TABLE OF CONTENTS

ABSTRACT	iii
DEDICATION	iv
LIST OF TABLES.....	vii
LIST OF FIGURES.....	viii
ACKNOWLEDGMENTS	x
CHAPTER 1 INTRODUCTION.....	1
CHAPTER 2 MATHEMATICAL PRELIMINARIES.....	5
2.1 Basic Definitions and Theorems.....	5
2.2 Semigroups.....	6
2.3 Well-Posedness Theorems	9
2.4 Semigroup Theorems.....	12
CHAPTER 3 LINEAR FEEDBACK CONTROL.....	14
3.1 Full State Feedback Design (LQR)	14
3.2 State Estimate Control Design	16
3.2.1 The Linear Quadratic Gaussian Tracking Problem (LQG)	17
3.2.2 Central Control Design.....	18
3.3 Useful Theorems	20
CHAPTER 4 MICRO AERIAL VEHICLE MODEL WITH SPATIAL HYS- TERESIS DAMPING	22

4.1	Model	22
4.1.1	Linearization of Lift Coefficient	26
CHAPTER 5 THEORETICAL ANALYSIS		29
5.1	Well-Posedness and Semigroup Results	29
CHAPTER 6 VARIATIONAL FORM AND APPROXIMATION THEORY		55
6.1	Numerical Methods	55
6.1.1	Weak Formulation	55
6.1.2	Discretization	59
6.2	Approximating Ricatti Solutions	65
6.2.1	Optimal Control Approximations	65
6.2.2	Observer Solutions Approximations	67
CHAPTER 7 NUMERICAL RESULTS		69
7.1	Numerical Results	69
7.1.1	Uncontrolled Simulation	70
7.1.2	Target Tracking Results	75
7.1.3	Morphing Trajectory Results	81
CHAPTER 8 CONCLUSIONS AND FUTURE WORK		89
APPENDIX A SPATIAL HYSTERESIS INEQUALITY		91
A.1	Proof of Theorem A.1	94
A.2	Observations	101
APPENDIX B CONVERGENCE OF BMB WITH KELVIN VOIGT PARAMETERS		103
BIBLIOGRAPHY		107

LIST OF TABLES

Table 4.1: Boundary Conditions	26
Table 7.1: System Parameter Values	69
Table 7.2: Cumulative Tracking Control Efforts.....	81
Table 7.3: Cumulative Morphing Control Efforts	87

LIST OF FIGURES

Figure 1.1: Dog faced fruit bat in flight. Credit for this image goes to Kenny Breuer in [24]	1
Figure 4.1: MAV beam-mass-beam system.	22
Figure 7.1: Uncontrolled Position: 6 Elements (Top Left), 12 Elements (Top Right), 20 Elements (Bottom Left), 30 Elements (Bottom Right)	71
Figure 7.2: Uncontrolled Slope: 6 Elements (First), 12 Elements (Second), 20 Elements (Third), 30 Elements (Fourth)	72
Figure 7.3: Uncontrolled Velocity: 6 Elements (First), 12 Elements (Second), 20 Elements (Third), 30 Elements (Fourth).....	73
Figure 7.4: Uncontrolled Angular Velocity: 6 Elements (First), 12 Elements (Second), 20 Elements (Third), 30 Elements (Fourth)	74
Figure 7.5: Target Tracking Goal: (Left) Position, (Right) Slope.....	76
Figure 7.6: LQR Full Order Control: Position (Top Left), Slope (Top Right), Velocity (Bottom Left), Angular Velocity (Bottom Right)	78
Figure 7.7: LQG State Estimate Control: Position (Top Left), Slope (Top Right), Velocity (Bottom Left), Angular Velocity (Bottom Right)	79
Figure 7.8: Central Controller State Estimate Control: Position (Top Left), Slope (Top Right), Velocity (Bottom Left), Angular Velocity (Bottom Right).....	80
Figure 7.9: Target Tracking Control Efforts: LQR (Top Left), LQG (Top Right), Central (Bottom)	81
Figure 7.10: Target States For Morphing Trajectories: Position (Top Left), Slope (Top Right), Velocity (Bottom Left), Angular Velocity (Bottom Right)	83

Figure 7.11: LQR Full Order Control Linear Morphing: Position (Top Left), Slope (Top Right), Velocity (Bottom Left), Angular Velocity (Bottom Right).....	84
Figure 7.12: LQG State Estimate Control Linear Morphing: Position (Top Left), Slope (Top Right), Velocity (Bottom Left), Angular Velocity (Bottom Right)	85
Figure 7.13: Central Controller State Estimate Control Linear Morphing: Position (Top Left), Slope (Top Right), Velocity (Bottom Left), Angular Velocity (Bottom Right)	86
Figure 7.14: Morphing Control Efforts: LQR (Top Left), LQG (Top Right), Central (Bottom)	87
Figure 2.1: Uncontrolled BMB with KV Kernel Simulation with 6 Elements: Position (Top Left), Slope (Top Right), Velocity (Bottom Left), Angular Velocity (Bottom Right)	104
Figure 2.2: Uncontrolled BMB with KV Kernel Simulation with 12 Elements: Position (Top Left), Slope (Top Right), Velocity (Bottom Left), Angular Velocity (Bottom Right)	105
Figure 2.3: Uncontrolled BMB with KV Kernel Simulation with 18 Elements: Position (Top Left), Slope (Top Right), Velocity (Bottom Left), Angular Velocity (Bottom Right)	106

ACKNOWLEDGMENTS

Foremost, I thank my Creator. It is through Him that I am able to do anything. Furthermore, I want to thank my family. Cathy, thank you for the unmatched support you have given me through the years. Without your love and sacrifice I could never have completed this work. My children, thank you for loving me through the good days and bad, the high points and low, and the seemingly long hours and short. I would also like to thank my parents in life, my parents in love, and my sisters and brothers for their love and support.

I would also like to thank my advisor, Dr. Katie Evans, for her countless hours of support, input, direction, and patience. Furthermore, Dr. Bernd Schröder has provided me with priceless help and theoretical insights. I would like to thank the rest of my committee members, Dr. Travis Atkison, Dr. Animesh Chakravarthy, and Dr. Steve Wells, for their ideas and feedback. I want to thank Dr. Lisa Kuhn for the time she has carved out of her schedule to discuss theoretical concepts with me .

I would like to thank all the faculty and staff in the mathematics department at Louisiana Tech for their support and help. Each person has influenced either my teaching or research in some way. I cannot thank them all enough. Lastly, I would like to thank the Louisiana Board of Regents for providing me with the research fellowship that has funded my work through the past three years.

CHAPTER 1

INTRODUCTION

A great deal is known about how to achieve stable flight for large aircraft that are in use every day around the world. What is strange is that little is known about the natural modes of flight that we see in the sky daily as well. Researchers such as Dr. Kenny Breuer at Brown University and Dr. Wei Shyy at Michigan University were both a part of a Multidisciplinary University Research Initiative (MURI), and as part of the project, explored the flight dynamics of creatures in nature. Their hope was that engineering methods and state of the art technology could be developed to mimic the flight capabilities seen in nature. For example many creatures such as insects and birds have flexible wings which can bend and morph shape to attain stable flight paths. Bats have been of particular interest in the realm of biologically inspired flight. The Air Force Research Laboratory Munitions Directorate suggested that unmanned



Figure 1.1: Dog faced fruit bat in flight. Credit for this image goes to Kenny Breuer in [24]

micro aerial vehicles, MAVs, with a flexible wing structure, similar to that of insects and birds, would be able to attain flight that small rigid wing vehicles can not. Thus, work began to achieve this goal at the turn of the millennium. A recent spur in the theory for DPS has developed into innovative research in what the Air Force originally proposed; see [6], [7], and [8]. A recent direction in creating a model for the proposed micro aerial vehicles has been to model flexible wing structures as Euler Bernoulli beams attached to a rigid fuselage considered to be a simple rigid mass.

The work in this thesis will build upon the partial differential equation model developed in [6], [7], [8], and [14]. The model in those works was created by modeling two flexible Euler-Bernoulli beams connected to a rigid mass. The properties of the model, such as well-posedness, and the heave dynamics were analyzed using semigroup analysis and finite element method. The model considered there consisted of a vehicle initially assumed to be in forward flight. The vehicle's lift force was modeled using a nonlinear lift coefficient obtained by adapting a model of lift determined experimentally for fruit fly wings [10]. Furthermore, the Euler Bernoulli beams were assumed to see an external viscous damping mechanism to simulate air damping and an internal damping mechanism called Kelvin Voigt damping to simulate internal damping effects since it is known that beams undergo internal damping at higher frequencies of oscillations [2],[20]. The model called BMB in the works mentioned above was proven to be well-posed and provided promising numerical results in the context of distributed parameter control. A modification to the model was also made in that the authors considered the addition of piezoceramic patch actuators (PZTs) as a realistic way of implementing control designs. Extensive theory can be found in [3] in relation

to piezoceramics and smart materials being used to control beams and plates. The well-posedness of the BMB model with PZTs was also considered and proven. However, numerical simulations for the controlled model with PZTs have not yet been performed.

In this work, we hope to gain insight into whether we should pursue a new material and model the vehicle with the more accurate non-local damping, or investigate other avenues of modeling and materials. The non-local damping model we consider will provide a more accurate description of the model using the material for the estimated parameters, than would previously have been considered with other damping models [2].

In Chapter 2, we will present a significant amount of theory which will be referenced while proving well-posedness of a linear approximation to the model developed in Chapter 4. The theory presented will rely heavily on the notions of functional analysis, Hilbert spaces and linear operators as well as semigroup theory. Chapter 3 will present a brief overview of the three different control designs used in this thesis and will provide a few theorems concerning the semigroups generated by the feedback control laws. In Chapter 4, the model with spatial hysteresis internal damping is presented. Also, a linear approximation to the model is developed which will be proven to be well-posed. After model development, theoretical results, well-posedness and exponentially stable semigroup results concerning our model are presented in Chapter 5. The finite element scheme used for our work and the Riccati Equation approximations used are presented in Chapter 6. Chapter 7 will show the numerical results we obtained using the control designs discussed in Chapter 3. Lastly, Chapter 8 will present some conclusions and future work.

As with any work, a certain amount of prior knowledge is assumed of the reader. This work assumes the reader is familiar with the following terms: linear operator, inner product, norm, Hilbert and Banach space, dual space, ordinary differential equation, and partial differential equation. Furthermore, the reader may benefit from familiarity with the finite element approach to solving partial differential equations.

CHAPTER 2

MATHEMATICAL PRELIMINARIES

In this chapter, we will provide a brief introduction to the methods used in the control of linear systems. The terms, definitions, and theorems of Section 2.1 are given in [17], [18], and [21]. The derivation and definitions given in Section 2.2 are taken from [19]. The discussion in Section 2.3 primarily follows that found in [3].

2.1 Basic Definitions and Theorems

We will provide some basic definitions and theorems which will be used throughout Chapter 5.

Definition 2.1. *Let H be a Hilbert space and let $\mathcal{A} : D(\mathcal{A}) \rightarrow H$ be a linear operator whose domain $D(\mathcal{A})$ is dense in H . Then \mathcal{A} is called self-adjoint if and only if $D(\mathcal{A}) = D(\mathcal{A}^*)$ and $\mathcal{A} = \mathcal{A}^*$. The adjoint of \mathcal{A} is defined as follows: $D(\mathcal{A}^*)$ is defined to be the set of all $x \in H$ so that $y \mapsto \langle x, \mathcal{A}y \rangle$ is continuous on $D(\mathcal{A})$. Then for all $x \in D(\mathcal{A}^*)$ and all $y \in D(\mathcal{A})$ the adjoint \mathcal{A}^* satisfies $\langle \mathcal{A}^*[x], y \rangle = \langle x, \mathcal{A}[y] \rangle$.*

Definition 2.2. *A self-adjoint operator \mathcal{A} is said to be coercive in a Hilbert space H if there is a positive constant c so that*

$$\langle \mathcal{A}\phi, \phi \rangle_H \geq c \|\phi\|_H^2 \tag{2.1}$$

for all $\phi \in H$.

The next theorem is a well known result in analysis and states a famous relationship between an inner product on a space and the norm of the elements of the inner product. It is known as the Cauchy-Schwarz inequality.

Theorem 2.3. Cauchy-Schwarz Inequality *Let X be an inner product space with inner product $\langle \cdot, \cdot \rangle_X$ and for all $x \in X$, let $\|x\|_X = \sqrt{\langle x, x \rangle}$. Then, for all $x, y \in X$ we have*

$$|\langle x, y \rangle_X| \leq \|x\|_X \|y\|_X. \quad (2.2)$$

To use the framework in Section 2.3 we require some operators to be self-adjoint. The next theorem will be needed in proving that our system operators are self-adjoint.

Theorem 2.4. Fundamental Theorem of Calculus of Variations *If $g : [x_1, x_2] \rightarrow \mathbb{R}$ is a fixed measurable function and $\int_{x_1}^{x_2} \zeta(x)g(x) dx = 0$ for every function $\zeta : [x_1, x_2] \rightarrow \mathbb{R}$ that is Lipschitzian on $[x_1, x_2]$ and vanishes at the endpoints, then $g(x) = 0$ for $x_1 < x < x_2$ except possibly on a set of measure zero.*

2.2 Semigroups

In this section, we will present the concept of a semigroup as well as a brief motivation for their use. Following the definitions, some theorems will be presented which give insight into the types of properties the semigroups we consider will be shown to have.

Definition 2.5. *A pair $(S, *)$ is called a semigroup if for all $u, v, w \in S$ we have*

$$u * (v * w) = (u * v) * w; \quad (2.3)$$

where $* : S \times S \rightarrow S$ is a binary operation.

Now if $M : S \times S \rightarrow S$ is the mapping of the binary relation then we have the following

$$M(M(u, v), w) = M(u, M(v, w)). \quad (2.4)$$

To solidify this concept of a semigroup we will consider the following IVP:

$$\dot{x} = Ax(t), \quad x(0) = f. \quad (2.5)$$

Then $x(t)$ is given by

$$x(t) = e^{At}. \quad (2.6)$$

Now define an operator $T(t)$ as $T(t)[x(s)] = x(t + s)$. Then $T(t)[f] = x(t)$ and $T(t)[x(s)] = x(t + s) = T(t + s)[f]$. Thus, the operator T satisfies the following:

1. $T(0) = \mathcal{I}$

and

2. $T(t + s) = T(t) \circ T(s)$.

We'll use this to define a semigroup of a family of linear operators.

Definition 2.6. *Let X be a Hilbert space. A family $T(t), 0 \leq t < \infty$ of bounded linear operators from $X \rightarrow X$ is called a semigroup if*

1. $T(0) = \mathcal{I}$, here \mathcal{I} is the identity on X , and

2. $T(s + t) = T(s) \circ T(t)$ for all $s, t > 0$.

It is important to note that the argument of the operators in the semigroup are the functions $x(t)$, and thus the linearity of T is such that $T(t)[x(s) + y(s)] = T(t)[x(s)] + T(t)[y(s)] = x(s + t) + y(s + t)$.

Definition 2.7. A linear operator \mathcal{A} defined by

$$D(\mathcal{A}) = \left\{ x \in X : \lim_{t \rightarrow 0^+} \frac{T(t)x - x}{t}, \text{ exists} \right\}$$

and

$$\mathcal{A}x = \lim_{t \rightarrow 0^+} \frac{T(t)x - x}{t} = \left. \frac{dT^+(t)x}{t} \right|_{t=0} \text{ for } x \in D(\mathcal{A})$$

is the infinitesimal generator of the semigroup $T(t)$, where $D(\mathcal{A})$ is the domain of \mathcal{A} .

Definition 2.8. Let X be a Hilbert Space. A semigroup $T(t), 0 \leq t < \infty$ of bounded linear operators is said to be strongly continuous if

$$\lim_{t \rightarrow 0^+} T(t)x = x \text{ for every } x \in X.$$

A strongly continuous semigroup of bounded linear operators is a semigroup of class C_0 . This will be abbreviated in writing as C_0 -semigroup.

Theorem 2.9. Let $T(t)$ be a C_0 -semigroup. There are constants $\omega \geq 0$ and $M \geq 1$ so that

$$\|T(t)\| \leq Me^{\omega t}, \text{ for } 0 \leq t < \infty.$$

If there is an $\omega < 0$ such that the inequality in Theorem 2.9 is satisfied then the semigroup is called **exponentially stable**.

Definition 2.10. An operator A is said to be exponentially stable if it generates an exponentially stable C_0 -semigroup.

2.3 Well-Posedness Theorems

Let V and H be complex Hilbert spaces with corresponding norms $\|\cdot\|_V$ and $\|\cdot\|_H$. Let $\langle \cdot, \cdot \rangle_H$ denote the inner product on H . We now assume that V is densely and continuously embedded in H . Therefore, V is dense in H and there is a positive constant c so that for all $\phi \in V$, we have $\|\phi\|_H \leq c\|\phi\|_V$. Now let H be identified with H^* through the Riesz map. Now for each $z \in H$ we define $\psi(z) \in V^*$ by $\psi(z)(\phi) = \langle z, \phi \rangle_H$ for $\phi \in V$. Through this mapping H is densely and continuously embedded into V^* . This common construction is what is known as a Gelfand triple and is denoted

$$V \hookrightarrow H \cong H^* \hookrightarrow V^*,$$

and we call H the pivot space. The duality pairing $\langle \cdot, \cdot \rangle_{V^*, V}$ will be utilized through the above Gelfand triple. Define $\phi^* \in V^*$ for $\phi \in V$ by

$$\phi^*(\phi) = \langle \phi^*, \phi \rangle_{V^*, V} = \lim_{n \rightarrow \infty} \langle z_n, \phi \rangle_H$$

where $z_n \in H$ is such that $z_n \rightarrow \phi^*$ in V^* . From here the proofs will use the above framework and the theory associated with sesquilinear forms which is now defined.

Definition 2.11. *Let V and H be vector fields over the same field $K = \mathbb{R}, \mathbb{C}$. A sesquilinear form \mathbf{a} is a function from $V \times H$ to K so that for all $v, v_1, v_2 \in V$, all $h, h_1, h_2 \in H$ and all scalars $\alpha, \beta \in K$ we have*

1. $\mathbf{a}(v_1 + v_2, h) = \mathbf{a}(v_1, h) + \mathbf{a}(v_2, h)$
2. $\mathbf{a}(v, h_1 + h_2) = \mathbf{a}(v, h_1) + \mathbf{a}(v, h_2)$
3. $\mathbf{a}(\alpha v, h) = \alpha \mathbf{a}(v, h)$
4. $\mathbf{a}(v, \beta h) = \bar{\beta} \mathbf{a}(v, h)$

This means that linearity in the first argument holds, but scalars factor out as their conjugate in the second argument, therefore implying conjugate linearity.

Assume now that we have a second order in time system given by

$$\ddot{z} + \mathcal{D}\dot{z} + \mathcal{A}z = f(t) \text{ in } V^* \tag{2.7}$$

$$z(0) = z_0, \dot{z}(0) = z_1.$$

To use the framework in this section, Gibson and Adamian state that \mathcal{A} must be coercive in H (the corresponding state space) [12]. Recall from Definition 2.2 that \mathcal{A} is coercive if there exists a constant c such that $\langle \mathcal{A}\phi, \phi \rangle_H \geq c\|\phi\|_H^2, \forall \phi \in \mathbf{D}(\mathcal{A})$. If the operator is not coercive we may choose a bounded, self-adjoint operator to add to \mathcal{A} such that their sum is coercive in H [12]. We now assume that \mathcal{A} and \mathcal{D} are generated by sesquilinear forms \mathbf{a} and \mathbf{d} . It was shown in [16] that there is a one-to-one correspondence between continuous sesquilinear forms on V and operators in $\mathcal{L}(V, V^*)$. Thus we have

$$\mathbf{a}(z, \phi) = \mathcal{A}z(\phi) = \langle \mathcal{A}z, \phi \rangle_{V^*, V} \quad z, \phi \in V \tag{2.8}$$

and

$$\mathbf{d}(z, \phi) = \mathcal{D}z(\phi) = \langle \mathcal{D}z, \phi \rangle_{V^*, V} \quad z, \phi \in V \tag{2.9}$$

We assume now that $\mathbf{a} : V \times V \rightarrow \mathbb{C}$ is a sesquilinear form on V that satisfies the following:

(H1) (Symmetry condition) For all $\phi, \psi \in V$ we have $\mathbf{a}(\phi, \psi) = \overline{\mathbf{a}(\psi, \phi)}$.

(H2) (Continuity condition) There exists a constant c_1 such that for all $\phi, \psi \in V$

$$\|\mathbf{a}(\phi, \psi)\| \leq c_1 \|\phi\|_V \|\psi\|_V \quad (2.10)$$

(H3) (Ellipticity condition) There exists a positive constant k_1 such that for all $\phi \in V$

$$\operatorname{Re}(\mathbf{a}(\phi, \phi)) = \mathbf{a}(\phi, \phi) \geq k_1 \|\phi\|^2. \quad (2.11)$$

The sesquilinear form \mathbf{d} is defined on a Hilbert space V_2 such that the following containments hold: $V \subseteq V_2 \subseteq H$. The Gelfand triple,

$$V \hookrightarrow V_2 \hookrightarrow H \cong H^* \hookrightarrow V_2^* \hookrightarrow V^*, \quad (2.12)$$

is considered with the duality pairing $\langle \cdot, \cdot \rangle_{V_2^*, V_2}$. Suppose that the sesquilinear form

$\mathbf{d} : V_2 \times V_2 \rightarrow \mathbb{C}$ satisfies:

(H4) (Continuity condition) There exists a constant c_2 such that for all $\phi, \psi \in V_2$

$$\|\mathbf{d}(\phi, \psi)\| \leq c_2 \|\phi\|_{V_2} \|\psi\|_{V_2}. \quad (2.13)$$

(H5) (Coercivity condition) There exists constants $k_2 > 0, \lambda_0 \geq 0$ such that for all

$$\phi \in V_2$$

$$\operatorname{Re}(\mathbf{d}(\phi, \phi)) + \lambda_0 \|\phi\|_H^2 \geq k_2 \|\phi\|_{V_2}^2 \quad (2.14)$$

Lastly, one regularity assumption is made about $f(t)$:

(H6) The input function f satisfies $f \in L^2[(0, T), V_2^*]$.

Using the above hypotheses we consider the variational form of (2.7) given by

$$\langle \dot{z}, \phi \rangle + \mathbf{d}(\dot{z}, \phi) + \mathbf{a}(z, \phi) = \langle f, \phi \rangle \text{ for } \phi \in V, \quad (2.15)$$

$$z(0) = z_0, \quad \dot{z}(0) = z_1.$$

Theorem 2.12 ([3]). *Suppose that \mathbf{a}, \mathbf{d} and f satisfy **H1-H6** and that $w_0 \in V, w_1 \in H$. Then there exists a unique solution w of (2.15) with $w \in L_2((0, T), V), \dot{w} \in L_2((0, T), V_2)$ and $\ddot{w} \in L_2((0, T), V^*)$. Moreover, solutions of (2.15) depend continuously on the data (w_0, w_1, f) in that the map $(w_0, w_1, f) \rightarrow (w, \dot{w})$ is continuous from $V \times H \times L_2((0, T), V_2^*)$ to $L_2((0, T), V) \times L_2((0, T), V_2)$.*

2.4 Semigroup Theorems

To consider the semigroup properties of the system, define the space $\mathcal{E} = V \times H$. Furthermore, foregoing motivation, let $\mathcal{H}_1 = \mathcal{R}(\zeta - \hat{\mathcal{A}})$ where \mathcal{R} is the range for some $\zeta > 0$ [3]. We consider rewriting (2.15) in first order form

$$\langle \hat{z}, v^* \rangle = \langle \hat{\mathcal{A}}\hat{z}(t), v^* \rangle + \langle F(t), v^* \rangle, \quad \hat{z}(0) = \hat{z}_0, \quad (2.16)$$

where $\mathbf{D}(\hat{\mathcal{A}}) = \{(\phi, \psi) \in \mathcal{H} : \psi \in V, \mathcal{A}\phi + \mathcal{D}\psi \in H\}$ and $v^* \in \mathbf{D}(\hat{\mathcal{A}}^*)$. The following theorem provides the criteria such that the semigroup generated by $\hat{\mathcal{A}}$ is strongly continuous.

Theorem 2.13 ([3]). *Under hypotheses **H1-H5** on \mathbf{a}, \mathbf{d} , the operator $\hat{\mathcal{A}}$ generates a C_0 -semigroup $\mathcal{T}(t)$ on $\mathcal{H} = V \times H$ which satisfies $\|\mathcal{T}(t)\|_{\mathcal{H}_1} \leq e^{\lambda t}$.*

The semigroup generated through this theorem is known as a contraction semigroup and is a stronger condition than the condition of a C_0 -semigroup. It does imply that provided we meet the hypotheses that we get a strongly continuous semigroup, but it is advantageous to know it has more properties which may be beneficial for future analysis. The next theorem states that if we add a bounded

linear operator to a generator of a strongly continuous semigroup then their sum will generate a strongly continuous semigroup. We will rephrase it to fit with the framework developed in this section.

Theorem 2.14 ([19]). *Suppose \hat{A} is the generator of a C_0 -semigroup. If \hat{B} is a bounded linear operator on \mathcal{H} , then $\hat{A} + \hat{B}$ is the infinitesimal generator of a C_0 -semigroup $S(t)$ on \mathcal{H} satisfying $\|S(t)\|_{\mathcal{H}} \leq Me^{(\omega + M\|\hat{B}\|_{\mathcal{H}})t}$, where ω is from the inequality in Theorem 2.9 for \hat{A} .*

The last theorem presented here shows that if the first order system generates a strongly continuous semigroup then the weak formulation of the system has a unique solution which can be represented in terms of the semigroup generated.

Theorem 2.15 ([1]). *There exists a unique solution of (2.16) which has continuous dependence on initial data if and only if \hat{A} is the infinitesimal generator of a C_0 -semigroup $T(t)$ of bounded linear operators on \mathcal{H} , and in this case \hat{z} is given by*

$$\hat{z}(t) = T(t)x + \int_0^t T(t-s)F(s)dx, \quad 0 \leq t \leq T. \quad (2.17)$$

CHAPTER 3

LINEAR FEEDBACK CONTROL

We will now discuss the basic theory behind linear quadratic control. The systems upon which control design is developed are assumed to be linear. The minimization that takes place is quadratic in the cost function. The infinite dimensional outline is given in this chapter; however, the layout follows closely to that in the finite dimensional text by Dorato et. al. [11]. The infinite dimensional treatises can be found in [9], [12], and [13].

3.1 Full State Feedback Design (LQR)

Full state feedback refers to the fact that complete information about the system is available for feedback. The Linear Quadratic Regulator (LQR) problem is constructed so that the state of the system is driven to zero.

Let E be a Hilbert space and the dynamics of a linear system be governed by the following:

$$\dot{\xi} = \mathcal{A}\xi + \mathcal{B}u, \quad \xi(0) = \xi_0, \quad (3.1)$$

where $\mathbf{D}(A) \subseteq X$, $\xi(t)$ is some state, and $u(t) \in \mathbb{R}^m$ is a control input vector which will be uniquely determined. Furthermore, $\mathcal{B} : \mathbb{R}^m \rightarrow E$ is the control operator. In

this work we wish to transform the state ξ starting at ξ_0 to another state $\tilde{\xi}$ using a linear feedback control. This type of linear tracking problem is called a disturbance rejection problem. In the disturbance rejection problem we assume that the system dynamics are given by

$$\dot{x} = \mathcal{A}x + \mathcal{B}u + w(t), \quad x(0) = x_0, \quad (3.2)$$

where $w(t) = A\tilde{\xi} - \dot{\tilde{\xi}} \neq 0$ is a disturbance signal and $x = \xi - \tilde{\xi}$. Our desire is to find a control input that minimizes the cost function

$$V(x, u) = \int_t^T (\langle x, \mathcal{Q}x \rangle_E + u' Ru) d\tau. \quad (3.3)$$

The operator $\mathcal{Q} : E \rightarrow E$ is positive-semidefinite and in this work will be $\mathcal{Q} = \mathcal{I}$, and $R : \mathbb{R}^m \rightarrow \mathbb{R}^m$ is positive definite which will take the form $R = cI$ where \mathcal{I} is the identity and c is some constant. To obtain the control law u for this so called Linear Quadratic Regulator (LQR) problem, we must solve the Differential Riccati Equation (DRE)

$$-\dot{\Pi} = \mathcal{A}^T \Pi(t) + \Pi(t) \mathcal{A} + \mathcal{Q} - \Pi(t) \mathcal{B} R^{-1} \mathcal{B}^T \Pi(t), \quad \Pi(T) = 0, \quad (3.4)$$

integrating backward in time from the final condition. The feedback gain operator \mathcal{K} is then defined as

$$\mathcal{K} = R^{-1} \mathcal{B}^* \Pi(t). \quad (3.5)$$

The feedforward signal $u_{fw}(t)$ is defined as

$$u_{fw} = -R^{-1}\mathcal{B}^*b(t). \quad (3.6)$$

Here $b(t)$ is given by solving the system

$$\dot{b}(t) = -[\mathcal{A} - \mathcal{B}R^{-1}\Pi(t)]^* b(t), \quad b(T) = 0. \quad (3.7)$$

Once we have $\Pi(t)$ and $b(t)$, the control law $u(t)$ is given by

$$u = -\mathcal{K}x(t) + u_{fw}. \quad (3.8)$$

If we substitute Equation (3.8) into Equation (3.2), we obtain the following closed-loop full state feedback-controlled system

$$\dot{x}(t) = [\mathcal{A} - \mathcal{B}\mathcal{K}]x(t) - \mathcal{B}u_{fw}. \quad (3.9)$$

In the limiting case as $T \rightarrow \infty$ the Differential Riccati Equation (3.4) becomes the Control Algebraic Riccati Equation (CARE)

$$\mathcal{A}^*\Pi(t) + \Pi(t)\mathcal{A} + \mathcal{Q} - \Pi(t)\mathcal{B}R^{-1}\mathcal{B}^*\Pi(t) = 0. \quad (3.10)$$

3.2 State Estimate Control Design

In reality we most likely do not have complete knowledge of the system for feedback purposes. However, we assume that we are able to measure the system in (3.2) and that measurement takes the form

$$y(t) = \mathcal{C}x(t), \quad (3.11)$$

where $\mathcal{C} : E \rightarrow \mathbb{R}^p$ is an operator that determines how we measure the system. We can use this information to provide some feedback into the system to apply control effort. In this section two state estimate control designs will be presented: the first will be Linear Quadratic Gaussian (LQG), the second will be Central Control Design.

3.2.1 The Linear Quadratic Gaussian Tracking Problem (LQG)

After measuring the system we have the estimate

$$\dot{x}_c = \mathcal{A}_c x_c(t) + \mathcal{F}y(t), \quad x_c(0) = x_{c0} \quad (3.12)$$

$$u = -\mathcal{K}x_c(t) - u_{fw}$$

Much of the theory of determining the operators \mathcal{A}_c , \mathcal{F} , and \mathcal{K} is found in [11] and [12].

$$\begin{bmatrix} \dot{x} \\ \dot{x}_c \end{bmatrix} = \begin{bmatrix} \mathcal{A} & -B\mathcal{K} \\ \mathcal{F}\mathcal{C} & \mathcal{A}_c \end{bmatrix} \begin{bmatrix} x \\ x_c \end{bmatrix} - \begin{bmatrix} B u_{fw} \\ 0 \end{bmatrix}, \quad \begin{bmatrix} x(0) \\ x_c(0) \end{bmatrix} = \begin{bmatrix} x_0 \\ x_{c0} \end{bmatrix}. \quad (3.13)$$

Definitions of stabilizable and detectable will now be presented to ensure that the feedback closed loop system operators can be found.

Definition 3.1. *The state $\Sigma(\mathcal{A}, \mathcal{B}, \mathcal{C})$ is said to be exponentially stable if \mathcal{A} is exponentially stable as an operator.*

Definition 3.2. *The state $\Sigma(\mathcal{A}, \mathcal{B}, \mathcal{C})$ is said to be stabilizable if there exists a linear operator $\mathcal{F} : X \rightarrow U$ such that $\mathcal{A} + B\mathcal{F}$ is exponentially stable as an operator. It is standard to refer to just the pair $(\mathcal{A}, \mathcal{B})$ as being stabilizable.*

Definition 3.3. *The state $\Sigma(\mathcal{A}, \mathcal{B}, \mathcal{C})$ is said to be detectable if there is a linear operator $\mathcal{L} : Y \rightarrow X$ such that $\mathcal{A} + \mathcal{L}\mathcal{C}$ is exponentially stable as an operator. It is standard to refer to just the pair $(\mathcal{A}, \mathcal{C})$ as being detectable.*

Under the assumptions of $(\mathcal{A}, \mathcal{B})$ and $(\mathcal{A}, \mathcal{C})$ being stabilizable and detectable respectively, the operators $\mathcal{A}_c, \mathcal{F}$, and \mathcal{K} are found by solving the ARE 3.10 and solving an additional Riccati equation known as the Filter Algebraic Riccati Equation (FARE):

$$\mathcal{A}P(t) + P(t)\mathcal{A}^* - P(t)\mathcal{C}^*\mathcal{R}^{-1}\mathcal{C}P(t) + \Omega = 0. \quad (3.14)$$

Here $\mathcal{R} = k\mathcal{I}$. In this work the operator Ω is also assumed to be \mathcal{I} . The control gain operator and control law are then given by

$$\begin{aligned} \mathcal{K} &= \mathcal{R}^{-1}\mathcal{B}^*\Pi \\ \mathcal{F} &= P\mathcal{C}^*\mathcal{R}^{-1} \\ \mathcal{A}_c &= \mathcal{A} - \mathcal{B}\mathcal{K} - \mathcal{F}\mathcal{C}. \end{aligned} \quad (3.15)$$

According to the previous assumptions the closed loop system (3.13) is stable.

3.2.2 Central Control Design

The design of what is known by Glover and McFarlane as the Central controller is presented in full in [13] and summarized by Skogestad and Postlethwaite in [22]. A proper treatise of the frequency domain and derivation of robustness conditions is given in [13]. Since the focus of the work here is not on maximizing robustness but rather on comparing controller effort for a specific model, we will forego the in depth

discussion of the Central controller's deep origins in the frequency domain. The first step in designing the Central controller is to calculate a parameter

$$\gamma_{min} = 1 + \sqrt{\sigma(\Pi P)}, \quad (3.16)$$

where σ is the spectral radius (in finite dimensions σ is just the maximum eigenvalue). Just as for the LQG controller, Π and P are solutions to the Algebraic and Filter Riccati Equations (3.10) and (3.14). As this controller only sees an estimate of the state we are given the state estimate system

$$\dot{x}_c = \mathcal{A}_c x_c(t) + \mathcal{F}y(t), \quad x_c(0) = x_{c0} \quad (3.17)$$

$$u = \mathcal{K}x_c(t) - u_{fw}$$

Note the difference in the control law u . Under the assumptions of stabilizability and detectability the closed loop system is stable and after Π and P are obtained we define the following:

$$\begin{aligned} \mathcal{K} &= \mathcal{B}^* \Pi \\ \mathcal{L} &= (1 - \gamma^2)I + \Pi P \\ \mathcal{F} &= \gamma^2 (\mathcal{L}^*)^{-1} P C^* \mathcal{R}^{-1} \\ \mathcal{A}_c &= \mathcal{A} - \mathcal{B} R^{-1} \mathcal{B} \Pi + \gamma^2 (\mathcal{L}^*)^{-1} P C^* \mathcal{C}. \end{aligned} \quad (3.18)$$

It is important enough to mention that if we choose $\gamma = \gamma_{min}$, then $\mathcal{L} = -\sigma(\Pi P)I + \Pi P$ is singular. This implies that with this choice of γ the controller cannot be directly implemented numerically. A common choice for γ is the multiple $\gamma = 1.1 * \gamma_{min}$ [22]. For computational purposes we have chosen $\gamma = 1.2 * \gamma_{min}$.

3.3 Useful Theorems

In this section we will state a few useful theorems from [12] for showing uniqueness of solutions to Riccati equations (3.10) and (3.14). Furthermore, we see the conditions that are needed for generation of exponentially stable semigroups by closed-loop feedback operators.

Theorem 3.4. *There exists a nonnegative self-adjoint solution of (3.10) if and only if, for each $z \in E$, there is a control u such that $V(x, u)$ is finite. If Π is the minimal nonnegative self-adjoint solutions of (3.10), then the unique control $u(\cdot)$ that minimizes $V(x, u)$ and optimal trajectory are given by*

$$u(t) = -R^{-1}\mathcal{B}^*\Pi z(t) \quad (3.19)$$

and

$$z(t) = S(t)z \quad (3.20)$$

where $S(t)$ is the semigroup generated by $\mathcal{A} - \mathcal{B}R^{-1}\mathcal{B}^*\Pi$. Furthermore, if \mathcal{Q} is coercive in E then $S(t)$ is uniformly exponentially stable.

Now define

$$\mathcal{A}_{\infty\infty} = \begin{bmatrix} \mathcal{A} & -\mathcal{B}\mathcal{K} \\ \mathcal{F}\mathcal{C} & \mathcal{A}_c \end{bmatrix} \quad (3.21)$$

from (3.13). Furthermore let $\hat{S}(t)$ be the semigroup generated by $\mathcal{A} - \mathcal{P}\mathcal{C}^*\mathcal{R}^{-1}\mathcal{C}$. If we replace $\mathcal{A}, \mathcal{B}, \mathcal{Q}, R, \Pi$ in Theorem 3.4 with $\mathcal{A}^*, \mathcal{C}^*, \Omega, R$, and P we obtain a unique minimal solution to the Filter Riccati Equation (3.14) and furthermore show that the $\hat{S}(t)$ is uniformly exponentially stable if Ω is coercive in E .

Theorem 3.5. *Suppose that there exist positive constants M_1, M_2, α_1 , and α_2 such that*

$$\|S(t)\|_E \leq M_1 e^{-\alpha_1 t}, \quad \|\hat{S}(t)\|_E \leq M_2 e^{-\alpha_2 t}, \quad t \geq 0. \quad (3.22)$$

Then, for each real $\alpha_3 < \min\{\alpha_1, \alpha_2\}$, there exists a constant M_3 such that

$$\|S_{\infty\infty}(t)\|_{E \times E} \leq M_3 e^{-\alpha_3 t}, \quad t \geq 0 \quad (3.23)$$

CHAPTER 4

MICRO AERIAL VEHICLE MODEL WITH SPATIAL HYSTERESIS DAMPING

4.1 Model

The model upon which this work builds was developed in [6]. The original beam-mass-beam model called “BMB” consists of two beams composed of latex and carbon graphite fiber with epoxy connected to a rigid mass. That initial model implemented viscous air damping and Kelvin Voigt internal damping. The initial model can be visualized as in Figure 4.1.

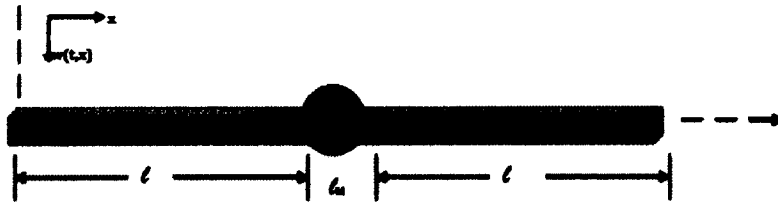


Figure 4.1: MAV beam-mass-beam system.

The system represents a one-dimensional micro aerial vehicle. The vehicle is only assumed to be capable of heave dynamics in this work. The vehicle is assumed to

be in balanced flight, i.e. lift and gravity are balanced at the start of any simulation, and the vehicle is gliding with flexible wings that can morph rather than flap.

The original model was analyzed in great depth (see [6], [7], [8], [14]). The first change made here will use the results in [2] which suggests that the BMB model can be improved by incorporating spatial hysteresis internal damping. Banks and Inman showed that spatial hysteresis damping more accurately describes the damping of a flexible beam than other internal damping models, such as Kelvin-Voigt, time hysteresis, and structural damping. Spatial hysteresis damping, as the term was coined by Banks, was introduced by Russell in [20]. It takes into account damping of a differential element of beam caused by internal friction with neighboring differential elements due to different bending rates. These damping effects are caused by energy dissipation within the beam due to fiber dynamics. This type of damping is often referred to as non-local damping because it takes into account the neighboring sections of the beam when considering damping properties.

The second change, in cooperation with the first, will be the adaptation of the material used experimentally and modeled in the work done by Banks and Inman. The flexible beam in [2] was composed of biaxial fiberglass roving, polyester yarn, and isophthalic polyester resin, which we will now consider to constitute our beams as well. Adapting the work done by Banks and Inman, we can modify the original BMB model

using the following equations for the left and right beams respectively:

$$\begin{aligned} & \rho A \ddot{w}_L(t, x_L) + \gamma \dot{w}_L(t, x_L) - \frac{\partial}{\partial x_L} \left[\int_0^\ell h(x_L, \xi) [\dot{w}'_L(t, x_L) - \dot{w}'_L(t, \xi)] d\xi \right] \\ & + EI w_L''''(t, x_L) = b(x_L) u_L(t) - 0.5 \rho_a v^2 c C_\ell, \end{aligned} \quad (4.1)$$

for $0 \leq x_L \leq \ell$ and $t \geq 0$, and

$$\begin{aligned} & \rho A \ddot{w}_R(t, x_R) + \gamma \dot{w}_R(t, x_R) - \frac{\partial}{\partial x_R} \left[\int_{\ell+\ell_M}^{\ell_M+2\ell} h(x_R, \xi) [\dot{w}'_R(t, x_R) - \dot{w}'_R(t, \xi)] d\xi \right] \\ & + EI w_R''''(t, x_R) = b(x_R) u_R(t) - 0.5 \rho_a v^2 c C_\ell, \end{aligned} \quad (4.2)$$

for $\ell + \ell_M \leq x_R \leq \ell_M + 2\ell$ and $t \geq 0$. Here the displacement $w(t, x)$ is a combination of beam displacement from equilibrium as well as over all rigid body displacement from the initial location in the air. Furthermore, ρ is the density of the beam material, A is the cross-sectional area of the beam, γ is the air damping coefficient, E is the modulus of the material, I is the area moment of inertia of the beam, b is the control input, u is the controller, ρ_a is the density of air at sea level, v is the forward velocity of the vehicle, c is the chord length of the beam, and C_ℓ is the aerodynamic lift coefficient.

The functions $h(x, \xi)$ and C_ℓ , $x \in \{x_L, x_R\}$, have the forms

$$h(x, \xi) = \frac{a}{b\sqrt{2\pi}} e^{-\frac{(x-\xi)^2}{2b^2}} \quad (4.3)$$

and

$$C_\ell = \left[k_1 + k_2 \sin \left(k_3 \arctan \left(\frac{\dot{w}(t, x) + k_5}{v} \right) + k_4 \right) \right]. \quad (4.4)$$

The aerodynamic lift coefficient, C_ℓ , was derived in [10] for a fruit fly model. It has been scaled here to accommodate the BMB model. The parameters k_1 , k_2 , k_3 , and

k_4 were best fit parameters from [10]. To scale up to an aircraft of the size we consider and to balance generated lift with gravity we have modified k_1 from that in [10] and let $k_4 = 0$. In [8], a new parameter k_5 was added to the lift coefficient to incorporate a vertical wind velocity, which will remain in this work as well. The way we interpret the lift force has changed from the early work done with the BMB model. Originally, the model included gravity and the total lift forces. However, we have streamlined the model in the assumption that the model is already in balanced flight or in an equilibrium. Therefore, the new interpretation of the lift force is that of a perturbation lift acting on the system that is already balanced. This interpretation of the lift force in the model is suggested by research collaborator Dr. Animesh Chakravarthy at Wichita State University.

The interaction kernel $h(x, \xi)$, as it is described in [2] and [20], is symmetric. Symmetry of $h(x, \xi)$ follows from Newton's second law [20]. Although we see a Gaussian form here, the term $h(x, \xi)$ can take different forms depending on what type of material composes the beam. We have chosen the above Gaussian form to make use of the results presented in [2]. We see here that h is nonnegative and bounded; thus, there are constants $\tau, \mu > 0$ where $\tau \leq h(x, \xi) \leq \mu$.

The boundary conditions presented in Table 4.1 are those from standard beam theory. Furthermore, they include the conditions for the beams which incorporate spatial hysteresis damping [2], [4].

Table 4.1: Boundary Conditions

Boundary Condition	Physical Interpretation
$EIw_L''(t, 0) = 0$ $EIw_R''(t, \ell_M + 2\ell) = 0$	Zero bending moment at the two free ends
$EIw_L''(t, 0) - \left[\int_0^\ell h(x_L, \xi) [\dot{w}'_L(t, x_L) - \dot{w}'_L(t, \xi)] d\xi \right]_{x_L=0} = 0$ $EIw_R''(t, \ell + \ell_M) - \left[\int_{\ell+\ell_M}^{\ell_M+2\ell} h(x_R, \xi) [\dot{w}'_R(t, x_R) - \dot{w}'_R(t, \xi)] d\xi \right]_{x_R=\ell_M+2\ell} = 0$	Zero shear force at the two free ends
$EIw_L'''(t, \ell) - \left[\int_0^\ell h(x_L, \xi) [\dot{w}'_L(t, x_L) - \dot{w}'_L(t, \xi)] d\xi \right]_{x_L=\ell} - EIw_R'''(t, \ell + \ell_M) + \left[\int_{\ell+\ell_M}^{\ell_M+2\ell} h(x_R, \xi) [\dot{w}'_R(t, x_R) - \dot{w}'_R(t, \xi)] d\xi \right]_{x_R=\ell+\ell_M} = m\ddot{w}_L(t, \ell)$	Change in shear force across the rigid mass equals the rigid mass (m) multiplied by its acceleration
$w_L(t, \ell) = w_R(t, \ell + \ell_M)$	Continuity of deflection across the rigid mass
$w'_L(t, \ell) = 0$ $w'_R(t, \ell + \ell_M) = 0$	Zero slope at each end of rigid mass

4.1.1 Linearization of Lift Coefficient

To apply linear control methods as described in [11], [12], and [22], we must obtain a linear system for which we can develop the controllers. The only nonlinearity in the system is seen in the aerodynamic lift coefficient, C_ℓ . The linearization process is now presented. The vehicle is assumed to be moving at a higher velocity in the forward direction than in the vertical direction. Thus, we can assume the following approximation holds:

$$\arctan\left(\frac{\dot{w}(t, x) + k_5}{v}\right) \approx \frac{\dot{w}(t, x) + k_5}{v}. \quad (4.5)$$

Now if we substitute this approximation into the Taylor Series expansion of C_ℓ and recall that $k_4 = 0$ we obtain

$$C_\ell = k_1 + k_2 \sum_{n=0}^{\infty} \frac{(-1)^n}{(2n+1)!} \left(\frac{k_3(\dot{w}(t, x) + k_5)}{v} \right)^{2n+1}. \quad (4.6)$$

In the linear approximation we keep only the linear term from the series which is $\frac{k_2 k_3}{v} \dot{w}(t, x)$. Note here that we do not keep the constant terms in the approximation. The constant terms are excluded due to the desire to have the lift be wholly a part of the damping operator for analysis purposes. We do not want to split the lift force into the damping operator and an external force operator. If the lift were split in this fashion, we would then be attempting to incorporate part of the lift into the controller and trying to reject part of the lift through some rejection process. We have elected to wholly absorb the lift force into the system operator. Thus, we have the final lift coefficient approximation

$$C_\ell \approx \frac{k_2 k_3}{v} \dot{w}(t, x). \quad (4.7)$$

Assuming a linearized lift function, (4.1) and (4.2) can be rewritten in a linear form as

$$\begin{aligned} \rho A \ddot{w}_L(t, x_L) + \gamma \dot{w}_L(t, x_L) - \frac{\partial}{\partial x_L} \left[\int_0^\ell h(x_L, \xi) [\dot{w}'_L(t, x_L) - \dot{w}'_L(t, \xi)] d\xi \right] \\ + EI w_L''''(t, x_L) = b(x_L) u_L(t) - \frac{0.5 \rho_a v^2 c k_2 k_3}{v} \dot{w}_L(t, x_L), \end{aligned} \quad (4.8)$$

for $0 \leq x_L \leq \ell$ and $t \geq 0$, and

$$\begin{aligned} \rho A \ddot{w}_R(t, x_R) + \gamma \dot{w}_R(t, x_R) - \frac{\partial}{\partial x_R} \left[\int_{\ell+\ell_M}^{\ell_M+2\ell} h(x_R, \xi) [\dot{w}'_R(t, x_R) - \dot{w}'_R(t, \xi)] d\xi \right] \\ + EI w_R''''(t, x_R) = b(x_R) u_R(t) - \frac{0.5 \rho_a v^2 c k_2 k_3}{v} \dot{w}_R(t, x_R) \end{aligned} \quad (4.9)$$

for $\ell + \ell_M \leq x_R \leq \ell_M + 2\ell$ and $t \geq 0$. As stated above, the control design will be developed on the linear approximation of the BMB model. Once the controllers are

developed they will then be applied to the nonlinear system that arises from (4.1) and (4.2). The next chapter will show that the control problem is well-posed and the first order system feedback operators used in the control design produce exponentially stable C_0 -semigroups for our particular system.

CHAPTER 5

THEORETICAL ANALYSIS

5.1 Well-Posedness and Semigroup Results

Using the framework developed in Chapter 2, the well-posedness of the linearized BMB model with spatial hysteresis damping will now be proven. Given two real Hilbert spaces V and S , let the state space be $S := L_2[0, \ell] \times L_2[\ell + \ell_M, \ell_M + 2\ell] \times \mathbb{R}$. Equations (4.8) and (4.9) along with the boundary conditions in Table 4.1 can be rewritten with acceleration terms first as:

$$\begin{aligned}
 & \rho A \ddot{w}_L(t, x_L) + \gamma \dot{w}_L(t, x_L) \\
 & - \frac{\partial}{\partial x_L} \left[\int_0^\ell h(x_L, \xi) \left[\frac{\partial}{\partial x_L} \dot{w}_L(t, x_L) - \frac{\partial}{\partial x_L} \dot{w}_L(t, \xi) \right] d\xi \right] \\
 & + EI \frac{\partial^4}{\partial x_L^4} w_L(t, x_L) = b(x_L) u_L(t) - \frac{0.5 \rho_a v^2 c k_2 k_3}{v} \dot{w}_L(t, x_L), \\
 & \rho A \ddot{w}_R(t, x_R) + \gamma \dot{w}_R(t, x_R) \\
 & - \frac{\partial}{\partial x_R} \left[\int_{\ell+\ell_M}^{\ell_M+2\ell} h(x_R, \xi) \left[\frac{\partial}{\partial x_R} \dot{w}_R(t, x_R) - \frac{\partial}{\partial x_R} \dot{w}_R(t, \xi) \right] d\xi \right] \\
 & + EI \frac{\partial^4}{\partial x_L^4} w_R(t, x_R) = b(x_R) u_R(t) - \frac{0.5 \rho_a v^2 c k_2 k_3}{v} \dot{w}_R(t, x_R),
 \end{aligned} \tag{5.1}$$

$$\begin{aligned}
& EI \frac{\partial^3}{\partial x_L^3} w_L(t, \ell) - \left[\int_0^\ell h(x_L, \xi) \left[\frac{\partial}{\partial x_L} \dot{w}_L(t, x_L) - \frac{\partial}{\partial x_L} \dot{w}_L(t, \xi) \right] d\xi \right]_{x_L=\ell} \\
& \quad - EI \frac{\partial^3}{\partial x_R^3} w_R(t, \ell + \ell_M) \\
& + \left[\int_{\ell+\ell_M}^{\ell_M+2\ell} h(x_R, \xi) \left[\frac{\partial}{\partial x_R} \dot{w}_R(t, x_R) - \frac{\partial}{\partial x_R} \dot{w}_R(t, \xi) \right] d\xi \right]_{x_L=\ell+\ell_M} = m\ddot{w}_L(t, \ell), \\
& EI \frac{\partial^2}{\partial x_L^2} w_L(t, 0) = 0, \\
& EI \frac{\partial^2}{\partial x_R^2} w_R(t, \ell_M + 2\ell) = 0, \\
& EI \frac{\partial^3}{\partial x_L^3} w_L(t, 0) - \left[\int_0^\ell h(x_L, \xi) \left[\frac{\partial}{\partial x_L} \dot{w}_L(t, x_L) - \frac{\partial}{\partial x_L} \dot{w}_L(t, \xi) \right] d\xi \right]_{x_L=0} = 0, \\
& EI \frac{\partial^3}{\partial x_R^3} w_R(t, \ell + \ell_M) \\
& - \left[\int_{\ell+\ell_M}^{\ell_M+2\ell} h(x_R, \xi) \left[\frac{\partial}{\partial x_R} \dot{w}_R(t, x_R) - \frac{\partial}{\partial x_R} \dot{w}_R(t, \xi) \right] d\xi \right]_{x_R=\ell_M+2\ell} = 0, \\
& w_L(t, \ell) - w_R(t, \ell + \ell_M) = 0, \\
& \frac{\partial}{\partial x_L} w_L(t, \ell) = 0, \\
& \frac{\partial}{\partial x_R} w_R(t, \ell + \ell_M) = 0.
\end{aligned}$$

Define the following operator such that

$$\begin{aligned} & \left(\gamma + 0.5\rho_a v c k_2 k_3 - \frac{\partial}{\partial x} \left[\int_{x_1}^{x_2} h(x, \xi) \left[\frac{\partial}{\partial x} - \frac{\partial}{\partial x} \Big|_{(t, \xi)} \right] d\xi \right] \right) \dot{w}(t, x) \\ &= \gamma \dot{w}(t, x) + 0.5\rho_a v c k_2 k_3 \dot{w}(t, x) - \frac{\partial}{\partial x} \left[\int_{x_1}^{x_2} h(x, \xi) \left[\frac{\partial}{\partial x} \dot{w}(t, x) - \frac{\partial}{\partial x} \dot{w}(t, \xi) \right] d\xi \right]. \end{aligned}$$

Now we can rewrite (5.1) as

$$\begin{aligned} & (\rho A) \ddot{w}_L(t, x_L) \\ &+ \left(\gamma + 0.5\rho_a v c k_2 k_3 - \frac{\partial}{\partial x_L} \left[\int_0^\ell h(x_L, \xi) \left[\frac{\partial}{\partial x_L} - \frac{\partial}{\partial x_L} \Big|_{(t, \xi)} \right] d\xi \right] \right) \dot{w}_L(t, x_L) \\ &+ EI \frac{\partial^4}{\partial x_L^4} w_L(t, x_L) = b(x_L) u_L(t), \\ & (\rho A) \ddot{w}_R(t, x_R) \\ &+ \left(\gamma + 0.5\rho_a v c k_2 k_3 - \frac{\partial}{\partial x_R} \left[\int_{\ell+\ell_M}^{\ell_M+2\ell} h(x_R, \xi) \left[\frac{\partial}{\partial x_R} - \frac{\partial}{\partial x_R} \Big|_{(t, \xi)} \right] d\xi \right] \right) \dot{w}_R(t, x_R) \\ &+ EI \frac{\partial^4}{\partial x_R^4} w_R(t, x_R) = b(x_R) u_R(t), \\ & m\ddot{w}_L(t, \ell) - EI \frac{\partial^3}{\partial x_L^3} w_L(t, \ell) \\ &+ \left[\int_0^\ell h(x_L, \xi) \left[\frac{\partial}{\partial x_L} - \frac{\partial}{\partial x_L} \Big|_{(t, \xi)} \right] d\xi \right]_{x_L=\ell} \dot{w}_L(t, x_L) + EI \frac{\partial^3}{\partial x_R^3} w_R(t, \ell + \ell_M) \\ &- \left[\int_{\ell+\ell_M}^{\ell_M+2\ell} h(x_R, \xi) \left[\frac{\partial}{\partial x_R} - \frac{\partial}{\partial x_R} \Big|_{(t, \xi)} \right] d\xi \right]_{x_R=\ell+\ell_M} \dot{w}_R(t, x_R) = 0 \end{aligned} \tag{5.2}$$

$$EI \frac{\partial^2}{\partial x_L^2} w_L(t, 0) = 0,$$

$$EI \frac{\partial^2}{\partial x_R^2} w_R(t, \ell_M + 2\ell) = 0,$$

$$EI \frac{\partial^3}{\partial x_L^3} w_L(t, 0) - \left[\int_0^\ell h(x_L, \xi) \left[\frac{\partial}{\partial x_L} - \frac{\partial}{\partial x_L} \Big|_{(t, \xi)} \right] d\xi \right]_{x_L=0} \dot{w}_L(t, x_L) = 0,$$

$$EI \frac{\partial^3}{\partial x_R^3} w_R(t, \ell + \ell_M)$$

$$- \left[\int_{\ell+\ell_M}^{\ell_M+2\ell} h(x_R, \xi) \left[\frac{\partial}{\partial x_R} - \frac{\partial}{\partial x_R} \Big|_{(t, \xi)} \right] d\xi \right]_{x_R=\ell_M+2\ell} \dot{w}_R(t, x_R) = 0,$$

$$w_L(t, \ell) - w_R(t, \ell + \ell_M) = 0,$$

$$\frac{\partial}{\partial x_L} w_L(t, \ell) = 0,$$

$$\frac{\partial}{\partial x_R} w_R(t, \ell + \ell_M) = 0.$$

Now divide through each equation by the constants in front of the acceleration terms.

Let $\Gamma = \frac{\gamma}{\rho A} + \frac{0.5\rho_a v c k_2 k_3}{\rho A}$ and $\Lambda = \frac{1}{\rho A}$ to obtain

$$\begin{aligned} \ddot{w}_L(t, x_L) + \left(\Gamma - \Lambda \frac{\partial}{\partial x_L} \left[\int_0^\ell h(x_L, \xi) \left[\frac{\partial}{\partial x_L} - \frac{\partial}{\partial x_L} \Big|_{(t, \xi)} \right] d\xi \right] \right) \dot{w}_L(t, x_L) \\ + \frac{EI}{\rho A} \frac{\partial^4}{\partial x_L^4} w_L(t, x_L) = \Lambda b(x_L) u_L(t), \end{aligned}$$

$$\begin{aligned}
& \ddot{w}_R(t, x_R) + \left(\Gamma - \Lambda \frac{\partial}{\partial x_R} \left[\int_{\ell+\ell_M}^{\ell_M+2\ell} h(x_R, \xi) \left[\frac{\partial}{\partial x_R} - \frac{\partial}{\partial x_R} \Big|_{(t, \xi)} \right] d\xi \right] \right) \dot{w}_R(t, x_R) \\
& \quad + \frac{EI}{\rho A} \frac{\partial^4}{\partial x_R^4} w_R(t, x_R) = \Lambda b(x_R) u_R(t), \\
& \ddot{w}_L(t, \ell) - \frac{EI}{m} \frac{\partial^3}{\partial x_L^3} w_L(t, \ell) + \frac{1}{m} \left[\int_0^\ell h(x_L, \xi) \left[\frac{\partial}{\partial x_L} - \frac{\partial}{\partial x_L} \Big|_{(t, \xi)} \right] d\xi \right]_{x_L=\ell} \dot{w}_L(t, x_L) \\
& \quad + \frac{EI}{m} \frac{\partial^3}{\partial x_R^3} w_R(t, \ell + \ell_M) \\
& \quad - \frac{1}{m} \left[\int_{\ell+\ell_M}^{\ell_M+2\ell} h(x_R, \xi) \left[\frac{\partial}{\partial x_R} - \frac{\partial}{\partial x_R} \Big|_{(t, \xi)} \right] d\xi \right]_{x_R=\ell+\ell_M} \dot{w}_R(t, x_R) = 0, \\
& \quad EI \frac{\partial^2}{\partial x_L^2} w_L(t, 0) = 0, \\
& \quad EI \frac{\partial^2}{\partial x_R^2} w_R(t, \ell_M + 2\ell) = 0, \\
& EI \frac{\partial^3}{\partial x_L^3} w_L(t, 0) - \left[\int_0^\ell h(x_L, \xi) \left[\frac{\partial}{\partial x_L} - \frac{\partial}{\partial x_L} \Big|_{(t, \xi)} \right] d\xi \right]_{x_L=0} \dot{w}_L(t, x_L) = 0, \\
& \quad EI \frac{\partial^3}{\partial x_R^3} w_R(t, \ell + \ell_M) \\
& \quad - \left[\int_{\ell+\ell_M}^{\ell_M+2\ell} h(x_R, \xi) \left[\frac{\partial}{\partial x_R} - \frac{\partial}{\partial x_R} \Big|_{(t, \xi)} \right] d\xi \right]_{x_R=\ell_M+2\ell} \dot{w}_R(t, x_R) = 0, \\
& \quad w_L(t, \ell) - w_R(t, \ell + \ell_M) = 0, \\
& \quad \frac{\partial}{\partial x_L} w_L(t, \ell) = 0, \\
& \quad \frac{\partial}{\partial x_R} w_R(t, \ell + \ell_M) = 0.
\end{aligned} \tag{5.3}$$

Let the state $z(t) = (z_1(t), z_2(t), z_3(t)) \in S$, where $z_1(t) = w_L(t, \cdot)$, $z_2(t) = w_R(t, \cdot)$, $z_3(t) = w_L(t, \ell)$. The inner product on S is taken to be

$$\langle z, \tilde{z} \rangle_S = \langle \rho A z_1, \tilde{z}_1 \rangle_{L_2[0, \ell]} + \langle \rho A z_2, \tilde{z}_2 \rangle_{L_2[\ell + \ell_M, \ell_M + 2\ell]} + m z_3 \tilde{z}_3. \quad (5.4)$$

From this, the system of second order differential equations

$$\ddot{z}(t) + \mathcal{D}_0 \dot{z}(t) + \mathcal{A}_0 z(t) = \mathcal{B}u(t) \quad \text{in } S \quad (5.5)$$

is obtained, where the operators \mathcal{D}_0 and \mathcal{A}_0 are given by

$$\mathcal{D}_0 z = \begin{bmatrix} \Gamma z_1 - \Lambda \frac{\partial}{\partial x_L} (\nu_L \mathcal{I} - \mathcal{G}_L) [z'_1(\cdot)] \\ \Gamma z_2 - \Lambda \frac{\partial}{\partial x_R} (\nu_R \mathcal{I} - \mathcal{G}_R) [z'_2(\cdot)] \\ \frac{1}{m} (\nu_L(\ell) z'_1(\ell) - \mathcal{G}_L(\ell) [z'_1(\cdot)] - \nu_R(\ell + \ell_M) z'_2(\ell + \ell_M) + \mathcal{G}_R(\ell + \ell_M) [z'_2(\cdot)]) \end{bmatrix}, \quad (5.6)$$

$$\mathcal{A}_0 z = \begin{bmatrix} \frac{EI}{\rho A} \frac{\partial^4}{\partial x_L^4} z_1(\cdot) \\ \frac{EI}{\rho A} \frac{\partial^4}{\partial x_R^4} z_2(\cdot) \\ -\frac{EI}{m} \frac{\partial^3}{\partial x_L^3} z_1(\ell) + \frac{EI}{m} \frac{\partial^3}{\partial x_R^3} z_2(\ell + \ell_M) \end{bmatrix}, \quad (5.7)$$

where $D(\mathcal{A}_0) = \{z \in S : z_1 \in H^4[0, \ell], z_2 \in H^4[\ell + \ell_M, \ell_M + 2\ell], z'_1(\ell) = 0,$

$z'_2(\ell + \ell_M) = 0, z_1(\ell) - z_3 = 0, z_2(\ell + \ell_M) - z_3 = 0\}$. Furthermore,

$\nu[\phi](x) = \int_\alpha^\beta h(x, \xi) d\xi \phi(x)$ and $\mathcal{G}[\phi](x) = \int_a^b h(x, \xi) \phi(\xi) d\xi$. That is, for the \mathcal{G}

operators in (5.6), the input is the function argument z as a function of the integration

variable. Furthermore,

$$\mathcal{B}u = \begin{bmatrix} \Lambda b \mathcal{I} & 0 & 0 \\ 0 & \Lambda b \mathcal{I} & 0 \\ 0 & 0 & \mathcal{I} \end{bmatrix} \begin{bmatrix} u_L(\cdot) \\ u_R(\cdot) \\ 0 \end{bmatrix} = \begin{bmatrix} \Lambda b u_L(\cdot) \\ \Lambda b u_R(\cdot) \\ 0 \end{bmatrix} \quad (5.8)$$

and $b(x) = b$ is constant across each beam.

Equation (5.5) can be rewritten in the form of (2.16) where $\hat{z}_1 = z$, $\hat{z}_2 = \dot{z}$, $F(t) = [0, \mathcal{B}]^T$, and

$$\hat{\mathcal{A}} = \begin{bmatrix} 0 & \mathcal{I} \\ -\mathcal{A}_0 & -\mathcal{D}_0 \end{bmatrix} \quad (5.9)$$

The operator \mathcal{A}_0 is not coercive in S since it was shown in [14] that the undamped uncontrolled system has an eigenvalue of zero. According to [12], a bounded, self-adjoint linear operator \mathcal{A}_1 can be chosen such that $\tilde{\mathcal{A}} = \mathcal{A}_0 + \mathcal{A}_1$ is coercive. The choice of operator suggested in [12] is one whose null space is the orthogonal complement of the eigenspace of \mathcal{A}_0 corresponding to nonpositive eigenvalues. Note here that there are infinitely many ways to choose \mathcal{A}_1 .

Consider $\mathcal{A}_1 = \mathcal{I}$. Note that $\mathcal{I} \in S$ is bounded, linear, and self-adjoint. Then define V to be the completion of $\mathbf{D}(\mathcal{A}_0)$ with respect to the inner product $\langle x, y \rangle_V = \langle \tilde{\mathcal{A}}x, y \rangle_S$ for $x, y \in \mathbf{D}(\mathcal{A}_0)$ (see [12]). Then $V = \mathbf{D}(\tilde{\mathcal{A}}^{1/2}) = \mathbf{D}(\mathcal{A}_0^{1/2})$ and $\mathbf{D}(\mathcal{A}_0^{1/2})$ is contained in the set $\{z \in S : z_1 \in H^2[0, \ell], z_2 \in H^2[\ell + \ell_M, \ell_M + 2\ell], z_1'(\ell) = 0, z_2'(\ell + \ell_M) = 0, z_1(\ell) - z_3 = 0, z_2(\ell + \ell_M) - z_3 = 0\}$. We now make the

following observation,

$$\begin{aligned}
\langle z, \tilde{z} \rangle_V &= \langle EIz_1'', \tilde{z}_1'' \rangle_{L_2[0, \ell]} + \langle EIz_2'', \tilde{z}_2'' \rangle_{L_2[\ell + \ell_M, \ell_M + 2\ell]} + \langle \mathcal{A}_1 z, \tilde{z} \rangle_S \\
&= \langle \tilde{\mathcal{A}} z, \tilde{z} \rangle_S \\
&= \langle \tilde{\mathcal{A}}^{1/2} z, \tilde{\mathcal{A}}^{1/2} \tilde{z} \rangle_S.
\end{aligned} \tag{5.10}$$

We note here that the last equality in (5.10) is due to the fact that square root operators are symmetric. To show that $\tilde{\mathcal{A}}$ is coercive we must first show that it is self-adjoint for consistency with Definition 2.2. The next lemma will show that $\mathbf{D}(\mathcal{A}_0)$ is densely defined. However, first note that $C_0^\infty[0, \ell] \subseteq H^4[0, \ell] \subseteq L_2[0, \ell]$ and similarly $C_0^\infty[\ell + \ell_M, \ell_M + 2\ell] \subseteq H^4[\ell + \ell_M, \ell_M + 2\ell] \subseteq L_2[\ell + \ell_M, \ell_M + 2\ell]$. However, it is well known that C_0^∞ is dense in L_2 . Hence, H^4 is dense in L_2 . We will use this result in the estimates for the proof of Lemma 5.1.

Lemma 5.1. *$\mathbf{D}(\mathcal{A}_0)$ is dense in S .*

Proof. The proof is similar to a proof provided in [23]. Let $\epsilon > 0$ and assume that $z = (z_1, z_2, z_3) \in S$. Let $\psi_1(\cdot) \in H^4[0, \ell]$ be such that $\psi_1'(\ell) = 0$, $\psi_1(\ell) = z_3$, and

$$\rho A \int_0^\ell |\psi_1(x_L) - z_1(x_L)|^2 dx_L < \frac{\epsilon}{2}.$$

Also, let $\psi_2(\cdot) \in H^4[\ell + \ell_M, \ell_M + 2\ell]$ be such that $\psi_2'(\ell + \ell_M) = 0$, $\psi_2(\ell + \ell_M) = z_3$,

and

$$\rho A \int_{\ell + \ell_M}^{\ell_M + 2\ell} |\psi_2(x_R) - z_2(x_R)|^2 dx_R < \frac{\epsilon}{2}$$

This construction implies that $\hat{z} = (\psi_1, \psi_2, z_3) \in \mathbf{D}(\mathcal{A}_0)$ and

$$\begin{aligned}
\|z - \hat{z}\|_S^2 &= \langle z - \hat{z}, z - \hat{z} \rangle_S \\
&= \rho A \int_0^\ell (z_1(x_L) - \psi_1(x_L))^2 dx_L \\
&\quad + \rho A \int_{\ell+\ell_M}^{\ell_M+2\ell} (z_2(x_R) - \psi_2(x_R))^2 dx_R + (z_3 - z_3)^2 \\
&\leq \rho A \int_0^\ell |z_1(x_L) - \psi_1(x_L)|^2 dx_L + \rho A \int_{\ell+\ell_M}^{\ell_M+2\ell} |z_2(x_R) - \psi_2(x_R)|^2 dx_R \\
&< \frac{\epsilon}{2} + \frac{\epsilon}{2} = \epsilon.
\end{aligned}$$

Therefore \mathcal{A}_0 is densely defined in S .

□

Theorem 5.2. *The operator \tilde{A} is self-adjoint with respect to the inner product on S defined in (5.4).*

Proof. By definition of \tilde{A} , all that needs to be shown is that \mathcal{A}_0 is self-adjoint. The proof will follow similarly to self-adjoint arguments in [5], [14], [16] and [23]. Recall from Definition 2.1 that we must show $\mathcal{A}_0^* = \mathcal{A}_0$ and $\mathbf{D}(\mathcal{A}_0^*) = \mathbf{D}(\mathcal{A}_0)$. For $\mathbf{D}(\mathcal{A}_0) \subseteq \mathbf{D}(\mathcal{A}_0^*)$, the containment is clear. The reverse containment will be provided later. Now to establish the definition of \mathcal{A}_0^* , assume there is a $\tilde{\Phi} \in S$ such that

$$\langle \mathcal{A}_0 z, \tilde{\Phi} \rangle_S - \langle z, \tilde{\Phi} \rangle_S = 0 \text{ for all } z \in \mathbf{D}(\mathcal{A}_0).$$

Equivalently, we can say that $\Phi \in \mathbf{D}(\mathcal{A}_0^*)$ if the above holds. The following is then obtained by definition of the inner product on S :

$$\begin{aligned}
& \int_0^\ell E I z_1''''(x_L) \phi_1(x_L) dx_L + \int_{\ell+\ell_M}^{\ell_M+2\ell} E I z_2''''(x_R) \phi_2(x_R) dx_R \\
& - E I z_1'''(\ell) \phi_3 + E I z_2'''(\ell + \ell_M) \phi_3 - \int_0^\ell \rho A z_1 \tilde{\phi}_1 dx_L - \int_{\ell+\ell_M}^{\ell_M+2\ell} \rho A z_2 \tilde{\phi}_2 dx_R \quad (5.11) \\
& - m z_3 \tilde{\phi}_3 = 0.
\end{aligned}$$

Now integrate the last two integrals by parts four times to obtain

$$\begin{aligned}
& \int_0^\ell \left[E I z_1''''(x_L) \phi_1(x_L) - \rho A \int_0^{x_L} \int_0^\xi \int_0^\zeta \int_0^\chi \tilde{\phi}_1(\tau) d\tau d\chi d\zeta d\xi z_1'''' \right] dx_L \\
& + \int_{\ell+\ell_M}^{\ell_M+2\ell} \left[E I z_2''''(x_R) \phi_2(x_R) - \rho A \int_{\ell+\ell_M}^{x_R} \int_{\ell+\ell_M}^\xi \int_{\ell+\ell_M}^\zeta \int_{\ell+\ell_M}^\chi \tilde{\phi}_2(\tau) d\tau d\chi d\zeta d\xi z_2'''' \right] dx_R \\
& - \rho A \left[z_1 \int_0^{x_L} \tilde{\phi}_1(\xi) d\xi \Big|_0^\ell - z_1' \int_0^{x_L} \int_0^\xi \tilde{\phi}_1(\zeta) d\zeta d\xi \Big|_0^\ell + z_1'' \int_0^{x_L} \int_0^\xi \int_0^\zeta \tilde{\phi}_1(\chi) d\chi d\zeta d\xi \Big|_0^\ell \right. \\
& - z_1''' \int_0^{x_L} \int_0^\xi \int_0^\zeta \int_0^\chi \tilde{\phi}_1(\tau) d\tau d\chi d\zeta d\xi \Big|_0^\ell + z_2 \int_{\ell+\ell_M}^{x_R} \tilde{\phi}_2(\xi) d\xi \Big|_{\ell+\ell_M}^{\ell_M+2\ell} \\
& - z_2' \int_{\ell+\ell_M}^{x_R} \int_{\ell+\ell_M}^\xi \tilde{\phi}_2(\zeta) d\zeta d\xi \Big|_{\ell+\ell_M}^{\ell_M+2\ell} + z_2'' \int_{\ell+\ell_M}^{x_R} \int_{\ell+\ell_M}^\xi \int_{\ell+\ell_M}^\zeta \tilde{\phi}_2(\chi) d\chi d\zeta d\xi \Big|_{\ell+\ell_M}^{\ell_M+2\ell} \\
& \left. - z_2''' \int_{\ell+\ell_M}^{x_R} \int_{\ell+\ell_M}^\xi \int_{\ell+\ell_M}^\zeta \int_{\ell+\ell_M}^\chi \tilde{\phi}_2(\tau) d\tau d\chi d\zeta d\xi \Big|_{\ell+\ell_M}^{\ell_M+2\ell} \right] - E I z_1'''(\ell) \phi_3 \\
& + E I z_2'''(\ell + \ell_M) \phi_3 - m z_3 \tilde{\phi}_3 = 0.
\end{aligned} \tag{5.12}$$

Now note that $\mathbf{D}(\mathcal{A}_0)$ contains $\mathcal{D}_1 = \{z \in S : z_1 \in H_0^4[0, \ell], z_2 = z_3 = 0\}$. Therefore, (5.12) holds for all $z \in \mathcal{D}_1$, and we can obtain the following:

$$\int_0^\ell z_1''''(x_L) \left[EI\phi_1(x_L) - \rho A \int_0^{x_L} \int_0^\xi \int_0^\zeta \int_0^x \tilde{\phi}_1(\tau) d\tau d\chi d\zeta d\xi \right] dx_L = 0. \quad (5.13)$$

Now, applying Theorem 2.4 we can write

$$EI\phi_1(x_L) - \rho A \int_0^{x_L} \int_0^\xi \int_0^\zeta \int_0^x \tilde{\phi}_1(\tau) d\tau d\chi d\zeta d\xi = d + cx_L + bx_L^2 + ax_L^3 \quad (5.14)$$

where a, b, c , and d are constants. This implies that

$$\phi_1(x_L) = \frac{1}{EI} \left[\rho A \int_0^{x_L} \int_0^\xi \int_0^\zeta \int_0^x \tilde{\phi}_1(\tau) d\tau d\chi d\zeta d\xi + d + cx_L + bx_L^2 + ax_L^3 \right] \quad (5.15)$$

Therefore, $\phi_1(x_L) \in H^4[0, \ell]$ and differentiating ϕ_1 four times yields

$$\phi_1'''' = \frac{\rho A}{EI} \tilde{\phi}_1(x_L) \iff \tilde{\phi}_1(x_L) = \frac{EI}{\rho A} \phi_1'''' \quad (5.16)$$

Similarly $\mathbf{D}(\mathcal{A}_0)$ contains $\mathcal{D}_2 = \{z \in S : z_2 \in H_0^4[\ell + \ell_M, \ell_M + 2\ell], z_1 = z_3 = 0\}$. Thus, we also have

$$\int_{\ell+\ell_M}^{\ell_M+2\ell} z_2''''(x_R) \left[EI\phi(x_R) - \rho A \int_{\ell+\ell_M}^{x_R} \int_{\ell+\ell_M}^\xi \int_{\ell+\ell_M}^\zeta \int_{\ell+\ell_M}^x \tilde{\phi}_2(\tau) d\tau d\chi d\zeta d\xi \right] dx_R = 0. \quad (5.17)$$

Applying Theorem 2.4, we write

$$EI\phi_2(x_R) - \rho A \int_{\ell+\ell_M}^{x_R} \int_{\ell+\ell_M}^{\xi} \int_{\ell+\ell_M}^{\zeta} \int_{\ell+\ell_M}^{\chi} \tilde{\phi}_2(\tau) d\tau d\chi d\zeta d\xi = \delta + \gamma x_R + \beta x_R^2 + \alpha x_R^3, \quad (5.18)$$

where α, β, γ , and δ are constants. Rewriting yields the following:

$$\phi_2(x_R) = \frac{1}{EI} \left[\rho A \int_{\ell+\ell_M}^{x_R} \int_{\ell+\ell_M}^{\xi} \int_{\ell+\ell_M}^{\zeta} \int_{\ell+\ell_M}^{\chi} \tilde{\phi}_2(\tau) d\tau d\chi d\zeta d\xi + \delta + \gamma x_R + \beta x_R^2 + \alpha x_R^3 \right]. \quad (5.19)$$

Therefore $\phi_2(x_R) \in H^4[\ell + \ell_M, \ell_M + 2\ell]$ and differentiating ϕ_2 four times yields

$$\phi_2''''(x_R) = \frac{\rho A}{EI} \tilde{\phi}_2(x_R) \iff \tilde{\phi}_2(x_R) = \frac{EI}{\rho A} \phi_2''''(x_R). \quad (5.20)$$

Substitute $\tilde{\phi}_1$ and $\tilde{\phi}_2$ into Equation (5.11) and integrate the first two integrals by parts four times to obtain

$$\begin{aligned} & \int_0^{\ell} EI z_1(x_L) \phi_1''''(x_L) dx_L - \int_0^{\ell} \rho A z_1 \frac{EI}{\rho A} \phi_1'''' dx_L \\ & + \int_{\ell+\ell_M}^{\ell_M+2\ell} EI z_2(x_R) \phi_2''''(x_R) dx_R - \int_{\ell+\ell_M}^{\ell_M+2\ell} \rho A z_2 \frac{EI}{\rho A} \phi_2''''(x_R) dx_R \\ & - EI z_1'''(\ell) \phi_3 + EI z_2'''(\ell + \ell_M) \phi_3 + EI \left[z_1''' \phi_1 \Big|_0^{\ell} - z_1'' \phi_1' \Big|_0^{\ell} + z_1' \phi_1'' \Big|_0^{\ell} - z_1 \phi_1''' \Big|_0^{\ell} \right] \\ & + EI \left[z_2''' \phi_2 \Big|_{\ell+\ell_M}^{\ell_M+2\ell} - z_2'' \phi_2' \Big|_{\ell+\ell_M}^{\ell_M+2\ell} + z_2' \phi_2'' \Big|_{\ell+\ell_M}^{\ell_M+2\ell} - z_2 \phi_2''' \Big|_{\ell+\ell_M}^{\ell_M+2\ell} \right] - m z_3 \tilde{\phi}_3 = 0. \end{aligned} \quad (5.21)$$

Canceling the first four integrals and evaluating the terms in brackets gives

$$\begin{aligned}
& -EIz_1'''(\ell)\phi_3 + EIz_2'''(\ell + \ell_M)\phi_3 + EIz_1'''(\ell)\phi_1(\ell) - EIz_1'''(0)\phi_1(0) - EIz_1''(\ell)\phi_1'(\ell) \\
& + EIz_1''(0)\phi_1'(0) + EIz_1'(\ell)\phi_1''(\ell) - EIz_1'(0)\phi_1''(0) - EIz_1(\ell)\phi_1'''(\ell) + EIz_1(0)\phi_1'''(0) \\
& + EIz_2'''(\ell_M + 2\ell)\phi_2(\ell_M + 2\ell) - EIz_2'''(\ell + \ell_M)\phi_2(\ell + \ell_M) \\
& - EIz_2''(\ell_M + 2\ell)\phi_2'(\ell_M + 2\ell) + EIz_2''(\ell + \ell_M)\phi_2'(\ell + \ell_M) \\
& + EIz_2'(\ell_M + 2\ell)\phi_2''(\ell_M + 2\ell) - EIz_2'(\ell + \ell_M)\phi_2''(\ell + \ell_M) \\
& - EIz_2(\ell_M + 2\ell)\phi_2'''(\ell_M + 2\ell) + EIz_2(\ell + \ell_M)\phi_2'''(\ell + \ell_M) - mz_3\tilde{\phi}_3 = 0.
\end{aligned} \tag{5.22}$$

Now using the properties of $\mathbf{D}(\mathcal{A}_0)$ applied to z and regrouping we are left with

$$\begin{aligned}
& EIz_1'''(\ell)[\phi_1(\ell) - \phi_3] + EIz_2'''(\ell + \ell_M)[\phi_3 - \phi_2(\ell + \ell_M)] - EIz_1'''(0)\phi_1(0) \\
& - EIz_1''(\ell)\phi_1'(\ell) + EIz_1''(0)\phi_1'(0) - EIz_1'(0)\phi_1''(0) + EIz_1(0)\phi_1'''(0) \\
& + EIz_2'''(\ell_M + 2\ell)\phi_2(\ell_M + 2\ell) - EIz_2''(\ell_M + 2\ell)\phi_2'(\ell_M + 2\ell) \\
& + EIz_2''(\ell + \ell_M)\phi_2'(\ell + \ell_M) + EIz_2'(\ell_M + 2\ell)\phi_2''(\ell_M + 2\ell) \\
& - EIz_2(\ell_M + 2\ell)\phi_2'''(\ell_M + 2\ell) + z_3 \left[EI\phi_2'''(\ell + \ell_M) - EI\phi_1'''(\ell) - m\tilde{\phi}_3 \right] = 0
\end{aligned} \tag{5.23}$$

Because (5.23) must hold for arbitrary $z \in S$, then it must be true that

$$z_3 \left[EI\phi_2'''(\ell + \ell_M) - EI\phi_1'''(\ell) - m\tilde{\phi}_3 \right] = 0. \tag{5.24}$$

Equation (5.24) implies

$$\tilde{\phi}_3 = -\frac{EI}{m} [\phi_1'''(\ell) - \phi_2'''(\ell + \ell_M)], \quad (5.25)$$

and the remaining terms in (5.23) must sum to zero. Choosing different subsets for z of $\mathbf{D}(\mathcal{A}_0)$, for which terms in (5.23) are eliminated, determines the domain of the adjoint. This implies that

$$\begin{aligned} \mathbf{D}(\mathcal{A}_0^*) &\subseteq \{ \Phi \in S : \phi_1 \in H^4[0, \ell], \phi_2 \in H^4[\ell + \ell_M, \ell_M + 2\ell], \phi_1'(\ell) = 0 \\ &\quad \phi_2'(\ell + \ell_M) = 0, \phi_1(\ell) - \phi_3 = 0, \phi_2(\ell + \ell_M) - \phi_3 = 0 \} \\ &= \mathbf{D}(\mathcal{A}_0). \end{aligned} \quad (5.26)$$

Thus $\mathbf{D}(\mathcal{A}_0^*) = \mathbf{D}(\mathcal{A}_0)$, and

$$\mathcal{A}_0^* \Phi = \tilde{\Phi} = \begin{bmatrix} \tilde{\phi}_1 \\ \tilde{\phi}_2 \\ \tilde{\phi}_3 \end{bmatrix} = \begin{bmatrix} \frac{EI}{\rho A} \phi_1'''' \\ \frac{EI}{\rho A} \phi_2'''' \\ \frac{EI}{m} \phi_2'''(\ell + \ell_M) - \frac{EI}{m} \phi_1'''(\ell) \end{bmatrix} = \mathcal{A}_0 \Phi. \quad (5.27)$$

Therefore $\mathcal{A}_0^* \Phi = \mathcal{A}_0 \Phi$ for all $\Phi \in \mathbf{D}(\mathcal{A}_0)$, and \mathcal{A}_0 is self-adjoint. Furthermore, this means that $\tilde{\mathcal{A}} = \mathcal{A}_0 + \mathcal{A}_1$ is self-adjoint.

□

A short computation will show that $\tilde{\mathcal{A}}$ is indeed coercive in the state space S .

Theorem 5.3. *The operator $\tilde{\mathcal{A}}$ of bounded perturbation of \mathcal{A}_0 is coercive in S .*

Proof.

$$\begin{aligned}
\langle \tilde{\mathcal{A}}z, z \rangle_S &= \langle z, z \rangle_V = \langle EIz_1'', z_1'' \rangle_{L_2[0, \ell]} + \langle EIz_2'', z_2'' \rangle_{L_2[\ell + \ell_M, \ell_M + 2\ell]} + \langle \mathcal{A}_1 z, z \rangle_S \\
&= \langle EIz_1'', z_1'' \rangle_{L_2[0, \ell]} + \langle EIz_2'', z_2'' \rangle_{L_2[\ell + \ell_M, \ell_M + 2\ell]} + \langle \rho A z_1, z_1 \rangle_{L_2[0, \ell]} \\
&\quad + \langle \rho A z_2, z_2 \rangle_{L_2[\ell + \ell_M, \ell_M + 2\ell]} + m z_3 z_3 \\
&\geq c \langle \rho A z_1, z_1 \rangle_{L_2[0, \ell]} + c \langle \rho A z_2, z_2 \rangle_{L_2[\ell + \ell_M, \ell_M + 2\ell]} + c m z_3 z_3 \\
&= c \|z\|_S^2
\end{aligned} \tag{5.28}$$

for $0 < c \leq 1$.

□

Now that we have a coercive operator we can exploit the theory developed in Chapter 2. The first thing will be to determine the sesquilinear forms associated with $\tilde{\mathcal{A}}$ and $\tilde{\mathcal{D}} = \mathcal{D}_0 + \mathcal{A}_1$. According to [3], when considering spatial hysteresis damping in a single Euler-Bernoulli beam, it is natural to let $V_2 = H^1[0, \ell]$. A slight modification will suit our multiple component model. Let $V_2 = H^1[0, \ell] \times H^1[\ell + \ell_M, \ell_M + 2\ell] \times \mathbb{R}$. The inner product on V_2 is taken as

$$\langle z, \tilde{z} \rangle_{V_2} = \langle z_1, \tilde{z}_1 \rangle_{H^1[0, \ell]} + \langle z_2, \tilde{z}_2 \rangle_{H^1[\ell + \ell_M, \ell_M + 2\ell]} + \langle \mathcal{A}_1 z, \tilde{z} \rangle_S. \tag{5.29}$$

Now let $\phi \in V$ and $z \in S$. Then

$$\begin{aligned} \langle \mathcal{A}_0 z, \Phi \rangle_S &= \langle E I z_1'''' , \phi_1 \rangle_{L_2[0, \ell]} + \langle E I z_2'''' , \phi_2 \rangle_{L_2[\ell + \ell_M, \ell_M + 2\ell]} \\ &\quad - E I z_1'''(\ell) \phi_3 + E I z_2'''(\ell + \ell_M) \phi_3. \end{aligned} \quad (5.30)$$

Now integrate by parts twice to obtain

$$\begin{aligned} \langle \mathcal{A}_0 z, \Phi \rangle_S &= \langle E I z_1'' , \phi_1'' \rangle_{L_2[0, \ell]} + \langle E I z_2'' , \phi_2'' \rangle_{L_2[\ell + \ell_M, \ell_M + 2\ell]} \\ &\quad + E I z_1'''(\ell) \phi_1(\ell) - E I z_1'''(0) \phi_1(0) - E I z_1''(\ell) \phi_1'(\ell) + E I z_1''(0) \phi_1'(0) \\ &\quad + E I z_2'''(\ell_M + 2\ell) \phi_2(\ell_M + 2\ell) - E I z_2'''(\ell + \ell_M) \phi_2(\ell + \ell_M) \\ &\quad - E I z_2''(\ell_M + 2\ell) \phi_2'(\ell_M + 2\ell) + E I z_2''(\ell + \ell_M) \phi_2'(\ell + \ell_M) \\ &\quad - E I z_1'''(\ell) \phi_3 + E I z_2'''(\ell + \ell_M) \phi_3. \end{aligned} \quad (5.31)$$

Regrouping (5.31) results in

$$\begin{aligned} \langle \mathcal{A}_0 z, \Phi \rangle_S &= \langle E I z_1'' , \phi_1'' \rangle_{L_2[0, \ell]} + \langle E I z_2'' , \phi_2'' \rangle_{L_2[\ell + \ell_M, \ell_M + 2\ell]} \\ &\quad + E I [z_1'''(\ell) (\phi_1(\ell) - \phi_3) - z_1'''(0) \phi_1(0) - z_1''(\ell) \phi_1'(\ell) + z_1''(0) \phi_1'(0)] \\ &\quad + E I [z_2'''(\ell_M + 2\ell) \phi_2(\ell_M + 2\ell) - z_2'''(\ell + \ell_M) (\phi_2(\ell + \ell_M) - \phi_3) \\ &\quad - z_2''(\ell_M + 2\ell) \phi_2'(\ell_M + 2\ell) + z_2''(\ell + \ell_M) \phi_2'(\ell + \ell_M)]. \end{aligned} \quad (5.32)$$

Substituting boundary conditions at the rigid mass location in for Φ and regrouping yields

$$\begin{aligned}
\langle \mathcal{A}_0 z, \Phi \rangle_S &= \langle EI z_1'', \phi_1'' \rangle_{L_2[0, \ell]} + \langle EI z_2'', \phi_2'' \rangle_{L_2[\ell + \ell_M, \ell_M + 2\ell]} \\
&\quad - EI z_1'''(0) \phi_1(0) + EI z_1''(0) \phi_1'(0) \\
&\quad + EI z_2'''(\ell_M + 2\ell) \phi_2(\ell_M + 2\ell) - EI z_2''(\ell_M + 2\ell) \phi_2'(\ell_M + 2\ell).
\end{aligned} \tag{5.33}$$

This will be used in defining the sesquilinear form \mathbf{a} later. A similar computation now with $\Phi \in V_2$, the damping operator \mathcal{D}_0 gives

$$\begin{aligned}
\langle \mathcal{D}_0 z, \Phi \rangle_S &= \langle \gamma z_1, \phi_1 \rangle_{L_2[0, \ell]} + \langle 0.5 \rho_a c v k_2 k_3 z_1, \phi_1 \rangle_{L_2[0, \ell]} - \left\langle \frac{\partial}{\partial x_L} (\nu_L - \mathcal{G}_L) [z_1'], \phi_1 \right\rangle_{L_2[0, \ell]} \\
&\quad + \langle \gamma z_2, \phi_2 \rangle_{L_2[\ell + \ell_M, \ell_M + 2\ell]} + \langle 0.5 \rho_a c v k_2 k_3 z_2, \phi_2 \rangle_{L_2[\ell + \ell_M, \ell_M + 2\ell]} \\
&\quad - \left\langle \frac{\partial}{\partial x_R} (\nu_R - \mathcal{G}_R) [z_2'], \phi_2 \right\rangle_{L_2[\ell + \ell_M, \ell_M + 2\ell]} + (\nu_L(\ell) - \mathcal{G}_L(\ell)) [z_1'] \phi_3 \\
&\quad - (\nu_R(\ell + \ell_M) - \mathcal{G}_R(\ell + \ell_M)) [z_2'] \phi_3.
\end{aligned} \tag{5.34}$$

If we integrate the third and sixth inner products by parts once each, we obtain the following:

$$\begin{aligned}
\langle \mathcal{D}_0 z, \Phi \rangle_S &= \langle \gamma z_1, \phi_1 \rangle_{L_2[0, \ell]} + \langle 0.5 \rho_a c v k_2 k_3 z_1, \phi_1 \rangle_{L_2[0, \ell]} + \langle (\nu_L - \mathcal{G}_L) [z'_1], \phi'_1 \rangle_{L_2[0, \ell]} \\
&+ \langle \gamma z_2, \phi_2 \rangle_{L_2[\ell + \ell_M, \ell_M + 2\ell]} + \langle 0.5 \rho_a c v k_2 k_3 z_2, \phi_2 \rangle_{L_2[\ell + \ell_M, \ell_M + 2\ell]} \\
&+ \langle (\nu_R - \mathcal{G}_R) [z'_2], \phi'_2 \rangle_{L_2[\ell + \ell_M, \ell_M + 2\ell]} + (\nu_L(\ell) - \mathcal{G}_L(\ell)) [z'_1] \phi_3 \\
&- (\nu_R(\ell + \ell_M) - \mathcal{G}_R(\ell + \ell_M)) [z'_2] \phi_3 \\
&- (\nu_L(\ell) - \mathcal{G}_L(\ell)) [z'_1] \phi_1(\ell) + (\nu_L(0) - \mathcal{G}_L(0)) [z'_1] \phi_1(0) \\
&- (\nu_R(\ell_M + 2\ell) - \mathcal{G}_R(\ell_M + 2\ell)) [z'_2] \phi_2(\ell_M + 2\ell) \\
&+ (\nu_R(\ell + \ell_M) - \mathcal{G}_R(\ell + \ell_M)) [z'_2] \phi_2(\ell + \ell_M).
\end{aligned} \tag{5.35}$$

As before, we can substitute boundary conditions at the mass location in for Φ to obtain

$$\begin{aligned}
\langle \mathcal{D}_0 z, \Phi \rangle_S &= \langle \gamma z_1, \phi_1 \rangle_{L_2[0, \ell]} + \langle 0.5 \rho_a c v k_2 k_3 z_1, \phi_1 \rangle_{L_2[0, \ell]} + \langle (\nu_L - \mathcal{G}_L) [z'_1], \phi'_1 \rangle_{L_2[0, \ell]} \\
&+ \langle \gamma z_2, \phi_2 \rangle_{L_2[\ell + \ell_M, \ell_M + 2\ell]} + \langle 0.5 \rho_a c v k_2 k_3 z_2, \phi_2 \rangle_{L_2[\ell + \ell_M, \ell_M + 2\ell]} \\
&+ \langle (\nu_R - \mathcal{G}_R) [z'_2], \phi'_2 \rangle_{L_2[\ell + \ell_M, \ell_M + 2\ell]} + (\nu_L(0) - \mathcal{G}_L(0)) [z'_1] \phi_1(0) \\
&- (\nu_R(\ell_M + 2\ell) - \mathcal{G}_R(\ell_M + 2\ell)) [z'_2] \phi_2(\ell_M + 2\ell).
\end{aligned} \tag{5.36}$$

Now a variational formulation of the system is given by

$$\langle \ddot{z}(t), \Phi \rangle_s + \mathbf{d}(\dot{z}(t), \Phi) + \mathbf{a}(z(t), \Phi) = \langle \mathcal{B}u(t), \Phi \rangle_S, \quad (5.37)$$

where the sesquilinear forms $\mathbf{a}(z(t), \Phi)$ and $\mathbf{d}(z(t), \Phi)$ are defined as

$$\mathbf{a}(z(t), \Phi) = \langle EIz_1'', \phi_1'' \rangle_{L_2[0, \ell]} + \langle EIz_2'', \phi_2'' \rangle_{L_2[\ell + \ell_M, \ell_M + 2\ell]} \quad (5.38)$$

and

$$\begin{aligned} \mathbf{d}(z(t), \Phi) &= \langle (\gamma + 0.5\rho_a cvk_2k_3) z_1, \phi_1 \rangle_{L_2[0, \ell]} + \langle (\nu_L - \mathcal{G}_L) z_1', \phi_1' \rangle_{L_2[0, \ell]} \\ &\quad + \langle (\gamma + 0.5\rho_a cvk_2k_3) z_2, \phi_2 \rangle_{L_2[\ell + \ell_M, \ell_M + 2\ell]} \\ &\quad + \langle (\nu_R - \mathcal{G}_R) z_2', \phi_2' \rangle_{L_2[\ell + \ell_M, \ell_M + 2\ell]}. \end{aligned} \quad (5.39)$$

To show that the system is wellposed, we will apply Theorem 2.12 to the system

$$\langle \ddot{z}(t), \Phi \rangle_s + \tilde{\mathbf{d}}(\dot{z}(t), \Phi) + \tilde{\mathbf{a}}(z(t), \Phi) = \langle \mathcal{B}u(t), \Phi \rangle_S \quad (5.40)$$

where $\tilde{\mathbf{a}}(z(t), \Phi) = \mathbf{a}(z(t), \Phi) + \langle \mathcal{A}_1 z, \Phi \rangle_S$ and $\tilde{\mathbf{d}}(z(t), \Phi) = \mathbf{d}(z(t), \Phi) + \langle \mathcal{A}_1 z, \Phi \rangle_S$.

Theorem 5.4. *The sesquilinear form $\tilde{\mathbf{a}}(\Phi, \Psi)$ satisfies **H1** - **H3** from Section 2.3.*

Proof. The symmetry property **H1** follows from the symmetry of the inner product on V . Thus, $\tilde{\mathbf{a}}(\Phi, \Psi) = \langle \Phi, \Psi \rangle_V = \overline{\langle \Psi, \Phi \rangle_V} = \langle \Psi, \Phi \rangle_V = \tilde{\mathbf{a}}(\Psi, \Phi)$, since V is a real

Hilbert space. Next, using the Cauchy-Schwarz inequality, we have

$$\|\tilde{\mathbf{a}}(\Phi, \Psi)\| = \|\langle \Phi, \Psi \rangle_V\| \leq k \|\Phi\|_V \|\Psi\|_V \quad (5.41)$$

for $k \geq 1$. Thus, $\tilde{\mathbf{a}}$ satisfies the continuity condition **H2**. Lastly,

$$\begin{aligned} \operatorname{Re}(\tilde{\mathbf{a}}(\Phi, \Phi)) &= \tilde{\mathbf{a}}(\Phi, \Phi) \\ &= \langle EI\phi_1'', \phi_1'' \rangle_{L_2[0, \ell]} + \langle EI\phi_2'', \phi_2'' \rangle_{L_2[\ell + \ell_M, \ell_M + 2\ell]} + \langle \mathcal{A}_1\Phi, \Phi \rangle_S \\ &\geq \epsilon \langle EI\phi_1'', \phi_1'' \rangle_{L_2[0, \ell]} + \epsilon \langle EI\phi_2'', \phi_2'' \rangle_{L_2[\ell + \ell_M, \ell_M + 2\ell]} + \epsilon \langle \mathcal{A}_1\Phi, \Phi \rangle_S \\ &= \epsilon \langle \Phi, \Phi \rangle_V = \epsilon \|\Phi\|_V^2, \end{aligned} \quad (5.42)$$

for $0 < \epsilon \leq 1$. Thus, $\tilde{\mathbf{a}}$ is V-elliptic satisfying condition **H3**. \square

It is well known from the theory that a sesquilinear form is continuous if and only if it satisfies the inequality in **H4** (hence the title ‘‘Continuity Condition’’). Thus, we will show that $\tilde{\mathbf{d}}$ is the sum of continuous functions and is therefore continuous, implying it satisfies **H4**.

Lemma 5.5. *Let $\Phi, \Psi \in V_2$. The following are continuous: $\langle \mathcal{A}_1\Phi, \Psi \rangle_S$,*

$$\langle (\gamma + 0.5\rho_a cvk_2k_3) \phi_1, \psi_1 \rangle_{L_2[0, \ell]}, \text{ and } \langle (\gamma + 0.5\rho_a cvk_2k_3z_1) \phi_2, \psi_2 \rangle_{L_2[\ell + \ell_M, \ell_M + 2\ell]}.$$

Proof. To begin, note that the proof is identical for the last two terms. Also note that $(\gamma + 0.5\rho_a cvk_2k_3)$ is a constant. Therefore continuity will follow quickly from the

Cauchy-Schwarz inequality. Consider,

$$\left| \langle (\gamma + 0.5\rho_a cvk_2k_3) \phi_1, \psi_1 \rangle_{L_2[0,\ell]} \right| \leq |(\gamma + 0.5\rho_a cvk_2k_3)| \left| \langle \phi_1, \psi_1 \rangle_{L_2[0,\ell]} \right|. \quad (5.43)$$

Now by the Cauchy-Schwarz inequality we have

$$\leq c \|\phi_1\|_{L_2[0,\ell]} \|\psi_1\|_{L_2[0,\ell]}.$$

Therefore, the last two terms listed in Lemma 5.5 are continuous. Lastly,

$$\langle \mathcal{A}_1 \Phi, \Psi \rangle_S = \langle \Phi, \Psi \rangle_S \leq \delta \|\Phi\|_S \|\Psi\|_S, \quad (5.44)$$

by Cauchy-Schwarz. Thus, the first term described in Lemma 5.5 is continuous, which finishes the proof. \square

Theorem 5.6. *The sesquilinear form $\tilde{\mathbf{d}}(\Phi, \Psi)$ satisfies **H4** – **H5** from Section 2.3.*

Proof. As noted, we only need to show that $\langle (\nu_L - \mathcal{G}_L) \phi'_1, \psi'_1 \rangle_{L_2[0,\ell]}$ is continuous for $\phi'_1, \psi'_1 \in L_2[0, \ell]$. The proof for $\langle (\nu_R - \mathcal{G}_R) \phi'_2, \psi'_2 \rangle_{L_2[\ell+\ell_M, \ell_M+2\ell]}$ is nearly identical. As noted above, we need to show that $\left| \langle (\nu_L - \mathcal{G}_L) \phi'_1, \psi'_1 \rangle_{L_2[0,\ell]} \right| \leq \epsilon \|\phi'_1\|_{L_2[0,\ell]} \|\psi'_1\|_{L_2[0,\ell]}$

for some constant ϵ . Now consider

$$\begin{aligned}
\left| \langle (\nu_L - \mathcal{G}_L)\phi'_1, \psi'_1 \rangle_{L_2[0,\ell]} \right| &\leq \left| \langle \nu\phi'_1, \psi'_1 \rangle_{L_2[0,\ell]} \right| + \left| \langle \mathcal{G}_L\phi'_1, \psi'_1 \rangle_{L_2[0,\ell]} \right| \\
&= \left| \left\langle \int_0^\ell h(x, \xi) d\xi \phi'_1(x), \psi'_1(x) \right\rangle_{L_2[0,\ell]} \right| \\
&\quad + \left| \int_0^\ell \int_0^\ell h(x, \xi) \phi'_1(\xi) d\xi \psi'_1(x) dx \right| \tag{5.45} \\
&\leq \mu\ell \left| \langle \phi'_1(x), \psi'_1(x) \rangle_{L_2[0,\ell]} \right| \\
&\quad + \left| \int_0^\ell \int_0^\ell h(x, \xi) \phi'_1(\xi) d\xi \psi'_1(x) dx \right|
\end{aligned}$$

(since $h(x, \xi) \leq \mu$)

$$\begin{aligned}
&\leq c_1 \|\phi'_1(x)\|_{L_2[0,\ell]} \|\psi'_1(x)\|_{L_2[0,\ell]} \\
&\quad + \left| \int_0^\ell \int_0^\ell h(x, \xi) \phi'_1(\xi) d\xi \psi'_1(x) dx \right|
\end{aligned}$$

(by Cauchy-Schwarz)

$$\begin{aligned}
&\leq c_1 \|\phi'_1(x)\|_{L_2[0,\ell]} \|\psi'_1(x)\|_{L_2[0,\ell]} \\
&\quad + \mu \int_0^\ell \int_0^\ell |\phi'_1(\xi)| |\psi'_1(x)| d\xi dx
\end{aligned}$$

(again since $h(x, \xi) \leq \mu$)

$$\begin{aligned}
&= c_1 \|\phi'_1(x)\|_{L_2[0,\ell]} \|\psi'_1(x)\|_{L_2[0,\ell]} \\
&\quad + \mu \langle |\phi'_1(\xi, \cdot)|, |\psi'_1(\cdot, x)| \rangle_{L_2[0,\ell] \times L_2[0,\ell]} \\
&\leq c_1 \|\phi'_1(x)\|_{L_2[0,\ell]} \|\psi'_1(x)\|_{L_2[0,\ell]} \\
&\quad + \mu \left| \langle |\phi'_1(\xi, \cdot)|, |\psi'_1(\cdot, x)| \rangle_{L_2[0,\ell] \times L_2[0,\ell]} \right| \\
&\leq c_1 \|\phi'_1(x)\|_{L_2[0,\ell]} \|\psi'_1(x)\|_{L_2[0,\ell]} \\
&\quad + \mu^* \|\phi'_1(\xi)\|_{L_2[0,\ell] \times L_2[0,\ell]} \|\psi'_1(x)\|_{L_2[0,\ell] \times L_2[0,\ell]}
\end{aligned}$$

(by Cauchy-Schwarz)

$$\begin{aligned}
&= c_1 \|\phi'_1(x)\|_{L_2[0,\ell]} \|\psi'_1(x)\|_{L_2[0,\ell]} \\
&\quad + \mu^* \left(\int_0^\ell \int_0^\ell (\phi'_1(\xi))^2 d\xi dx \right)^{\frac{1}{2}} \left(\int_0^\ell \int_0^\ell (\psi'_1(x))^2 d\xi dx \right)^{\frac{1}{2}}.
\end{aligned}$$

Note that the first integral only involves an integrand as a function of ξ and similarly the second integral an integrand as a function of x . Therefore, the second term gives us the multiplication of two $(\ell)^{\frac{1}{2}}$'s. Thus, we get that the above is

$$\begin{aligned}
&= c_1 \|\phi'_1(x)\|_{L_2[0,\ell]} \|\psi'_1(x)\|_{L_2[0,\ell]} \\
&\quad + \mu^*(\ell)^{\frac{1}{2}} \left(\int_0^\ell (\phi'_1(\xi))^2 d\xi \right)^{\frac{1}{2}} (\ell)^{\frac{1}{2}} \left(\int_0^\ell (\psi'_1(x))^2 dx \right)^{\frac{1}{2}} \\
&\leq c_1 \|\phi'_1\|_{L_2[0,\ell]} \|\psi'_1\|_{L_2[0,\ell]} \\
&\quad + c_2 \|\phi'_1\|_{L_2[0,\ell]} \|\psi'_1\|_{L_2[0,\ell]} \\
&= \epsilon \|\phi'_1\|_{L_2[0,\ell]} \|\psi'_1\|_{L_2[0,\ell]},
\end{aligned}$$

where $c_2 = (\mu^*)(\ell)$ and $\epsilon = c_1 + c_2$. Thus, by this argument and Lemma 5.5, the sesquilinear form $\tilde{\mathbf{d}}$ satisfies continuity condition **H4**.

To prove that the sesquilinear form is elliptic in V_2 we will make use of the highly non-trivial result in Appendix A; it states that the following inequality holds:

$$\int_{x_1}^{x_2} \int_{x_1}^{x_2} h(x, \xi) (\phi'(x) - \phi'(\xi)) d\xi \phi'(x) dx + \int_{x_1}^{x_2} (\phi(x))^2 dx \geq L \int_{x_1}^{x_2} (\phi'(x))^2 dx, \quad (5.46)$$

where L is some positive constant. This, when rewritten in terms of the $L_2[x_1, x_2]$ inner product, is just

$$\langle (\nu - \mathcal{G})\phi'(x), \phi'(x) \rangle_{L_2[x_1, x_2]} + \langle \phi(x), \phi(x) \rangle_{L_2[x_1, x_2]} \geq L \langle \phi'(x), \phi'(x) \rangle_{L_2[x_1, x_2]}. \quad (5.47)$$

Now let $\lambda = 0$ from **H5**. Then we have

$$\begin{aligned}
\operatorname{Re} \left(\tilde{\mathbf{d}}(\Phi, \Phi) \right) &= \tilde{\mathbf{d}}(\Phi, \Phi) \\
&= \langle \gamma \phi_1, \phi_1 \rangle_{L_2[0, \ell]} + \langle 0.5 \rho_a c v k_2 k_3 \phi_1, \phi_1 \rangle_{L_2[0, \ell]} \\
&\quad + \langle (\nu_L - \mathcal{G}_L) \phi'_1, \phi'_1 \rangle_{L_2[0, \ell]} + \langle \gamma \phi_2, \phi_2 \rangle_{L_2[\ell + \ell_M, \ell_M + 2\ell]} \\
&\quad + \langle 0.5 \rho_a c v k_2 k_3 \phi_2, \phi_2 \rangle_{L_2[\ell + \ell_M, \ell_M + 2\ell]} \\
&\quad + \langle (\nu_R - \mathcal{G}_R) \phi'_2, \phi'_2 \rangle_{L_2[\ell + \ell_M, \ell_M + 2\ell]} + \langle \mathcal{A}_1 \Phi, \Phi \rangle_S. \tag{5.48} \\
&\geq \langle \gamma \phi_1, \phi_1 \rangle_{L_2[0, \ell]} + \kappa \langle \phi_1, \phi_1 \rangle_{L_2[0, \ell]} \\
&\quad + \kappa \langle (\nu_L - \mathcal{G}_L) \phi'_1, \phi'_1 \rangle_{L_2[0, \ell]} \\
&\quad + \langle \gamma \phi_2, \phi_2 \rangle_{L_2[\ell + \ell_M, \ell_M + 2\ell]} + \kappa \langle \phi_2, \phi_2 \rangle_{L_2[\ell + \ell_M, \ell_M + 2\ell]} \\
&\quad + \kappa \langle (\nu_R - \mathcal{G}_R) \phi'_2, \phi'_2 \rangle_{L_2[\ell + \ell_M, \ell_M + 2\ell]} + \langle \mathcal{A}_1 \Phi, \Phi \rangle_S \\
&\quad \text{(for } \kappa := \min\{1, 0.5 \rho_a c v k_2 k_3\}), \\
&\geq \langle \gamma \phi_1, \phi_1 \rangle_{L_2[0, \ell]} + \kappa L_1 \langle \phi'_1, \phi'_1 \rangle_{L_2[0, \ell]} \\
&\quad + \langle \gamma \phi_2, \phi_2 \rangle_{L_2[\ell + \ell_M, \ell_M + 2\ell]} + \kappa L_2 \langle \phi'_2, \phi'_2 \rangle_{L_2[\ell + \ell_M, \ell_M + 2\ell]} \\
&\quad + \langle \mathcal{A}_1 \Phi, \Phi \rangle_S. \\
&\quad \text{(by (5.47)),}
\end{aligned}$$

$$\begin{aligned}
&\geq k \langle \phi_1, \phi_1 \rangle_{L_2[0,\ell]} + k \langle \phi'_1, \phi'_1 \rangle_{L_2[0,\ell]} + k \langle \phi_2, \phi_2 \rangle_{L_2[\ell+\ell_M, \ell_M+2\ell]} \\
&\quad + k \langle \phi'_2, \phi'_2 \rangle_{L_2[\ell+\ell_M, \ell_M+2\ell]} + k \langle \mathcal{A}_1 \Phi, \Phi \rangle_S \\
&= k \langle \Phi, \Phi \rangle_{V_2} = k \|\Phi\|_{V_2}^2,
\end{aligned}$$

for $k := \min\{\kappa L_1, \kappa L_2, \gamma, 1\}$. Thus, $\tilde{\mathbf{d}}$ satisfies coercivity/ellipticity condition **H5** with $\lambda = 0$ and $k_2 = k$. \square

By Theorem 2.12 the system in (5.40) is well-posed. By Theorem 2.13, the first order system operator, defined on $E = V \times S$,

$$\tilde{\mathcal{A}} = \hat{\mathcal{A}} + \begin{bmatrix} 0 & 0 \\ -\mathcal{I} & -\mathcal{I} \end{bmatrix} \quad (5.49)$$

generates a C_0 -semigroup of contractions. Furthermore, by Theorem 2.14, the operator $\hat{\mathcal{A}}$ generates a C_0 -semigroup. Now, by Theorem 2.15, we have that the first order weak formulation of the system with $\tilde{\mathcal{A}}$ is well-posed which implies that the equivalent second order weak formulation (5.37) is well-posed.

To show that the closed-loop feedback operators $\hat{\mathcal{A}} - \hat{\mathcal{B}}\mathcal{K}$ and $\hat{\mathcal{A}} - \mathcal{F}\hat{\mathcal{C}}$ generate exponentially stable semigroups, it suffices to show that \mathcal{Q} and Ω are coercive in E [12]. In our work, we choose the identity for both \mathcal{Q} and Ω . Thus, we have that both are coercive in E and the semigroups generated are exponentially stable. Furthermore, by Theorem 3.5, we have the semigroup, $S_{\infty\infty}$, produced by the state estimate operator in (3.13) is exponentially stable.

CHAPTER 6

VARIATIONAL FORM AND APPROXIMATION THEORY

6.1 Numerical Methods

We now use a Galerkin finite element approach to find numerical solutions to the BMB model with spatial hysteresis damping.

6.1.1 Weak Formulation

As is standard in Finite Element approaches we desire a solution $[w_L(t, x_L), w_R(t, x_R)]^T \in U \subseteq H = H^2[0, \ell] \times H^2[\ell + \ell_M, \ell_M + 2\ell]$. Here the Hilbert space H^2 is the Sobolev space $W^{2,2}$. We multiply (4.1) and (4.2) by test functions $\phi_L(x_L)$ and $\phi_R(x_R)$, respectively, and integrate to obtain

$$\begin{aligned} & \int_0^\ell \left[\rho A \ddot{w}_L(t, x_L) + \gamma \dot{w}_L(t, x_L) - \frac{\partial}{\partial x_L} \left[\int_0^\ell h(x_L, \xi) [\dot{w}'_L(t, x_L) - \dot{w}'_L(t, \xi)] d\xi \right] \right. \\ & \left. + EI w_L''''(t, x_L) \right] \phi_L(x_L) dx_L = \int_0^\ell [b(x_L) u_L(t) - 0.5 \rho_a v^2 c C_\ell] \phi_L(x_L) dx_L \end{aligned} \tag{6.1}$$

and

$$\begin{aligned}
& \int_{\ell+\ell_M}^{\ell_M+2\ell} \left[\rho A \ddot{w}_R(t, x_R) + \gamma \dot{w}_R(t, x_R) - \frac{\partial}{\partial x_R} \left[\int_{\ell+\ell_M}^{\ell_M+2\ell} h(x_R, \xi) [\dot{w}'_R(t, x_R) - \dot{w}'_R(t, \xi)] d\xi \right] \right. \\
& \left. + EI w_R'''(t, x_R) \phi_R(x_R) \right] dx_R = \int_{\ell+\ell_M}^{\ell_M+2\ell} [b(x_R) u_R(t) - 0.5 \rho_a v^2 c C_\ell] \phi_R(x_R) dx_R
\end{aligned} \tag{6.2}$$

for all $[\phi_L(x_L), \phi_R(x_R)]^T \in U = \{[\phi_L(\cdot), \phi_R(\cdot)]^T \in S : \phi_L(\ell) = \phi_R(\ell + \ell_M), \phi'_L(\ell) = 0, \phi'_R(\ell + \ell_M) = 0\}$. Integration by parts of (6.1) and (6.2) yields the following

$$\begin{aligned}
& \int_0^\ell \left[\rho A \ddot{w}_L(t, x_L) \phi_L(x_L) + \gamma \dot{w}_L(t, x_L) \phi_L(x_L) \right. \\
& \left. + \left[\int_0^\ell h(x_L, \xi) [\dot{w}'_L(t, x_L) - \dot{w}'_L(t, \xi)] d\xi \right] \phi'_L(x_L) + EI w_L''(t, x_L) \phi_L''(x_L) \right] dx_L \\
& - \left[\int_0^\ell h(x_L, \xi) [\dot{w}'_L(t, x_L) - \dot{w}'_L(t, \xi)] d\xi \right]_{x_L=\ell} \phi_L(\ell) \\
& + \left[\int_0^\ell h(x_L, \xi) [\dot{w}'_L(t, x_L) - \dot{w}'_L(t, \xi)] d\xi \right]_{x_L=0} \phi_L(0) \\
& + EI w_L'''(t, \ell) \phi_L(\ell) - EI w_L'''(t, 0) \phi_L(0) - EI w_L''(t, \ell) \phi'_L(\ell) + EI w_L''(t, 0) \phi'_L(0) \\
& = \int_0^\ell [b(x_L) u_L(t) - 0.5 \rho_a v^2 c C_\ell] \phi_L(x_L) dx_L
\end{aligned} \tag{6.3}$$

and

$$\begin{aligned}
& \int_{\ell+\ell_M}^{\ell_M+2\ell} \left[\rho A \ddot{w}_R(t, x_R) \phi_R(x_R) + \gamma \dot{w}_R(t, x_R) \phi_R(x_R) \right. \\
& + \left. \left[\int_{\ell+\ell_M}^{\ell_M+2\ell} h(x_R, \xi) [\dot{w}'_R(t, x_R) - \dot{w}'_R(t, \xi)] d\xi \right] \phi'_R(x_R) + EI w''_R(t, x_R) \phi''_R(x_R) \right] dx_R \\
& - \left[\int_{\ell+\ell_M}^{\ell_M+2\ell} h(x_R, \xi) [\dot{w}'_R(t, x_R) - \dot{w}'_R(t, \xi)] d\xi \right]_{x_R=\ell_M+2\ell} \phi_R(\ell_M+2\ell) \\
& + \left[\int_{\ell+\ell_M}^{\ell_M+2\ell} h(x_R, \xi) [\dot{w}'_R(t, x_R) - \dot{w}'_R(t, \xi)] d\xi \right]_{x_R=\ell+\ell_M} \phi_R(\ell+\ell_M) \\
& + EI w'''_R(t, \ell_M+2\ell) \phi_R(\ell_M+2\ell) - EI w'''_R(t, \ell+\ell_M) \phi_R(\ell+\ell_M) \\
& - EI w''_R(t, \ell_M+2\ell) \phi'_R(\ell_M+2\ell) + EI w''_R(t, \ell+\ell_M) \phi'_R(\ell+\ell_M) \\
& = \int_{\ell+\ell_M}^{\ell_M+2\ell} [b(x_R) u_R(t) - 0.5 \rho_a v^2 c C_\ell] \phi_R(x_R) dx_R
\end{aligned} \tag{6.4}$$

Adding (6.3) and (6.4) gives

$$\begin{aligned}
& \int_0^\ell \left[\rho A \ddot{w}_L(t, x_L) \phi_L(x_L) + \gamma \dot{w}_L(t, x_L) \phi_L(x_L) \right. \\
& + \left. \left[\int_0^\ell h(x_L, \xi) [\dot{w}'_L(t, x_L) - \dot{w}'_L(t, \xi)] d\xi \right] \phi'_L(x_L) + EI w''_L(t, x_L) \phi''_L(x_L) \right] dx_L \\
& - \left[\int_0^\ell h(x_L, \xi) [\dot{w}'_L(t, x_L) - \dot{w}'_L(t, \xi)] d\xi \right]_{x_L=\ell} \phi_L(\ell) \\
& + \left[\int_0^\ell h(x_L, \xi) [\dot{w}'_L(t, x_L) - \dot{w}'_L(t, \xi)] d\xi \right]_{x_L=0} \phi_L(0) + EI w'''_L(t, \ell) \phi_L(\ell) \\
& - EI w'''_L(t, 0) \phi_L(0) - EI w''_L(t, \ell) \phi'_L(\ell) + EI w''_L(t, 0) \phi'_L(0)
\end{aligned} \tag{6.5}$$

$$\begin{aligned}
& + \int_{\ell+\ell_M}^{\ell_M+2\ell} \left[\rho A \ddot{w}_R(t, x_R) \phi_R(x_R) + \gamma \dot{w}_R(t, x_R) \phi_R(x_R) \right. \\
& + \left. \left[\int_{\ell+\ell_M}^{\ell_M+2\ell} h(x_R, \xi) [\dot{w}'_R(t, x_R) - \dot{w}'_R(t, \xi)] d\xi \right] \phi'_R(x_R) + EI w''_R(t, x_R) \phi''_R(x_R) \right] dx_R \\
& - \left[\int_{\ell+\ell_M}^{\ell_M+2\ell} h(x_R, \xi) [\dot{w}'_R(t, x_R) - \dot{w}'_R(t, \xi)] d\xi \right]_{x_R=\ell_M+2\ell} \phi_R(\ell_M + 2\ell) \\
& + \left[\int_{\ell+\ell_M}^{\ell_M+2\ell} h(x_R, \xi) [\dot{w}'_R(t, x_R) - \dot{w}'_R(t, \xi)] d\xi \right]_{x_R=\ell+\ell_M} \phi_R(\ell + \ell_M) \\
& + EI w'''_R(t, \ell_M + 2\ell) \phi_R(\ell_M + 2\ell) - EI w'''_R(t, \ell + \ell_M) \phi_R(\ell + \ell_M) \\
& - EI w''_R(t, \ell_M + 2\ell) \phi'_R(\ell_M + 2\ell) + EI w''_R(t, \ell + \ell_M) \phi'_R(\ell + \ell_M) \\
& = \int_0^\ell [b(x_L) u_L(t) - 0.5 \rho_a v^2 c C_\ell] \phi_L(x_L) dx_L \\
& + \int_{\ell+\ell_M}^{\ell_M+2\ell} [b(x_R) u_R(t) - 0.5 \rho_a v^2 c C_\ell] \phi_R(x_R) dx_R.
\end{aligned}$$

An application of the boundary conditions in Table 4.1 leaves only

$$\begin{aligned}
& \int_0^\ell \left[\rho A \ddot{w}_L(t, x_L) \phi_L(x_L) + \gamma \dot{w}_L(t, x_L) \phi_L(x_L) \right. \\
& + \left. \left[\int_0^\ell h(x_L, \xi) [\dot{w}'_L(t, x_L) - \dot{w}'_L(t, \xi)] d\xi \right] \phi'_L(x_L) + EI w''_L(t, x_L) \phi''_L(x_L) \right] dx_L \\
& + \int_{\ell+\ell_M}^{\ell_M+2\ell} \left[\rho A \ddot{w}_R(t, x_R) \phi_R(x_R) + \gamma \dot{w}_R(t, x_R) \phi_R(x_R) \right. \\
& + \left. \left[\int_{\ell+\ell_M}^{\ell_M+2\ell} h(x_R, \xi) [\dot{w}'_R(t, x_R) - \dot{w}'_R(t, \xi)] d\xi \right] \phi'_R(x_R) + EI w''_R(t, x_R) \phi''_R(x_R) \right] dx_R
\end{aligned} \tag{6.6}$$

$$\begin{aligned}
+m\ddot{w}_L(t, \ell) \phi_L(\ell) &= \int_0^\ell [b(x_L) u_L(t) - 0.5\rho_a v^2 c C_\ell] \phi_L(x_L) dx_L \\
+ \int_{\ell+\ell_M}^{\ell_M+2\ell} [b(x_R) u_R(t) - 0.5\rho_a v^2 c C_\ell] \phi_R(x_R) dx_R.
\end{aligned}$$

6.1.2 Discretization

We choose a basis $\{e_j\}_{j=1}^N$ of the approximating space $U^N \subset U$. Here N will represent the total number of basis functions used. We will approximate the displacements of the left and right beams with cubic Hermite interpolating polynomials.

Then the basis functions take the form:

$$e_j^N = \begin{bmatrix} b_{L,j}^N \\ b_{R,j}^N \end{bmatrix} \text{ for } j = 1, \dots, N. \quad (6.7)$$

The displacements of the left and right beams will be approximated, respectively, using the following:

$$\begin{bmatrix} w_L(t, x_L) \\ w_R(t, x_R) \end{bmatrix} \approx \begin{bmatrix} w_L^N(t, x_L) \\ w_R^N(t, x_R) \end{bmatrix} = \begin{bmatrix} \sum_{i=1}^N \alpha_i^N(t) b_{L,i}(x_L) \\ \sum_{i=1}^N \beta_i^N(t) b_{R,i}(x_R) \end{bmatrix}. \quad (6.8)$$

If we substitute this approximation into (6.6) we have

$$\begin{aligned}
& \int_0^\ell \left[\rho A \ddot{w}_L^N(t, x_L) \phi_L(x_L) + \gamma \dot{w}_L^N(t, x_L) \phi_L(x_L) \right. \\
& + \left. \left[\int_0^\ell h(x_L, \xi) \left[(\dot{w}_L^N)'(t, x_L) - (\dot{w}_L^N)'(t, \xi) \right] d\xi \right] \phi_L'(x_L) + EI (w_L^N)''(t, x_L) \phi_L''(x_L) \right] dx_L \\
& + \int_{\ell+\ell_M}^{\ell_M+2\ell} \left[\rho A \ddot{w}_R^N(t, x_R) \phi_R(x_R) + \gamma \dot{w}_R^N(t, x_R) \phi_R(x_R) \right. \\
& + \left. \left[\int_{\ell+\ell_M}^{\ell_M+2\ell} h(x_R, \xi) \left[(\dot{w}_R^N)'(t, x_R) - (\dot{w}_R^N)'(t, \xi) \right] d\xi \right] \phi_R'(x_R) + EI (w_R^N)''(t, x_R) \phi_R''(x_R) \right] dx_R \\
& + m \ddot{w}_L^N(t, \ell) \phi_L(\ell) = \int_0^\ell [b(x_L) u_L(t) - 0.5 \rho_a v^2 c C_\ell] \phi_L(x_L) dx_L \\
& + \int_{\ell+\ell_M}^{\ell_M+2\ell} [b(x_R) u_R(t) - 0.5 \rho_a v^2 c C_\ell] \phi_R(x_R) dx_R.
\end{aligned} \tag{6.9}$$

The last equality in (6.8) gives

$$\begin{aligned}
& \int_0^\ell \left[\rho A \sum_{i=1}^N \ddot{\alpha}_i^N(t) b_{L,i}(x_L) \phi_L(x_L) + \gamma \sum_{i=1}^N \dot{\alpha}_i^N(t) b_{L,i}(x_L) \phi_L(x_L) \right. \\
& + \left. \left(\int_0^\ell h(x_L, \xi) \left[\sum_{i=1}^N \dot{\alpha}_i^N(t) b'_{L,j}(x_L) - \sum_{i=1}^N \dot{\alpha}_i^N(t) b'_{L,i}(\xi) \right] d\xi \right) \phi_L'(x_L) \right. \\
& + \left. EI \sum_{i=1}^N \alpha_i^N(t) b''_{L,i}(x_L) \phi_L''(x_L) \right] dx_L \\
& + \int_{\ell+\ell_M}^{\ell_M+2\ell} \left[\rho A \sum_{i=1}^N \ddot{\beta}_i^N(t) b_{R,i}(x_R) \phi_R(x_R) + \gamma \sum_{i=1}^N \dot{\beta}_i^N(t) b_{R,i}(x_R) \phi_R(x_R) \right. \\
& + \left. \left(\int_{\ell+\ell_M}^{\ell_M+2\ell} h(x_R, \xi) \left[\sum_{i=1}^N \dot{\beta}_i^N(t) b'_{R,i}(x_R) - \sum_{i=1}^N \dot{\beta}_i^N(t) b'_{R,i}(\xi) \right] d\xi \right) \phi_R'(x_R) \right] dx_R
\end{aligned} \tag{6.10}$$

$$\begin{aligned}
& +EI \sum_{i=1}^N \beta_i^N(t) b_{R,i}''(x_R) \phi_R''(x_R) \Big] dx_R + m \sum_{i=1}^N \ddot{\alpha}_i^N(t) b_{L,i}(\ell) \phi_L(\ell) \\
& = \int_0^\ell [b(x_L) u_L(t) - 0.5\rho_a v^2 c C_\ell] \phi_L(x_L) dx_L \\
& + \int_{\ell+\ell_M}^{\ell_M+2\ell} [b(x_R) u_R(t) - 0.5\rho_a v^2 c C_\ell] \phi_R(x_R) dx_R.
\end{aligned}$$

Now the test functions will also span the appropriate basis functions to obtain,

$$\begin{aligned}
& \int_0^\ell \left[\rho A \sum_{i,j=1}^N \ddot{\alpha}_i^N(t) b_{L,i}(x_L) b_{L,j}(x_L) + \gamma \sum_{i,j=1}^N \dot{\alpha}_i^N(t) b_{L,i}(x_L) b_{L,j}(x_L) \right. \\
& + \sum_{i,j=1}^N \dot{\alpha}_i^N(t) \left(\int_0^\ell h(x_L, \xi) [b'_{L,i}(x_L) - b'_{L,i}(\xi)] d\xi \right) b'_{L,j}(x_L) \\
& \left. + EI \sum_{i,j=1}^N \alpha_i^N(t) b_{L,i}''(x_L) b_{L,j}''(x_L) \right] dx_L \\
& + \int_{\ell+\ell_M}^{\ell_M+2\ell} \left[\rho A \sum_{i,j=1}^N \ddot{\beta}_i^N(t) b_{R,i}(x_R) b_{R,j}(x_R) + \gamma \sum_{i,j=1}^N \dot{\beta}_i^N(t) b_{R,i}(x_R) b_{R,j}(x_R) \right. \\
& \left. + \sum_{i,j=1}^N \dot{\beta}_i^N(t) \left(\int_{\ell+\ell_M}^{\ell_M+2\ell} h(x_R, \xi) [b'_{R,i}(x_R) - b'_{R,i}(\xi)] d\xi \right) b'_{R,j}(x_R) \right. \\
& \left. + EI \sum_{i,j=1}^N \beta_i^N(t) b_{R,i}''(x_R) b_{R,j}''(x_R) \right] dx_R + m \sum_{i,j=1}^N \ddot{\alpha}_i^N(t) b_{L,i}(\ell) b_{L,j}(\ell) \\
& = \int_0^\ell [b(x_L) u_L(t) - 0.5\rho_a v^2 c C_\ell] b_{L,j}(x_L) dx_L \\
& + \int_{\ell+\ell_M}^{\ell_M+2\ell} [b(x_R) u_R(t) - 0.5\rho_a v^2 c C_\ell] b_{R,j}(x_R) dx_R,
\end{aligned} \tag{6.11}$$

which we can rewrite in the following way

$$\begin{aligned}
& \int_0^\ell \rho A b_{L,i}(x_L) b_{L,j}(x_L) dx_L \sum_{i,j=1}^N \ddot{\alpha}_i^N(t) \\
& + \int_0^\ell \gamma b_{L,i}(x_L) b_{L,j}(x_L) dx_L \sum_{i,j=1}^N \dot{\alpha}_i^N(t) \\
& + \int_0^\ell \left(\int_0^\ell h(x_L, \xi) [b'_{L,i}(x_L) - b'_{L,i}(\xi)] d\xi \right) b'_{L,j}(x_L) dx_L \sum_{i,j=1}^N \dot{\alpha}_i^N(t) \\
& + \int_0^\ell EI b''_{L,i}(x_L) b''_{L,j}(x_L) dx_L \sum_{i,j=1}^N \alpha_i^N(t) \\
& + \int_{\ell+\ell_M}^{\ell_M+2\ell} \rho A b_{R,i}(x_R) b_{R,j}(x_R) dx_R \sum_{i,j=1}^N \ddot{\beta}_i^N(t) \\
& + \int_{\ell+\ell_M}^{\ell_M+2\ell} \gamma b_{R,i}(x_R) b_{R,j}(x_R) dx_R \sum_{i,j=1}^N \dot{\beta}_i^N(t) \\
& + \int_{\ell+\ell_M}^{\ell_M+2\ell} \left(\int_{\ell+\ell_M}^{\ell_M+2\ell} h(x_R, \xi) [b'_{R,i}(x_R) - (t)b'_{R,i}(\xi)] d\xi \right) b'_{R,j}(x_R) dx_R \sum_{i,j=1}^N \dot{\beta}_i^N(t) \\
& + \int_{\ell+\ell_M}^{\ell_M+2\ell} EI b''_{R,i}(x_R) b''_{R,j}(x_R) dx_R \sum_{i,j=1}^N \beta_i^N(t) + m b_{L,i}(\ell) b_{L,j}(\ell) \sum_{i,j=1}^N \ddot{\alpha}_i^N(t) \\
& = \int_0^\ell [b(x_L) u_L(t) - 0.5 \rho_a v^2 c C_\ell] b_{L,j}(x_L) dx_L \\
& + \int_{\ell+\ell_M}^{\ell_M+2\ell} [b(x_R) u_R(t) - 0.5 \rho_a v^2 c C_\ell] b_{R,j}(x_R) dx_R.
\end{aligned} \tag{6.12}$$

In the matrix representation we can rewrite (6.12) as

$$\begin{aligned}
 & M_L \ddot{\alpha}(t) + M_R \ddot{\beta}(t) + D_L \dot{\alpha}(t) + D_R \dot{\beta}(t) + K_L \alpha(t) + K_R \beta(t) \\
 & = B_L u_L(t) + B_R u_R(t) + F_L + F_R,
 \end{aligned} \tag{6.13}$$

where

$$\begin{aligned}
 [M_L]_{i,j} &= \int_0^\ell \rho A b_{L,i}(x_L) b_{L,j}(x_L) dx_L + m b_{L,i}(\ell_1) b_{L,j}(\ell_1) \\
 [M_R]_{i,j} &= \int_{\ell+\ell_M}^{\ell_M+2\ell} \rho A b_{R,i}(x_R) b_{R,j}(x_R) dx_R \\
 [D_L]_{i,j} &= \int_0^\ell \gamma b_{L,i}(x_L) b_{L,j}(x_L) dx_L \\
 &+ \int_0^\ell \left(\int_0^\ell h(x_L, \xi) [b'_{L,i}(x_L) - b'_{L,i}(\xi)] d\xi \right) b'_{L,j}(x_L) dx_L \\
 [D_R]_{i,j} &= \int_{\ell+\ell_M}^{\ell_M+2\ell} \gamma b_{R,i}(x_R) b_{R,j}(x_R) dx_R \\
 &+ \int_{\ell+\ell_M}^{\ell_M+2\ell} \left(\int_{\ell+\ell_M}^{\ell_M+2\ell} h(x_R, \xi) [b'_{R,i}(x_R) - b'_{R,i}(\xi)] d\xi \right) b'_{R,j}(x_R) dx_R \\
 [K_L]_{i,j} &= \int_0^\ell EI b''_{L,i}(x_L) b''_{L,j}(x_L) dx_L \\
 [K_R]_{i,j} &= \int_{\ell+\ell_M}^{\ell_M+2\ell} EI b''_{R,i}(x_R) b''_{R,j}(x_R) dx_R
 \end{aligned} \tag{6.14}$$

$$\begin{aligned}
[B_L]_j &= \int_0^\ell b(x_L) u_L(t) b_{L,j}(x_L) dx_L \\
[B_R]_j &= \int_{\ell+\ell_M}^{\ell_M+2\ell} b(x_R) u_R(t) b_{R,j}(x_R) dx_L \\
[F_L]_j &= \int_0^\ell -0.5\rho_a v^2 c C_\ell b_{L,j}(x_L) dx_L \\
[F_R]_j &= \int_{\ell+\ell_M}^{\ell_M+2\ell} -0.5\rho_a v^2 c C_\ell b_{R,j}(x_R) dx_R.
\end{aligned}$$

We can rewrite (6.13) as the following:

$$\ddot{c}(t) = M^{-1} (-D\dot{c}(t) - Kc(t) + \bar{B} + \bar{F}), \quad (6.15)$$

where

$$c(t) = \begin{bmatrix} \alpha(t) \\ \beta(t) \end{bmatrix} \Rightarrow \dot{c}(t) = \begin{bmatrix} \dot{\alpha}(t) \\ \dot{\beta}(t) \end{bmatrix} \Rightarrow \ddot{c}(t) = \begin{bmatrix} \ddot{\alpha}(t) \\ \ddot{\beta}(t) \end{bmatrix}. \quad (6.16)$$

Also,

$$M = \begin{bmatrix} M_L & 0 \\ 0 & M_R \end{bmatrix}, \quad D = \begin{bmatrix} D_L & 0 \\ 0 & D_R \end{bmatrix}, \quad K = \begin{bmatrix} K_L & 0 \\ 0 & K_R \end{bmatrix}, \quad (6.17)$$

$$\bar{B} = \begin{bmatrix} B_L \\ B_R \end{bmatrix}, \quad \bar{F} = \begin{bmatrix} F_L \\ F_R \end{bmatrix}.$$

We can now rewrite (6.15) as a first order system of ordinary differential equations

$$\dot{x}(t) = Ax(t) + Bu(t) + F(x(t)), \quad (6.18)$$

where

$$x(t) = \begin{bmatrix} c(t) \\ \dot{c}(t) \end{bmatrix}, \quad A = \begin{bmatrix} 0 & I \\ -M^{-1}K & -M^{-1}D \end{bmatrix} \quad (6.19)$$

$$B = \begin{bmatrix} 0 \\ M^{-1}\bar{B} \end{bmatrix}, \quad F = \begin{bmatrix} 0 \\ M^{-1}\bar{F}(x(t)) \end{bmatrix}.$$

6.2 Approximating Riccati Solutions

In this section we will describe the routines and theory for calculating solutions for the finite dimensional approximations to the Riccati equations (3.10) and (3.14). The results here follow from the work done in [12]. The spaces S , V , and $E = V \times S$ will be defined as in Chapter 5, as well as their corresponding inner products. Furthermore, let \mathcal{A}_1 , \mathcal{Q} , and \mathcal{M} be as defined in Chapter 5.

6.2.1 Optimal Control Approximations

To calculate the solutions to the appropriate Riccati equations for a system with a mode problem, we calculate

$$\tilde{K} = K + [\langle \mathcal{A}_1 e_i, e_j \rangle_S] = K + M, \quad (6.20)$$

since $\mathcal{A}_1 = \mathcal{I}$. The Grammian matrix then is defined as

$$W = \begin{bmatrix} \tilde{K} & 0 \\ 0 & M \end{bmatrix}. \quad (6.21)$$

Now, since $Q \in \mathcal{L}(E)$, we can write Q as

$$Q = \begin{bmatrix} Q_0 & Q_1 \\ Q_1^* & Q_2 \end{bmatrix}, \quad (6.22)$$

where $Q_0 \in \mathcal{L}(V)$, $Q_1 \in \mathcal{L}(H, V)$, and $Q_2 \in \mathcal{L}(H)$. Now let Q be the approximation of Q matrix, which is substituted into the finite dimensional Control Algebraic Riccati Equation as

$$A^T \Pi^N + \Pi^N A - \Pi^N B R^{-1} B^T \Pi^N + Q = 0. \quad (6.23)$$

Then, defining a matrix \tilde{Q} as

$$\tilde{Q} = \begin{bmatrix} \tilde{Q}_0 & \tilde{Q}_1 \\ \tilde{Q}_1^T & \tilde{Q}_2 \end{bmatrix}, \quad (6.24)$$

direct computation shows that $Q = W^{-1} \tilde{Q}$. Here, we have

$$\tilde{Q}_0 = [\langle e_i, Q_0 e_j \rangle_V], \quad \tilde{Q}_1 = [\langle e_i, Q_1 e_j \rangle_V], \quad \tilde{Q}_2 = [\langle e_i, Q_2 e_j \rangle_S]. \quad (6.25)$$

Since $Q = \mathcal{I}$, we have that $\tilde{Q} = W$. Then (6.23) is equivalent to the following Riccati equation:

$$W^{-1}A^TW\Pi^N + \Pi^NA - \Pi^NBR^{-1}B^TW\Pi^N + Q = 0. \quad (6.26)$$

If we premultiply (6.26) by W , we have

$$A^T\tilde{\Pi}^N + \tilde{\Pi}^NA - \tilde{\Pi}^NBR^{-1}B^T\tilde{\Pi}^N + \tilde{Q} = 0, \quad (6.27)$$

which is the matrix Riccati equation used in implementation. Here $\tilde{\Pi}^N = W\Pi^N$.

Furthermore, the gain matrix $K_g = -R^{-1}B^T\tilde{\Pi}^N$.

6.2.2 Observer Solutions Approximations

To calculate the solutions to the finite dimensional approximation to the Filter Algebraic Riccati Equation, we start with

$$AP + PA^T - PC^TR^{-1}CP + \Omega^N = 0. \quad (6.28)$$

Similar to the approach in the previous section, Ω has a representation as in (6.22).

Then we have the following

$$\tilde{P} = PW^{-1} \quad (6.29)$$

and

$$\tilde{\Omega}^N = \Omega^NW^{-1}. \quad (6.30)$$

Then the approximating Filter Algebraic Riccati Equation to be solved is

$$A\tilde{P} + \tilde{P}A^T - \tilde{P}C^T R^{-1} C\tilde{P} + \tilde{\Omega}^N = 0. \quad (6.31)$$

The observer gain is then given by

$$F = \tilde{P}C^T R^{-1}. \quad (6.32)$$

We note here that if $\Omega = \mathcal{I}$ then $\tilde{\Omega}^N = W^{-1}$. The Riccati equation solutions presented here are used for the development of all three control designs in Chapter 7.

CHAPTER 7

NUMERICAL RESULTS

7.1 Numerical Results

Here we present the numerical simulations for the BMB system with spatial hysteresis damping. The parameters used for the simulations are presented in Table 7.1. The values for the modulus of the material and the external damping coefficient were estimated in [2] for spatial hysteresis damping. Banks and Inman note that the external or viscous damping coefficient cannot be determined independently of the internal damping features.

Table 7.1: System Parameter Values

Parameter	Value	Units
ℓ	0.3048	m
ℓ_M	0.0508	m
ρ	1710	kg/m ³
\hat{w} , width	0.127	m
h , height	0.0254	m
$a = \hat{w}h$	0.0032	m ²
E	2.68×10^{10}	N/m ²
$I = (\hat{w}h^3)/12$	1.734×10^{-7}	m ⁴
m	1.927	kg
m_b	3.363	kg
γ	0.090189	kg/(m sec)

The uncontrolled system will be presented first and will require a little discussion before the controlled results are presented. For the controlled results we are assuming that the controllers are able to act over the entire beam.

7.1.1 Uncontrolled Simulation

Incorporating spatial hysteresis damping led to some unexpected convergence issues. Because of the nature of the damping we were not able to see convergence in uncontrolled simulations with a low number of elements. We believe this is due to the fact that spatial hysteresis damping fundamentally relies on the surrounding beam elements to interact with a given beam element to produce internal damping effects. The fewer elements we use, the less internal friction, and thus internal damping, the system experiences. However, due the Gaussian nature of the kernel function, we expect to see the convergence appear with a higher number of elements. As the number of elements per beam increases we do, in fact, see the system deviate less from the previous simulation with fewer elements (See Figure 7.1). To try to eliminate the possibility of a coding error, we ran the same code with a constant kernel function. In [20] it is proven that a constant kernel function will produce the effects of Kelvin Voigt damping. Thus, we ran the code with $h(x, \xi) = 100$ (the Kelvin Voigt damping constant used in [7],[8], and [14]), and the results were consistent with previous simulations using explicit Kelvin Voigt damping. The results for Kelvin Voigt kernel simulations can be seen in Appendix B. We were unable to run simulations with higher numbers of elements due to time constraints on the Louisiana Optical Network Initiative (LONI supercomputer). The simulations we did run were with 3

elements per beam (6 elements total), 6 elements per beam (12 elements total), 10 elements per beam (20 elements total), and 15 elements per beam (30 elements total). The uncontrolled position, slope, velocity, and angular velocity plots can be seen in Figure 7.1, Figure 7.2, Figure 7.3, and Figure 7.4, respectively.

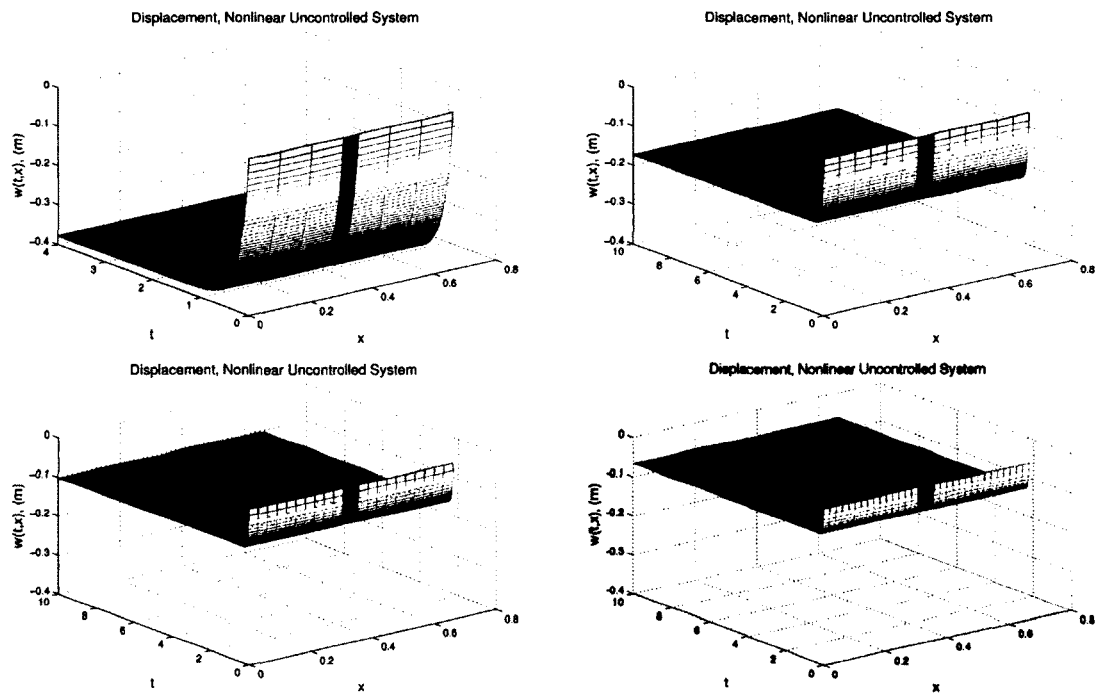


Figure 7.1: Uncontrolled Position: 6 Elements (Top Left), 12 Elements (Top Right), 20 Elements (Bottom Left), 30 Elements (Bottom Right)

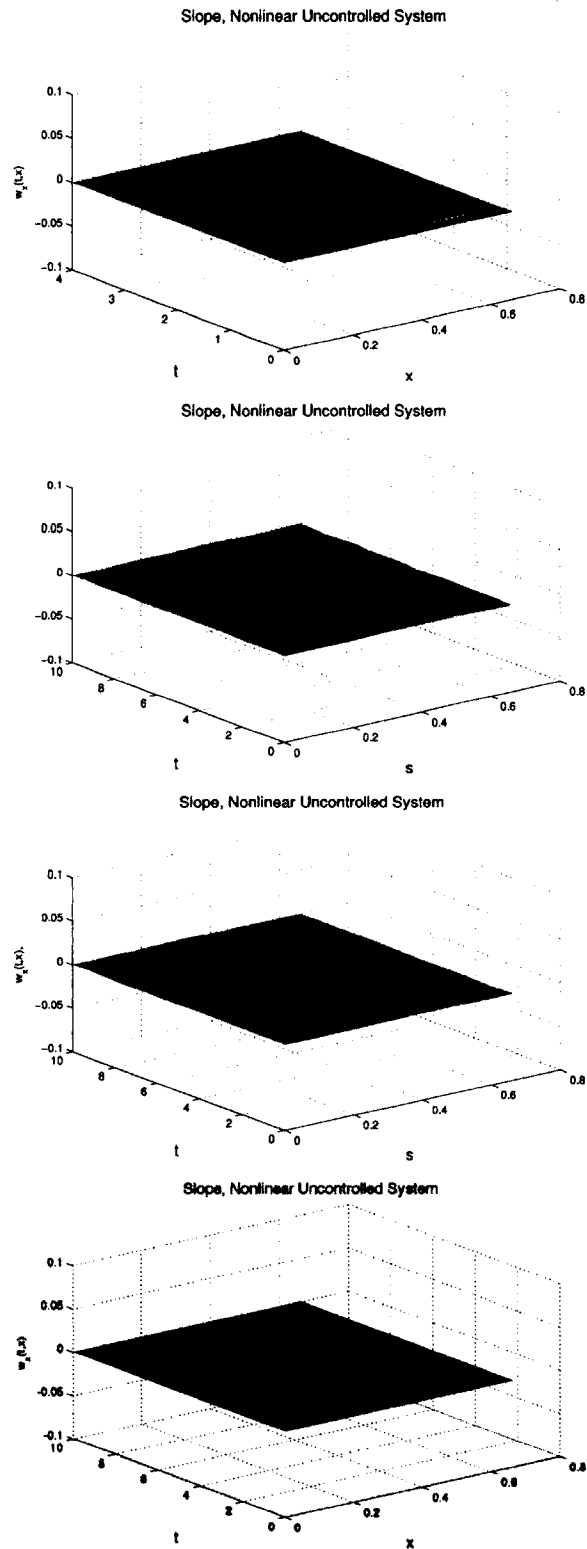


Figure 7.2: Uncontrolled Slope: 6 Elements (First), 12 Elements (Second), 20 Elements (Third), 30 Elements (Fourth)

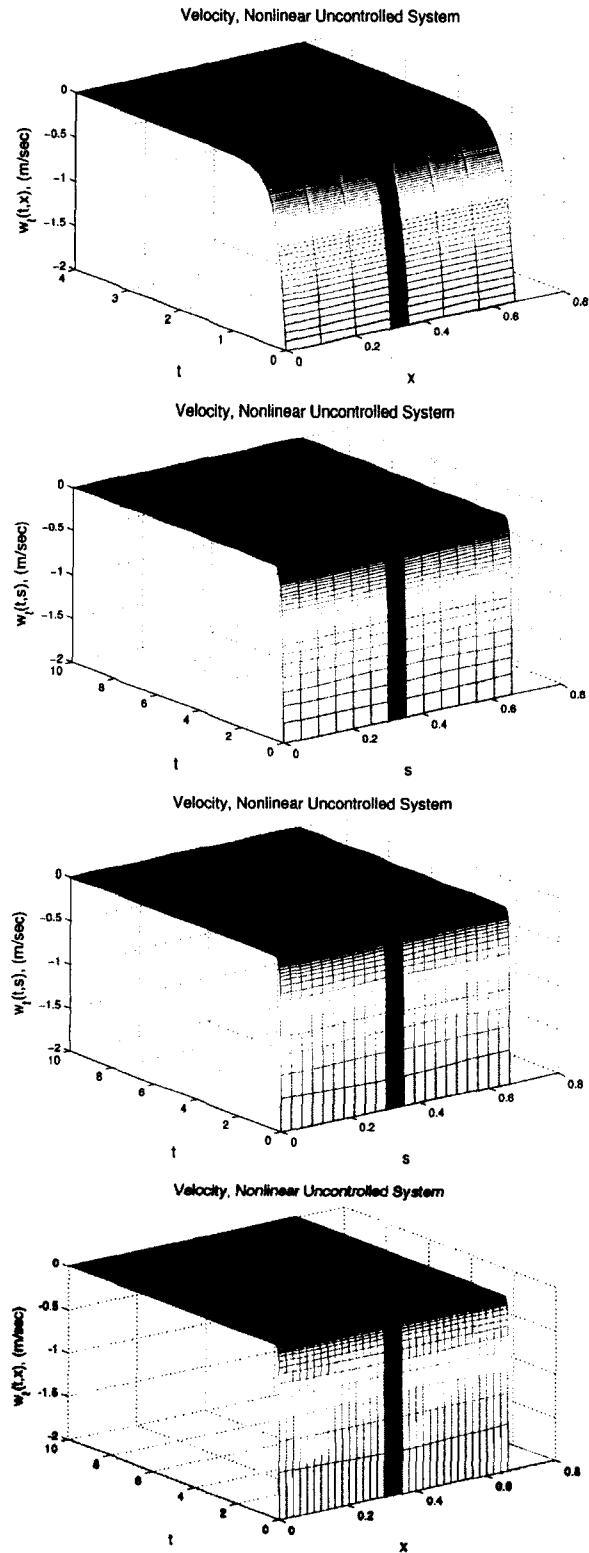


Figure 7.3: Uncontrolled Velocity: 6 Elements (First), 12 Elements (Second), 20 Elements (Third), 30 Elements (Fourth)

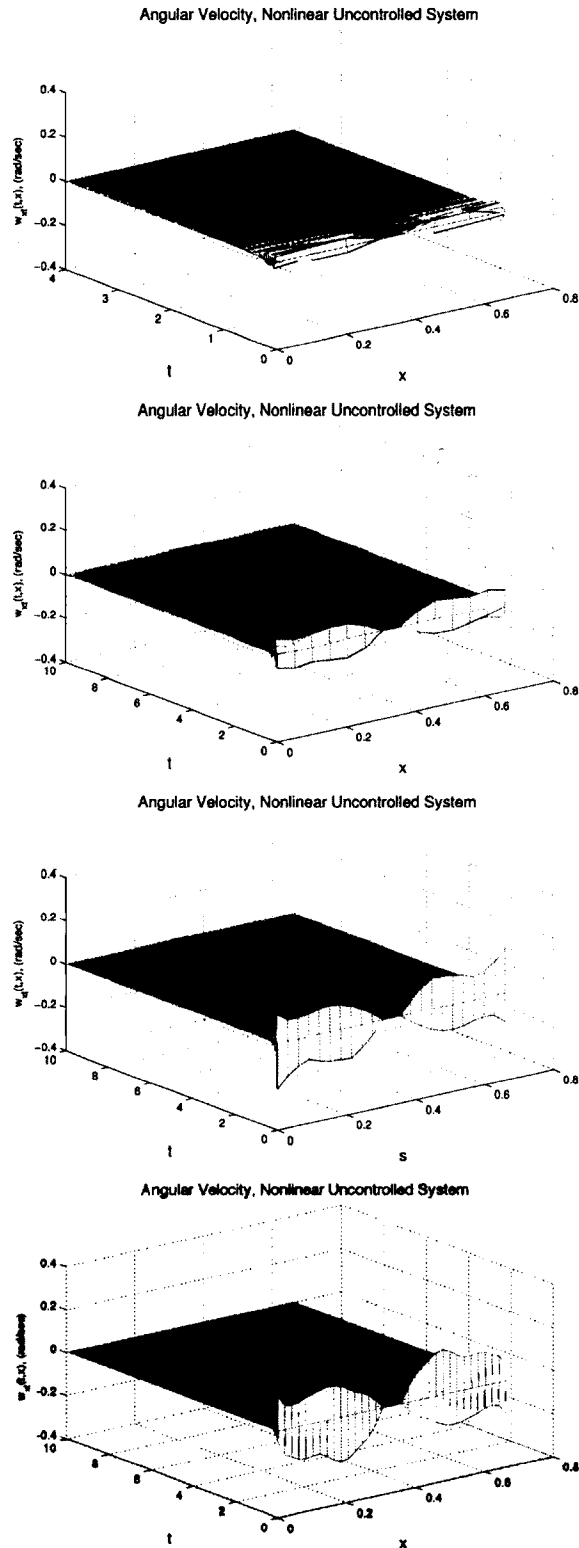


Figure 7.4: Uncontrolled Angular Velocity: 6 Elements (First), 12 Elements (Second), 20 Elements (Third), 30 Elements (Fourth)

It is important to note here that the magnitude of the slope and angular velocity states is very minor; although, we also note here that both slope and angular velocity state grows slightly with the number of elements used. This will be important in interpreting the data from the controlled simulations.

7.1.2 Target Tracking Results

In this section the goal of our controllers is to track the BMB system to a certain shape. For the LQR, LQG, and Central Controllers we assume input functions of the form

$$b_L(x_L) = b_R(x_R) = 56, \quad (7.1)$$

for $0 \leq x_L \leq \ell$ and $\ell + \ell_M \leq x_R \leq \ell_M + 2\ell$. We also assume state estimates of the form

$$y_L = 28w_L(t, x_L), \quad y_R = 28w_R(t, x_R) \quad (7.2)$$

for $0 \leq x_L \leq \ell$ and $\ell + \ell_M \leq x_R \leq \ell_M + 2\ell$. The desired target tracking position and slope are given by

$$w(t, x) = \frac{5x(x - 2\ell)(x - \ell)^2}{2w_{peak}} \quad (7.3)$$

and

$$w'(t, x) = \frac{5x(x - \ell)(8x^2 - 8x\ell + \ell^2)^2}{4w_{peak}} \quad (7.4)$$

respectively. Here $0 \leq x \leq 2\ell$ and $w_{peak} = 0.0762$ m. Figure 7.5 shows the shape of these targets.

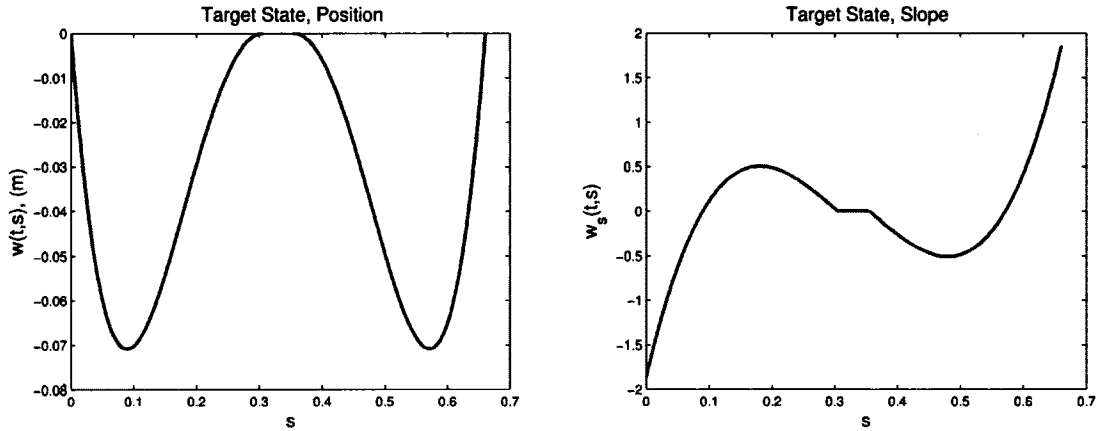


Figure 7.5: Target Tracking Goal: (Left) Position, (Right) Slope.

We assume a linear approximation of the aerodynamic lift term which aids in development of control design. Assuming a linearized lift coefficient we then obtain the following, modified, first order linear system:

$$\dot{x}(t) = \tilde{A}x(t) + Bu(t) \quad (7.5)$$

where

$$\tilde{A} = \begin{bmatrix} 0 & I \\ -M^{-1}K & -M^{-1}\tilde{D} \end{bmatrix} \quad (7.6)$$

and

$$\tilde{D} = \begin{bmatrix} \tilde{D}_L & 0 \\ 0 & \tilde{D}_R \end{bmatrix} \quad (7.7)$$

such that

$$\begin{aligned}
\left[\tilde{D}_L\right]_{i,j} &= \int_0^\ell \gamma b_{L,i}(x_L) b_{L,j}(x_L) dx_L \\
&+ \int_0^\ell \left(\int_0^\ell h(x_L, \xi) [b'_{L,i}(x_L) - b'_{L,i}(\xi)] d\xi \right) b'_{L,j}(x_L) dx_L \\
&+ \int_0^\ell \Xi b_{L,i}(x_L) b_{L,j}(x_L) dx_L \\
\left[\tilde{D}_R\right]_{i,j} &= \int_{\ell+\ell_M}^{\ell_M+2\ell} \gamma b_{R,i}(x_R) b_{R,j}(x_R) dx_R \\
&+ \int_{\ell+\ell_M}^{\ell_M+2\ell} \left(\int_{\ell+\ell_M}^{\ell_M+2\ell} h(x_R, \xi) [b'_{R,i}(x_R) - b'_{R,i}(\xi)] d\xi \right) b'_{R,j}(x_R) dx_R \\
&+ \int_{\ell+\ell_M}^{\ell_M+2\ell} \Xi b_{R,i}(x_R) b_{R,j}(x_R) dx_R,
\end{aligned} \tag{7.8}$$

were $\Xi = -0.5\rho_a v c k_2 k_3$.

The initial condition for the system is chosen as $x(0) = [0, 0, -2, 0]^T$ that is no initial displacement, slope, or angular velocity, but some initial velocity. Also it is assumed that the initial condition of the state estimate is such that $x_c(0) = 0.75x(0)$. It is assumed that the position and slope states are available for measurement for the state estimate controllers (See Chapter 3). The finite element discretization was done with $N = 21$ nodes, i.e. 10 elements per beam. Matlab's ODE15s stiff differential equation solver was used to solve the systems. The target tracking results for the LQR, LQG, and Central controllers are seen in Figures 7.6, 7.7, and 7.8, respectively. The control efforts for each of the controllers here are presented in Figure 7.9.

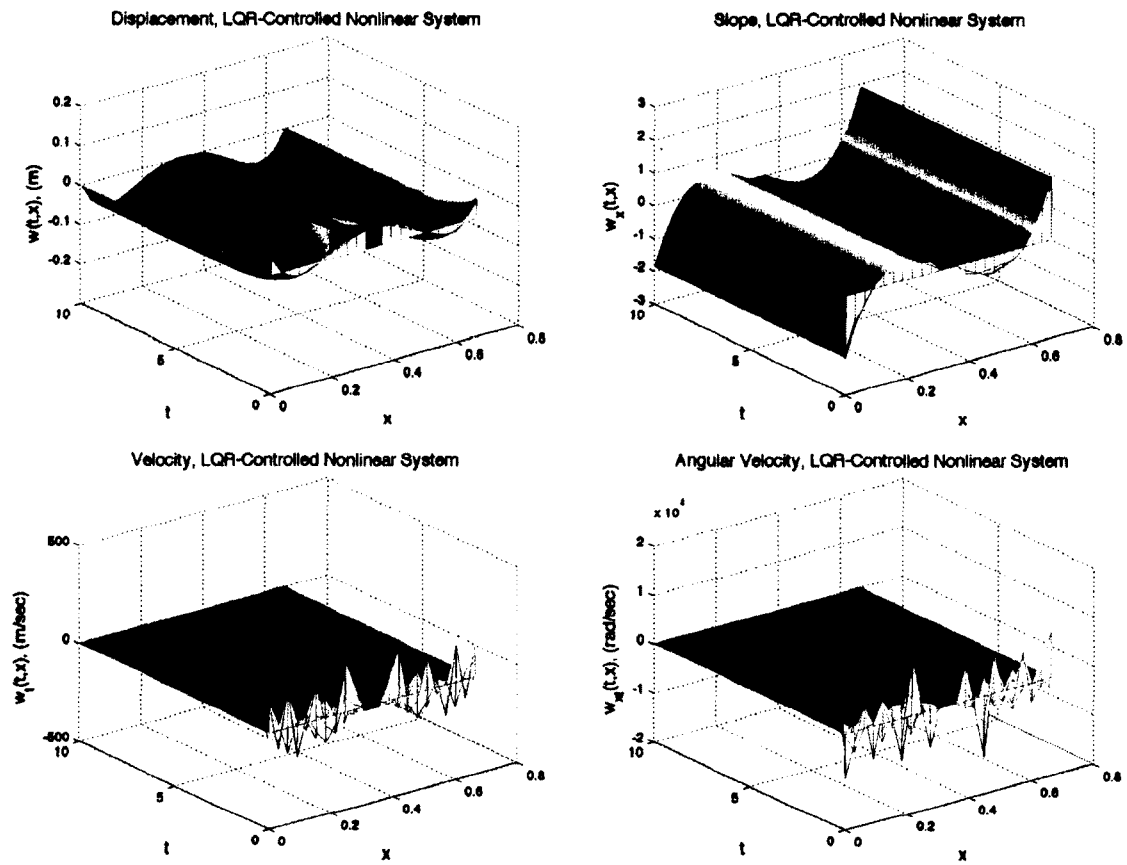


Figure 7.6: LQR Full Order Control: Position (Top Left), Slope (Top Right), Velocity (Bottom Left), Angular Velocity (Bottom Right)

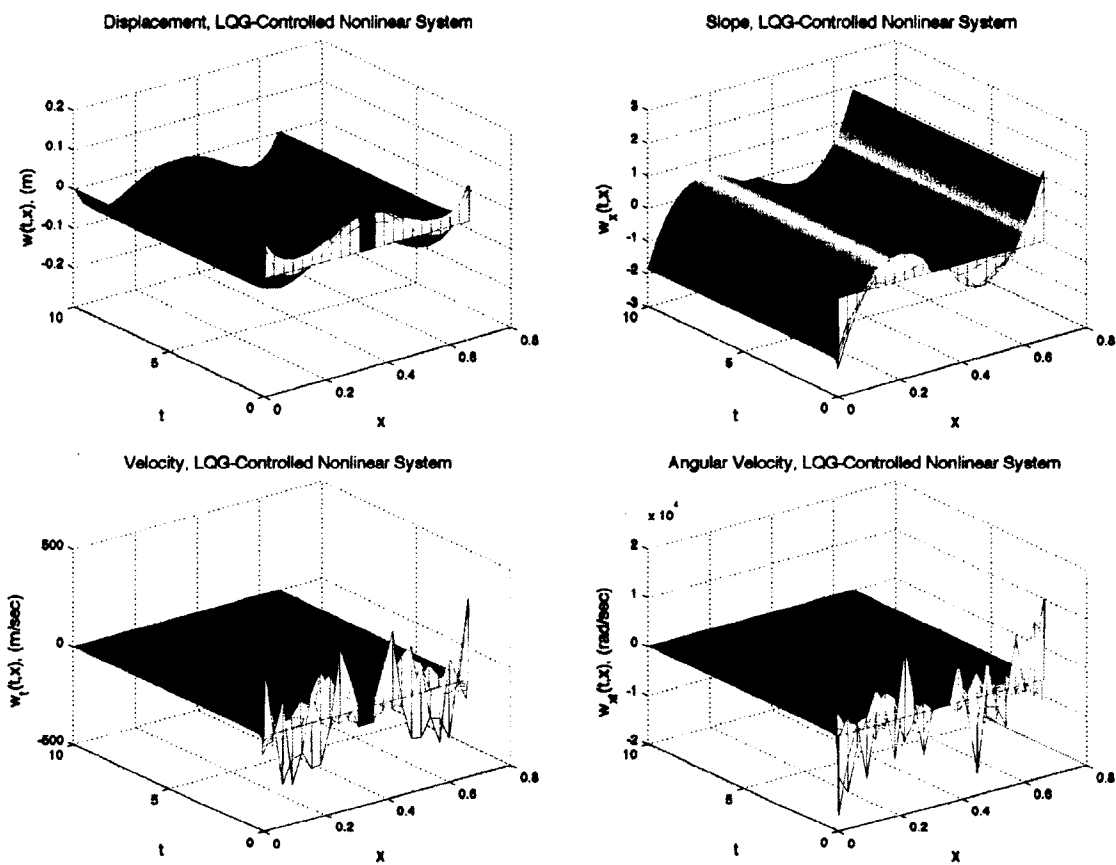


Figure 7.7: LQG State Estimate Control: Position (Top Left), Slope (Top Right), Velocity (Bottom Left), Angular Velocity (Bottom Right)

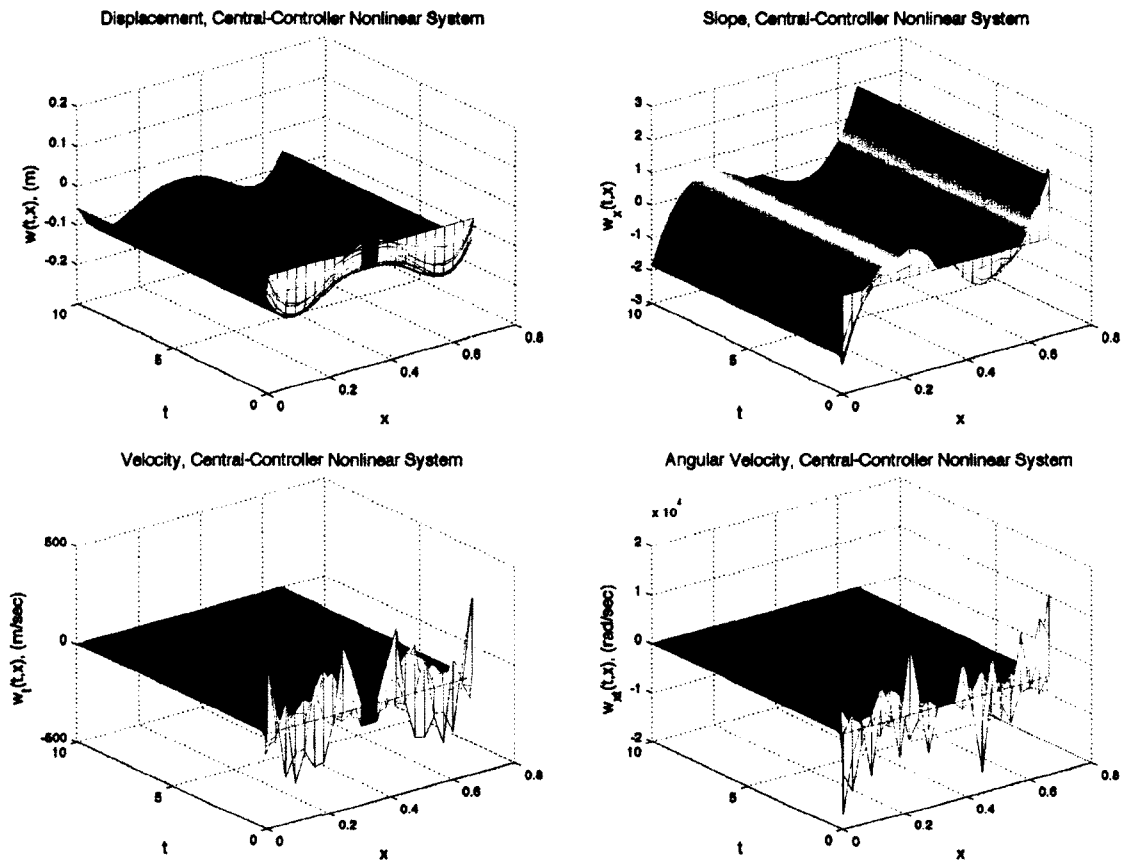


Figure 7.8: Central Controller State Estimate Control: Position (Top Left), Slope (Top Right), Velocity (Bottom Left), Angular Velocity (Bottom Right)

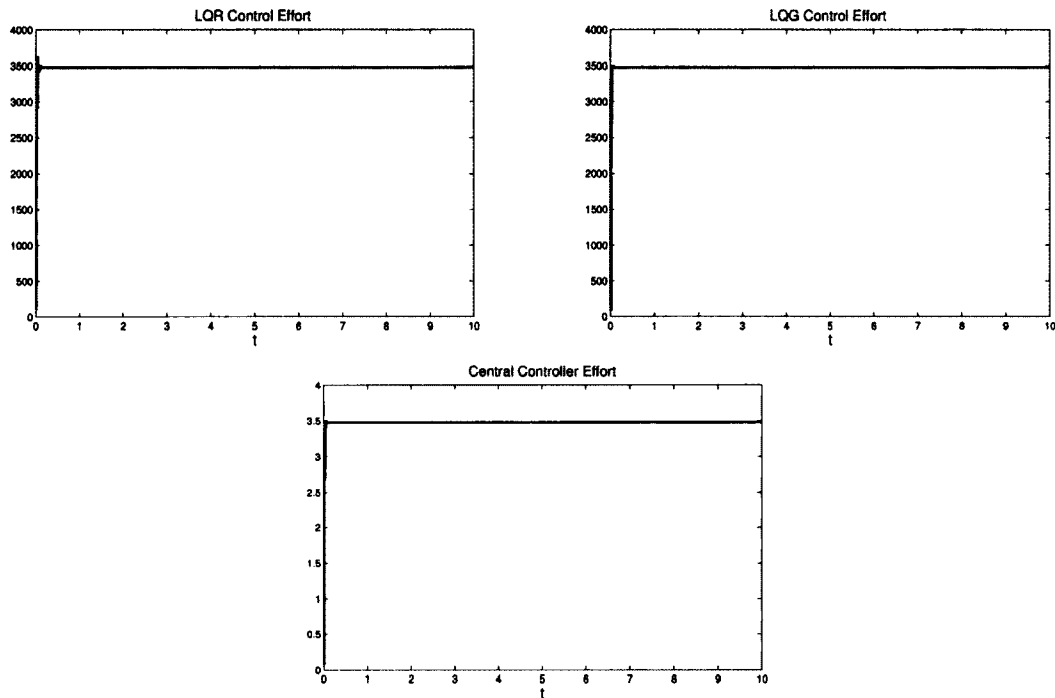


Figure 7.9: Target Tracking Control Efforts: LQR (Top Left), LQG (Top Right), Central (Bottom)

In addition to plotting the control efforts over time, we calculated the total area under the control effort curve using a trapezoid rule. The total area for each curve is presented in Table 7.2.

Table 7.2: Cumulative Tracking Control Efforts

Controller	Area Under Control Effort Curve
LQR Controller	3.4758e+04
LQG Controller	3.4771e+04
Central Controller	34.7697

7.1.3 Morphing Trajectory Results

In this section we seek to morph the BMB system linearly over five seconds to a desired state. To obtain solutions to the Ricatti equations we choose control input

functions, for LQR, LQG, and Central Controllers, of the form

$$b_L(x_L) = b_R(x_R) = 56, \quad (7.9)$$

for $0 \leq x_L \leq \ell$ and $\ell + \ell_M \leq x_R \leq \ell_M + 2\ell$. We also assume state measurements of the form

$$y_L = 28w_L(t, x_L), \quad y_R = 28w_R(t, x_R) \quad (7.10)$$

for $0 \leq x_L \leq \ell$ and $\ell + \ell_M \leq x_R \leq \ell_M + 2\ell$.

The initial conditions for the system are given as $x(0) = [0, 0, 0, 0]^T$, that is, no initial displacement, slope, velocity, or angular velocity from equilibrium. Similar to the target tracking simulations we assume $x_c(0) = 0.75x(0)$. The spatial discretization for the finite element scheme is done with $N = 21$, i.e. 10 elements per beam. We are again using Matlab's ODE15s stiff differential equation solver to solve each feedback control system. For the morphing trajectory results, the target states are presented in Figure 7.10. The results here have been accepted for publication by the Conference on Decision and Control [25].

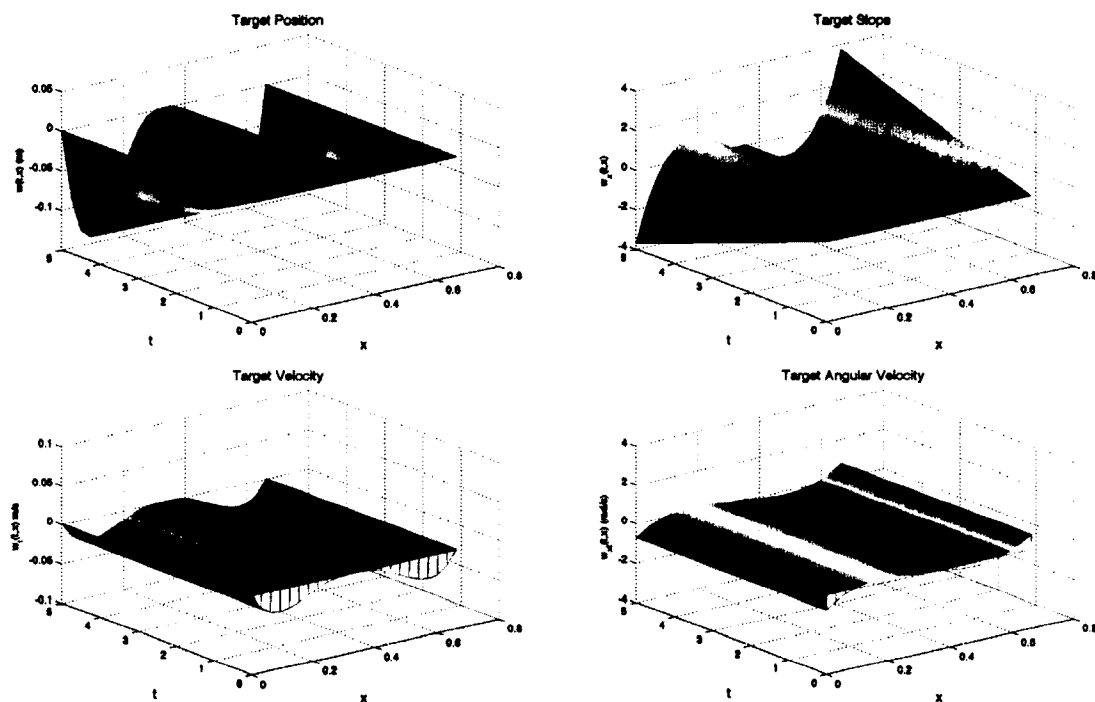


Figure 7.10: Target States For Morphing Trajectories: Position (Top Left), Slope (Top Right), Velocity (Bottom Left), Angular Velocity (Bottom Right)

The controlled simulations are presented in Figure 7.11, Figure 7.12, and Figure 7.13 for the LQR, LQG, and Central controllers, respectively. Furthermore, the control efforts are presented in Figure 7.14.

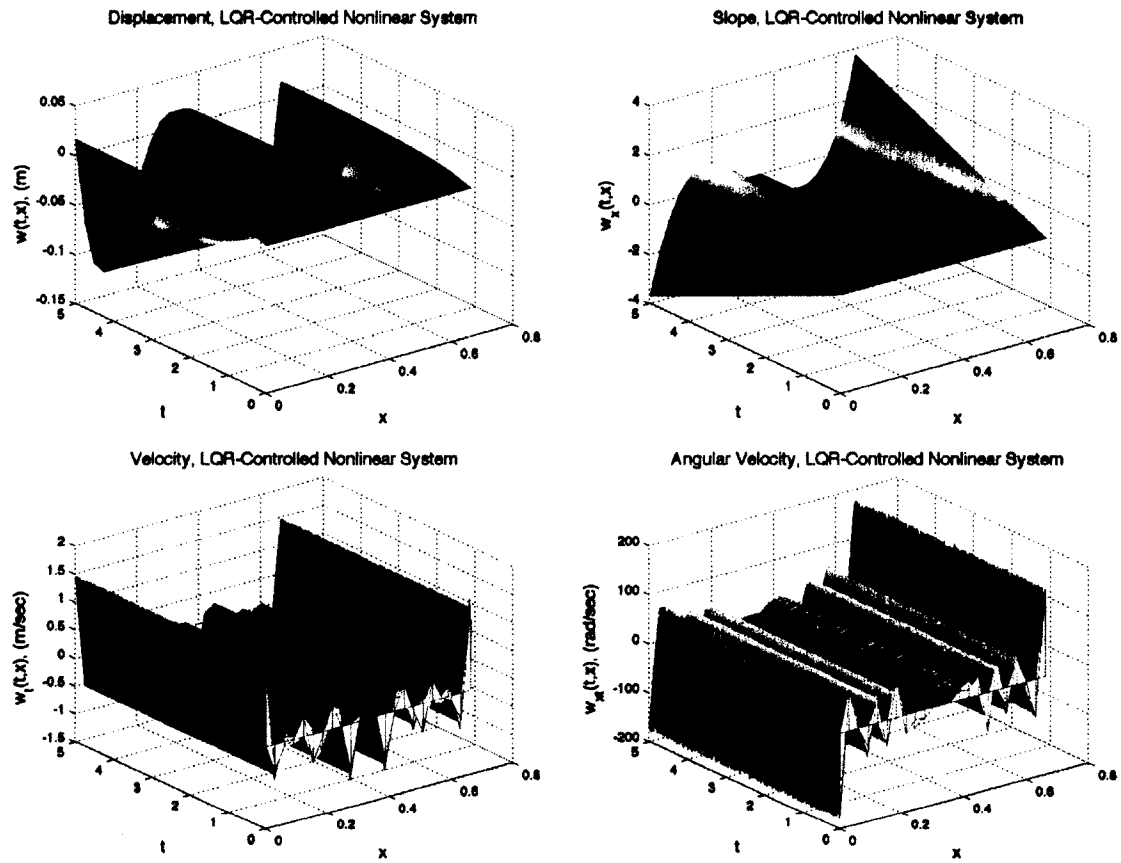


Figure 7.11: LQR Full Order Control Linear Morphing: Position (Top Left), Slope (Top Right), Velocity (Bottom Left), Angular Velocity (Bottom Right)

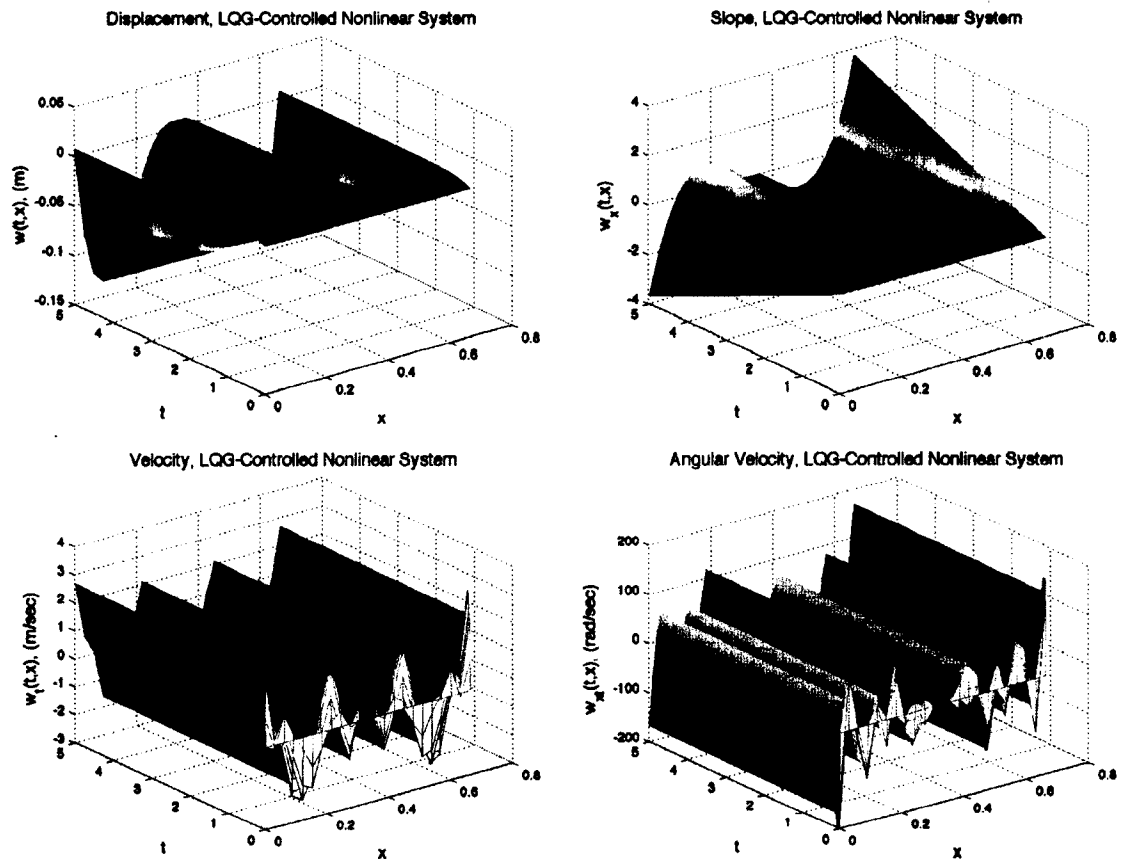


Figure 7.12: LQG State Estimate Control Linear Morphing: Position (Top Left), Slope (Top Right), Velocity (Bottom Left), Angular Velocity (Bottom Right)

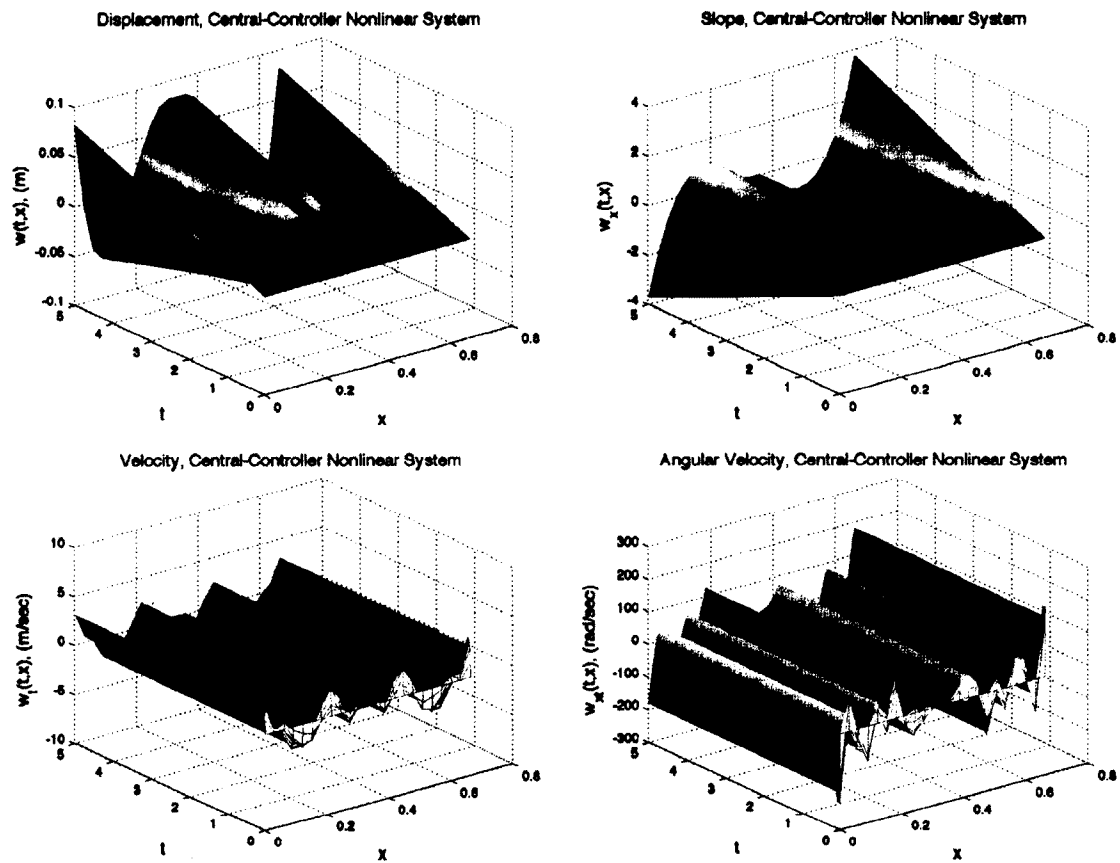


Figure 7.13: Central Controller State Estimate Control Linear Morphing: Position (Top Left), Slope (Top Right), Velocity (Bottom Left), Angular Velocity (Bottom Right)

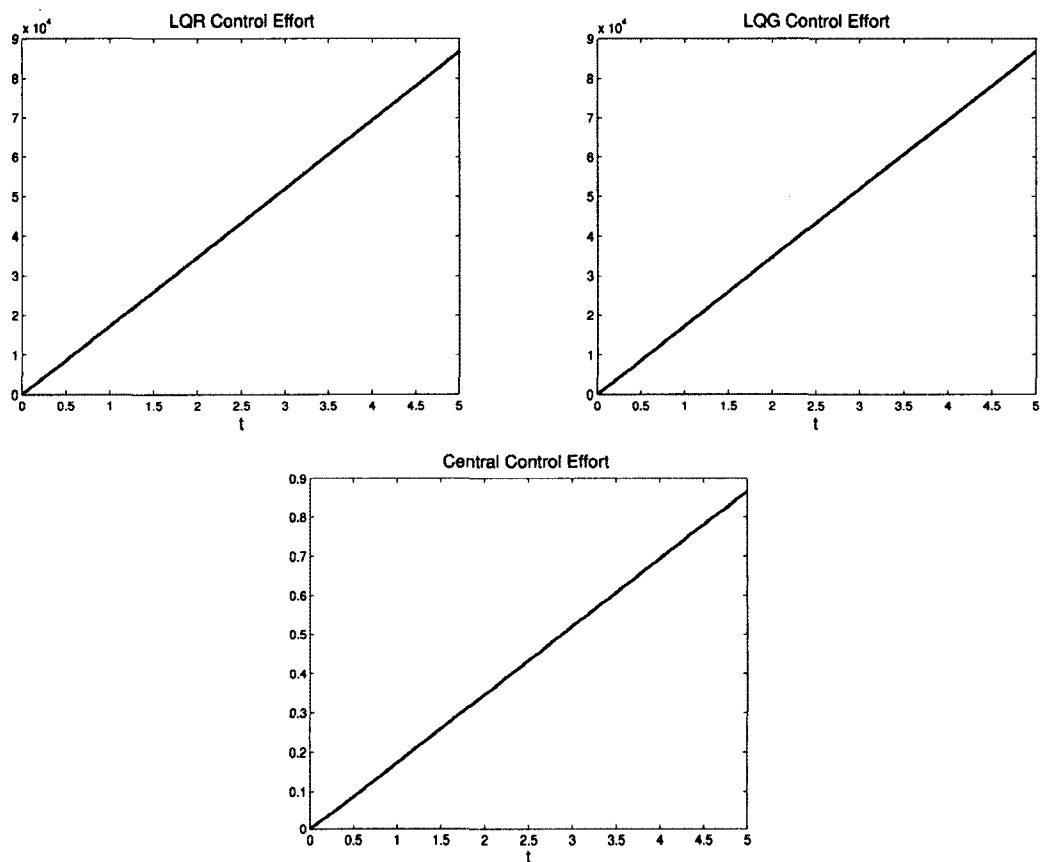


Figure 7.14: Morphing Control Efforts: LQR (Top Left), LQG (Top Right), Central (Bottom)

Again we calculated the cumulative control effort for each controller by computer the area under the control effort curve for each controller. The total area under each curve is presented in Table 7.3.

Table 7.3: Cumulative Morphing Control Efforts

Controller	Area Under Control Effort Curve
LQR Controller	2.1712e+05
LQG Controller	2.1716e+05
Central Controller	2.1716

We see here that for the tracking results, LQR and LQG controllers reach the target position and slope. For the tracking control, the central controller cannot compensate for the initial condition. Although we see a small amount of control effort, the performance is not satisfactory for the central controller. This is not surprising since increasing robustness usually decreases performance. For the central controller, we can guarantee a stability margin, but we cannot reach our target position. The velocities and angular velocities for tracking control are not within reason. Attempting to linearly control these angular velocities leads to unrealistic control efforts which are reflected in Figure 7.9. We infer that the LQR and LQG controller are able to successfully control the vehicle, albeit with an unrealistic amount of input, but the central controller does not even reach the target position.

The morphing strategy results provide a marginally better outlook than the tracking strategy. For morphing control, LQR and LQG controllers overshoot the target position slightly but are within centimeters of the target, and the slope states for each reach their target. The velocities for each are not at target but they are within reason. However, the angular velocities for the morphing strategy still require unrealistic amounts of control input as seen in Figure 7.14. We conclude for this strategy that the LQR and LQG controllers can theoretically control the vehicle but may not realistically be able to achieve this control. Lastly, we see that the Central controller used here overshoots the target position without an attempt to return to target. The same constants b, c, R, \mathcal{R} for all three controllers may not be optimal, but they were chosen to numerically solve the Ricatti equations.

CHAPTER 8

CONCLUSIONS AND FUTURE WORK

In the work herein we have described a model incorporating a non-local damping type called spatial hysteresis for modeling the heave motion of a one dimensional micro aerial vehicle. Furthermore, we presented the simulations of uncontrolled and controlled motion of the vehicle due to some initial disturbance. The vehicle is shown to undergo little bending during the initial drop in position. The control strategies then are seen to require unrealistically high angular velocity states to achieve the desired position. The density as well as the flexural rigidity of the beam are contributing factors of this inherent problem. Although the morphing over time strategy is not as extreme as the optimal in time target tracking, the angular velocity state still needs to achieve some impossible rates. Due to this difficulty we propose that using the material adapted in Chapter 4 is not a plausible choice for a flexible, morphing wing MAV with these tracking strategies.

Due to the numerical results discussed previously we propose going back to a previous model with beams composed of a different fiber structure than that described in Chapter 4. Although the spatial hysteresis parameters for the beam composite used in previous research have not been experimentally estimated, we do know parameters

for the internal damping mechanism known as Kelvin-Voigt damping. We hope to implement control design on the previous BMB model with piezoceramic patches.

Another future direction for research might include experimentation on a beam composed of carbon graphite fiber with epoxy to estimate spatial hysteresis damping parameters. If an experiment could be performed on such a beam, then there would be an even greater mesh of the research to date and the literature concerning appropriate damping models for flexible beams of a composite structure. Perhaps a collaboration of faculty and students could achieve such research together. Also, from here, research could be done with functional gains and sensitivity analysis to consider optimal patch placement.

Other avenues of research include a two dimensional plate model that is currently under investigation by research collaborators Dr. Lisa Kuhn and Dr. Cody Ray. Although it is a formidable task, Dr. Kuhn has already begun the modeling process and hopes to begin running numerical simulations soon. The work done by Kuhn and Ray focuses more on a bat type wing which has a longer chord length than the model presented here. Dr. Katie Evans suggests considering beam-like plates, where beam-like means a small chord length to beam length ratio.

Furthermore, incorporation of roll motion and yaw motion is currently a focus of research collaborator Dr. Animesh Chakravarthy. Furthermore, he has done a frequency domain analysis of the model with Kelvin-Voigt damping. His recommendation for future work is to look at trying to do frequency domain analysis of the model with spatial hysteresis damping. Lastly, we would like to develop a theory, similar to that in [12] for the MinMax controller.

APPENDIX A

SPATIAL HYSTERESIS INEQUALITY

The work in this appendix has been submitted for publication (see [15]).

In this note, we prove the following Cacciopoli-type inequality. (The interval $[0, L]$ is chosen for convenience only and can be replaced with any finite interval $[a, b]$. Scaling up to multidimensional domains, if possible at all, is more sophisticated than a simple application of Fubini's Theorem, because of the double integral on the left side.)

Theorem A.1. *Let $L > 0$ and $p \geq 1$. There is a constant $C_p > 0$ so that, for all functions $\phi \in W^{1,p}[0, L]$, we have that*

$$\int_0^L \int_0^L |\phi'(x) - \phi'(\xi)|^p dx d\xi + \int_0^L |\phi(x)|^p dx \geq C_p \int_0^L |\phi'(x)|^p dx.$$

Unlike for the Cacciopoli inequalities we were able to find in the literature, there are no restrictions on $\phi \in W^{1,p}[0, L]$. This freedom comes at the price of needing the extra term $\int_0^L \int_0^L |\phi'(x) - \phi'(\xi)|^p dx d\xi$ on the left side. Because the left side is a sum of two terms, the inequality could also be considered a relative of the Gagliardo-Nirenberg inequality. However, the Gagliardo-Nirenberg inequality involves L^p norms with four different values for p , whereas this inequality stays with one p . Consideration of straight lines $\phi(x) = ax$ shows that, just like the integral $\int_0^L |\phi(x)|^p dx$, the extra term is not solely responsible for the truth of the inequality in Theorem A.1.

Clearly, for $\phi, \psi \in L^2[0, L]$, the L^2 -inner products $\langle \nu[\psi], \phi \rangle$ and $\langle \mathcal{G}[\psi], \phi \rangle$ are bilinear forms and so is their difference. For the bilinear form $\langle (\nu - \mathcal{G})[\psi], \phi \rangle$ associated with spatial hysteresis internal damping, the kernel function h in ν and \mathcal{G} is so that, for all $(x, \xi) \in [0, L]^2$, we have $h(x, \xi) = h(\xi, x)$, and, there are $\kappa, \mu > 0$ so

that, for all $(x, \xi) \in [0, L]^2$, we have $\kappa \leq h(x, \xi) \leq \mu$. To assure that the bilinear form associated with spatial hysteresis internal damping for an Euler-Bernoulli beam is coercive with respect to the damping space $H^1[0, L]$ and the state space $L^2[0, L]$ (see [3] for more details), there must be an $C > 0$ so that, for all functions $\phi \in H^1[0, L] = W^{1,2}[0, L]$ that satisfy $\phi(0) = 0$, we have that

$$\int_0^L (\nu - \mathcal{G})[\psi](x)\psi(x) dx + \int_0^L |\phi(x)|^2 dx \geq C \int_0^L |\phi'(x)|^2 dx,$$

The inequality above follows from Theorem A.1 because Proposition A.2 below shows that, for symmetric kernels, the first term above can safely be replaced with the simpler term we use in Theorem A.1. Hence, the model under consideration is well-posed. To our knowledge, this is the first time a formal proof of the above inequality appears in the literature.

Proposition A.2. *Let $L > 0$ and let $h \in L^2[0, L]^2$ be a kernel function so that, for all $(x, \xi) \in [0, L]^2$, we have $h(x, \xi) = h(\xi, x)$ and so that there are $\kappa, \mu > 0$ so that, for all $(x, \xi) \in [0, L]^2$, we have $\kappa \leq h(x, \xi) \leq \mu$. Then, for all $\psi \in L^2[0, L]$, we have that*

$$\begin{aligned} \frac{\kappa}{2} \int_0^L \int_0^L (\psi(x) - \psi(\xi))^2 dx d\xi &\leq \int_0^L (\nu - \mathcal{G})[\psi](x)\psi(x) dx \\ &\leq \frac{\mu}{2} \int_0^L \int_0^L (\psi(x) - \psi(\xi))^2 dx d\xi. \end{aligned}$$

Proof. First note the following.

$$\int_0^L (\nu - \mathcal{G})[\psi](x)\psi(x) dx$$

$$\begin{aligned}
&= \int_0^L \left(\int_0^L h(x, \xi) d\xi \psi(x) - \int_0^L h(x, \xi) \psi(\xi) d\xi \right) \psi(x) dx \\
&= \int_0^L \int_0^L h(x, \xi) ((\psi(x))^2 - \psi(\xi)\psi(x)) d\xi dx \\
&= \frac{1}{2} \int_0^L \int_0^L h(x, \xi) ((\psi(x))^2 - \psi(\xi)\psi(x)) d\xi dx \\
&\quad + \frac{1}{2} \int_0^L \int_0^L h(\xi, x) ((\psi(\xi))^2 - \psi(x)\psi(\xi)) dx d\xi \\
&= \frac{1}{2} \int_0^L \int_0^L h(x, \xi) ((\psi(x))^2 - \psi(\xi)\psi(x)) d\xi dx \\
&\quad + \frac{1}{2} \int_0^L \int_0^L h(x, \xi) (-\psi(\xi)\psi(x) + (\psi(\xi))^2) d\xi dx \\
&= \frac{1}{2} \int_0^L \int_0^L h(x, \xi) ((\psi(x))^2 - 2\psi(\xi)\psi(x) + (\psi(\xi))^2) d\xi dx \\
&= \frac{1}{2} \int_0^L \int_0^L h(x, \xi) (\psi(x) - \psi(\xi))^2 d\xi dx
\end{aligned}$$

The inequalities now follow from $0 < \kappa \leq h \leq \mu$. □

Note that one, maybe even surprising, consequence of Proposition A.2 is that

$$\int_0^L (\nu - \mathcal{G})[\psi](x)\psi(x) dx \text{ is nonnegative.}$$

Although we only needed Theorem A.1 for $p = 2$ and with the additional boundary conditions $\phi(0) = 0$ and $\phi'(0) = 0$ (clamped beam) imposed, we prove it first without boundary conditions for $p = 2$ (see Lemma A.3) and then generalize to p^{th} powers. This gives us the most general version of the inequality without much extra work.

A.1 Proof of Theorem A.1

We will need the following lemma.

Lemma A.3. *Let $\{f_n\}_{n=1}^\infty$ be a sequence in $C^1([0, L])$ such that*

- (i) $|f'_n(x)| \leq 1$;
(ii) $\lim_{n \rightarrow \infty} \int_0^L |f_n(x)|^2 dx = 0$;
(iii) $\lim_{n \rightarrow \infty} \int_0^L \int_0^L |f'_n(x) - f'_n(y)|^2 dx dy = 0$.

Then we must have

$$\lim_{n \rightarrow \infty} \int_0^L |f'_n(x)|^2 dx = 0.$$

Proof. Suppose for a contradiction that this is not true. Then, without loss of generality, there exists a sequence $\{f_n\}_{n=1}^{\infty}$ that satisfies (i)-(iii) and an $\varepsilon > 0$ such that

$$\int_0^L |f'_n(x)|^2 dx \geq \varepsilon, \quad n \geq 1.$$

For any $n \geq 1$, we have

$$\int_0^L \int_0^L (f'_n(x) - f'_n(y))^2 dx dy = 2L \int_0^L (f'_n(x))^2 dx - 2(f_n(L) - f_n(0))^2.$$

Hence

$$\lim_{n \rightarrow \infty} L \int_0^L (f'_n(x))^2 dx - (f_n(L) - f_n(0))^2 = 0.$$

On the other hand, using the assumption (i), we get

$$|f_n(L) - f_n(0)| = \left| \int_0^L f'_n(x) dx \right| \leq \int_0^L |f'_n(x)| dx \leq L,$$

for any $n \geq 1$. So there exists a subsequence $\{f_{\psi(n)}\}_{n=1}^{\infty}$ such that

$$A := \lim_{n \rightarrow \infty} f_{\psi(n)}(L) - f_{\psi(n)}(0)$$

exists. Hence

$$\lim_{n \rightarrow \infty} L \int_0^L \left(f'_{\psi(n)}(x) \right)^2 dx - A^2 = 0,$$

which implies

$$\varepsilon \leq \lim_{n \rightarrow \infty} \int_0^L \left(f'_{\psi(n)}(x) \right)^2 dx = \frac{A^2}{L}.$$

In particular we have $A \neq 0$. Next we prove that $\{f_{\psi(n)}(0)\}_{n=1}^{\infty}$ converges and compute the limit. Indeed, we have

$$\begin{aligned} \left| f_{\psi(n)}^2(L) - f_{\psi(n)}^2(0) \right| &= \left| \int_0^L \frac{d}{dx} f_{\psi(n)}^2(x) dx \right| \\ &= 2 \left| \int_0^L f_{\psi(n)}(x) f'_{\psi(n)}(x) dx \right| \\ &\leq 2 \left(\int_0^L f_{\psi(n)}^2(x) dx \right)^{1/2} \left(\int_0^L \left[f'_{\psi(n)}(x) \right]^2 dx \right)^{1/2} \\ &\leq 2\sqrt{L} \left(\int_0^L f_{\psi(n)}^2(x) dx \right)^{1/2}, \end{aligned}$$

for any $n \geq 1$. Hence

$$\lim_{n \rightarrow \infty} \left| f_{\psi(n)}^2(L) - f_{\psi(n)}^2(0) \right| = 0.$$

Since $A = \lim_{n \rightarrow \infty} f_{\psi(n)}(L) - f_{\psi(n)}(0) \neq 0$ and

$$f_{\psi(n)}(L) + f_{\psi(n)}(0) = \frac{f_{\psi(n)}^2(L) - f_{\psi(n)}^2(0)}{f_{\psi(n)}(L) - f_{\psi(n)}(0)}, \quad n = 1, 2, \dots,$$

we get

$$\lim_{n \rightarrow \infty} f_{\psi(n)}(L) + f_{\psi(n)}(0) = \frac{0}{A} = 0.$$

Putting everything together, we get

$$\lim_{n \rightarrow \infty} f_{\psi(n)}(L) = \frac{A}{2}, \quad \text{and} \quad \lim_{n \rightarrow \infty} f_{\psi(n)}(0) = -\frac{A}{2}.$$

Next note that we have

$$\begin{aligned} |f_{\psi(n)}(x)| &\leq |f_{\psi(n)}(x) - f_{\psi(n)}(0)| + |f_{\psi(n)}(0)| \\ &\leq \int_0^x |f'_{\psi(n)}(x)| \, dx + |f_{\psi(n)}(0)| \\ &\leq \int_0^x dx + |f_{\psi(n)}(0)| \\ &\leq x + |f_{\psi(n)}(0)| \\ &\leq L + \sup_{n \geq 1} |f_{\psi(n)}(0)| =: M, \end{aligned}$$

for any $x \in [0, L]$, that is, the sequence $\{f_{\psi(n)}(x)\}$ is uniformly bounded on $[0, L]$.

Using this fact, we obtain the following

$$\begin{aligned} |f_{\psi(n)}^3(L) - f_{\psi(n)}^3(0)| &= \left| \int_0^L \frac{d}{dx} f_{\psi(n)}^3(x) \, dx \right| \\ &= 3 \left| \int_0^L f_{\psi(n)}^2(x) f'_{\psi(n)}(x) \, dx \right| \\ &\leq 3 \left(\int_0^L f_{\psi(n)}^4(x) \, dx \right)^{1/2} \left(\int_0^L [f'_{\psi(n)}(x)]^2 \, dx \right)^{1/2} \\ &\leq 3\sqrt{L} \left(\int_0^L f_{\psi(n)}^4(x) \, dx \right)^{1/2} \\ &\leq 3\sqrt{L} \left(\int_0^L M^2 f_{\psi(n)}^2(x) \, dx \right)^{1/2} \\ &= 3M\sqrt{L} \left(\int_0^L f_{\psi(n)}^2(x) \, dx \right)^{1/2}, \end{aligned}$$

for any $n \geq 1$. Hence

$$\lim_{n \rightarrow \infty} \left| f_{\psi(n)}^3(L) - f_{\psi(n)}^3(0) \right| = 0,$$

which implies

$$\lim_{n \rightarrow \infty} f_{\psi(n)}^3(L) - f_{\psi(n)}^3(0) = \left(\frac{A}{2} \right)^3 - \left(-\frac{A}{2} \right)^3 = \frac{A^3}{4} = 0,$$

a contradiction. □

Proof of Theorem A.1. First note that, for $f' = 0$, the inequality is true for any constant C_p . So we may restrict our proof to $f' \neq 0$. Because C^1 is dense in $W^{1,p}$, we may assume that all functions are in $C^1([0, L])$. Let $f \in C^1([0, L])$ be such that $f' \neq 0$. Because f' is continuous, we have that $M := \sup_{x \in [0, L]} |f'(x)| \in (0, \infty)$. Set $g(x) = \frac{1}{M} f(x)$. It is clear that f satisfies the inequality if and only if g satisfies the same inequality with the same constant. So it is enough to prove the inequality for $f \in C^1([0, L])$ such that $|f'(x)| \leq 1$. Suppose for a contradiction that the inequality is not true. Then there exists a sequence $\{f_n\}_{n=1}^\infty$ in $C^1([0, L])$ and an $\varepsilon > 0$ such that

- (i) $|f'_n(x)| \leq 1$;
- (ii) $\int_0^L |f'_n(x)|^p dx \geq \varepsilon$;
- (iii) $\int_0^L \int_0^L |f'_n(x) - f'_n(y)|^p dx dy + \int_0^L |f_n(x)|^p dx \rightarrow 0$ as $n \rightarrow \infty$.

Clearly (iii) implies

$$\lim_{n \rightarrow \infty} \int_0^L \int_0^L |f'_n(x) - f'_n(y)|^p dx dy = 0, \quad \text{and} \quad \lim_{n \rightarrow \infty} \int_0^L |f_n(x)|^p dx = 0.$$

Using (i), we get

$$\begin{aligned}
\int_0^L \int_0^L |f'_n(x) - f'_n(y)|^2 dx dy &= \int_0^L \int_0^L |f'_n(x) - f'_n(y)| |f'_n(x) - f'_n(y)| dx dy \\
&\leq 2 \int_0^L \int_0^L |f'_n(x) - f'_n(y)| dx dy \\
&\leq 2 \left[\int_0^L \int_0^L |f'_n(x) - f'_n(y)|^p dx dy \right]^{1/p} \left[\int_0^L \int_0^L dx dy \right]^{1/q} \\
&\leq 2L^{2/q} \left[\int_0^L \int_0^L |f'_n(x) - f'_n(y)|^p dx dy \right]^{1/p}
\end{aligned}$$

where, for $p > 1$, q is the conjugate of p , i.e., $q = \frac{p}{p-1}$. (For $p = 1$ we stop after the first inequality, which suffices for the following.) Hence

$$\lim_{n \rightarrow \infty} \int_0^L \int_0^L (f'_n(x) - f'_n(y))^2 dx dy = 0.$$

Next we claim that $\{f_n(0)\}_{n=1}^\infty$ is bounded. Assume this is not the case. Then there exists a subsequence $\{f_{\psi(n)}(0)\}_{n=1}^\infty$ such that $|f_{\psi(n)}(0)| \geq 2L$. Note that

$$|f_n(x) - f_n(0)| = \left| \int_0^x f'_n(t) dt \right| \leq \int_0^x |f'_n(t)| dt \leq \int_0^L |f'_n(t)| dt \leq L$$

for any $x \in [0, L]$ and $n \geq 1$. Hence

$$L \leq |f_{\psi(n)}(0)| - L \leq |f_{\psi(n)}(x)|; \quad x \in [0, L].$$

This implies

$$L^{p+1} \leq \int_0^L |f_{\psi(n)}(x)|^p dx,$$

a contradiction. Hence $\{f_n(0)\}_{n=1}^\infty$ is bounded and we obtain that

$$M := \sup_{x \in [0, L], n \geq 1} |f_n(x)| \leq \sup_{n \geq 1} |f_n(0)| + L < \infty,$$

that is, that the sequences $\{f_n(x)\}_{n=1}^\infty$ are uniformly bounded on $[0, L]$. Next note

that we have

$$\begin{aligned} \int_0^L |f_n(x)|^2 dx &= \int_0^L |f_n(x)| |f_n(x)| dx \\ &\leq M \int_0^L |f_n(x)| dx \\ &\leq M L^{1/q} \left[\int_0^L |f_n(x)|^p dx \right]^{1/p}, \end{aligned}$$

(again with q being the conjugate of the last step omitted) which implies that

$$\lim_{n \rightarrow \infty} \int_0^L |f_n(x)|^2 dx = 0.$$

So we have

$$\left\{ \begin{array}{l} |f'_n(x)| \leq 1, \quad n = 1, 2, \dots \\ \lim_{n \rightarrow \infty} \int_0^L |f_n(x)|^2 dx = 0 \\ \lim_{n \rightarrow \infty} \int_0^L \int_0^L |f'_n(x) - f'_n(y)|^2 dx dy = 0. \end{array} \right.$$

and by Lemma A.3 we infer

$$\lim_{n \rightarrow \infty} \int_0^L |f'_n(x)|^2 dx = 0.$$

On the other hand, we have

$$\begin{aligned} \int_0^L |f'_n(x)|^p dx &= \int_0^L |f'_n(x)|^{p-1} |f'_n(x)| dx \\ &\leq \int_0^L |f'_n(x)| dx \\ &\leq L^{1/2} \left[\int_0^L |f'_n(x)|^2 dx \right]^{1/2}, \end{aligned}$$

which implies

$$\frac{\varepsilon^2}{L} \leq \int_0^L |f'_n(x)|^2 dx,$$

a contradiction. □

A.2 Observations

The proof primarily relies on the homogeneity of the inequality, so that the following result is an easy consequence.

Theorem A.4. *Let $L > 0$, $p \geq 1$ and let $H : [0, \infty) \times [0, \infty) \rightarrow [0, \infty)$ be so that*

1. $H(u, v) = 0$ iff $u = v = 0$,
2. For all $c \geq 0$ we have $H(cu, cv) = cH(u, v)$,
3. H is continuous.

Then there is a constant $C_{p,H} > 0$ so that, for all functions $\phi \in W^{1,p}[0, L]$, we have that

$$H \left(\int_0^L \int_0^L |\phi'(x) - \phi'(\xi)|^p dx d\xi, \int_0^L |\phi(x)|^p dx \right) \geq C_{p,H} \int_0^L |\phi'(x)|^p dx.$$

Although Theorem A.4 looks rather technical, with $H(u, v) = (u^m + v^m)^{\frac{1}{m}}$, we see that we can attach exponents to all three terms in Theorem A.1 and then obtain, for example, that the corresponding inequality for the norms

$$\|\phi'(x) - \phi'(\xi)\|_{L^p[0,L]^2} + \|\phi(x)\|_{L^p[0,L]} \geq C_p \|\phi'(x)\|_{L^p[0,L]} \text{ holds, too.}$$

APPENDIX B

CONVERGENCE OF BMB WITH KELVIN VOIGT PARAMETERS

Here it is shown that the Matlab code used for spatial hysteresis damping converges for a constant kernel function which as stated in [20] is equivalent to Kelvin Voigt damping.

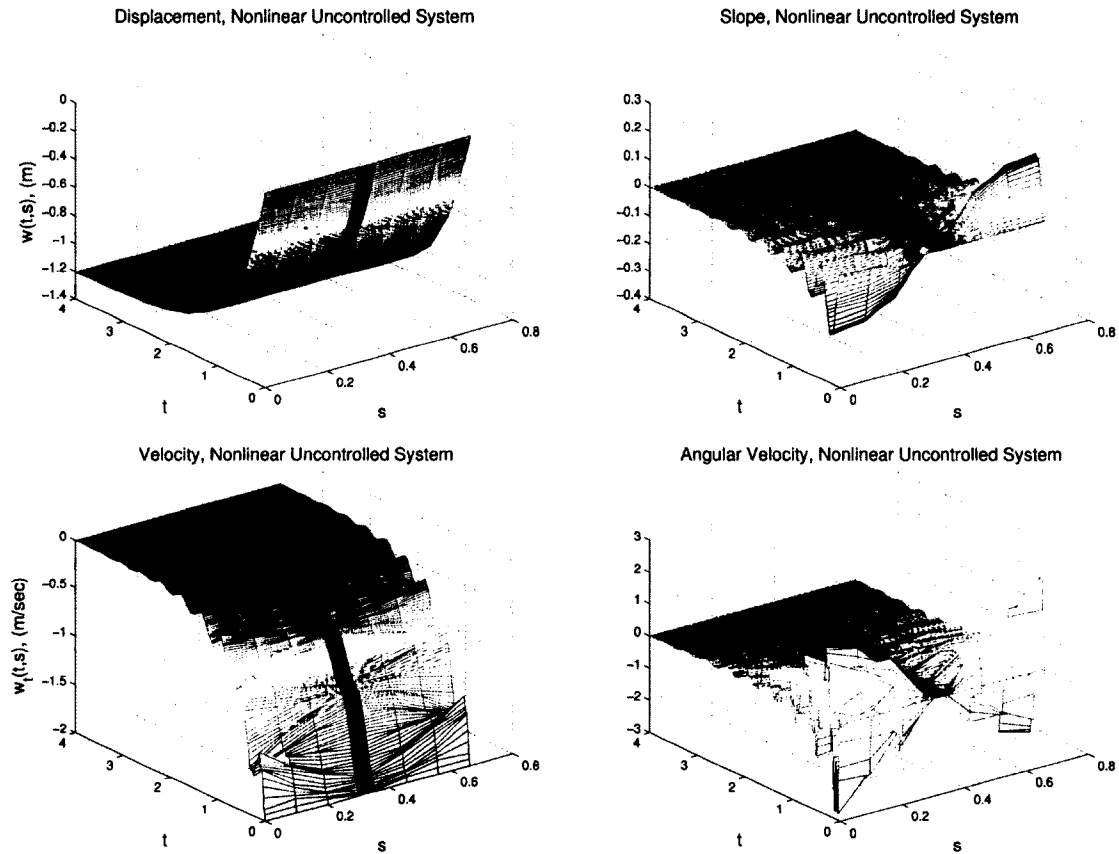


Figure 2.1: Uncontrolled BMB with KV Kernel Simulation with 6 Elements: Position (Top Left), Slope (Top Right), Velocity (Bottom Left), Angular Velocity (Bottom Right)

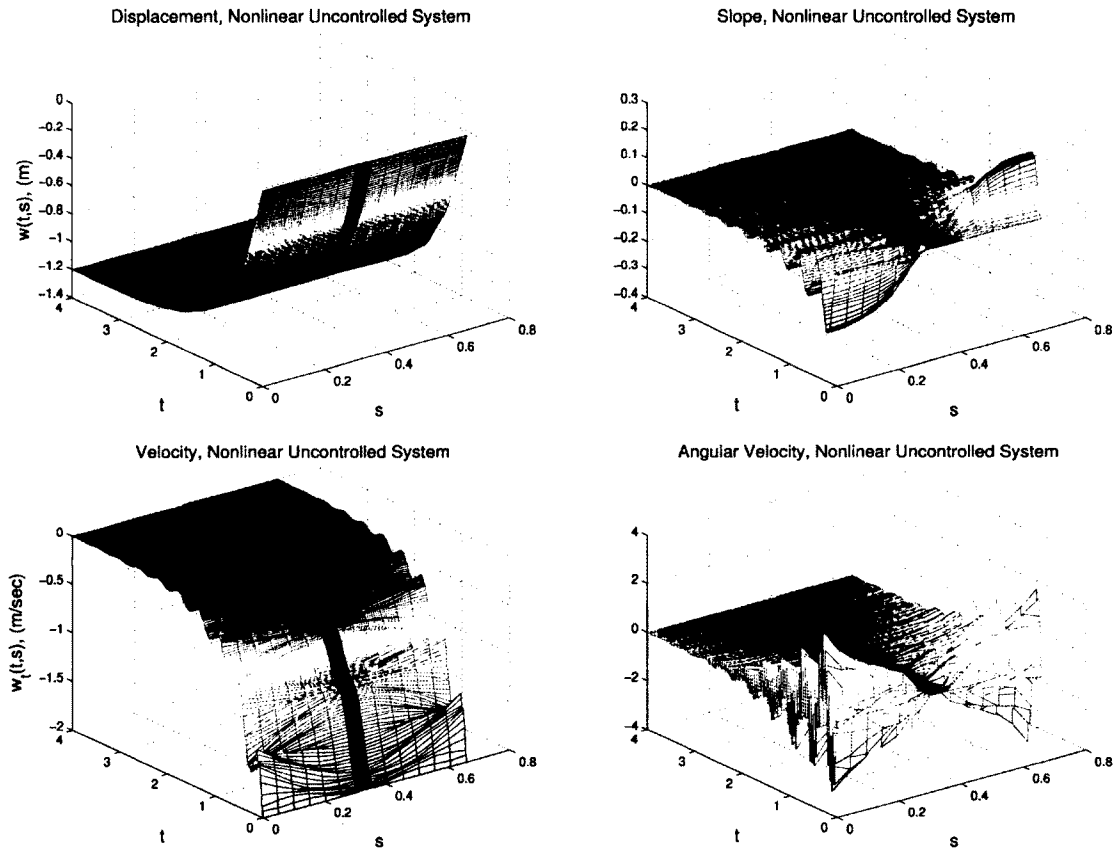


Figure 2.2: Uncontrolled BMB with KV Kernel Simulation with 12 Elements: Position (Top Left), Slope (Top Right), Velocity (Bottom Left), Angular Velocity (Bottom Right)

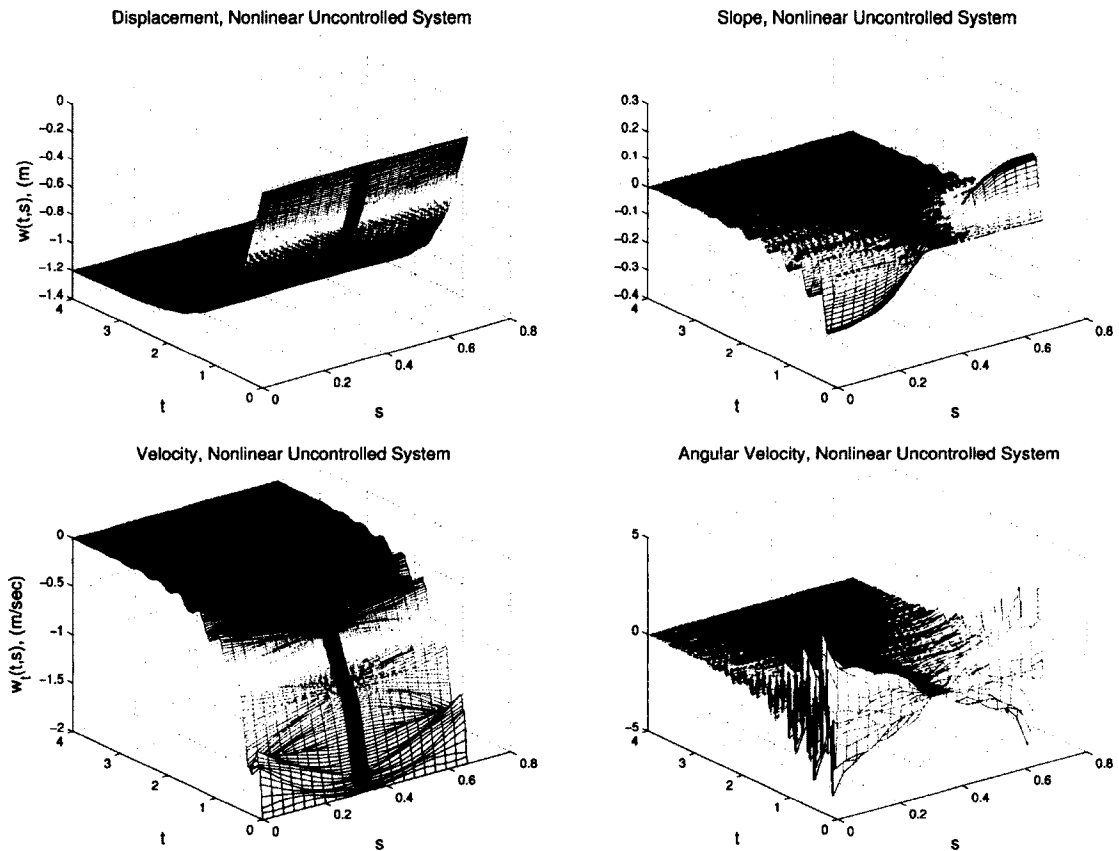


Figure 2.3: Uncontrolled BMB with KV Kernel Simulation with 18 Elements: Position (Top Left), Slope (Top Right), Velocity (Bottom Left), Angular Velocity (Bottom Right)

BIBLIOGRAPHY

- [1] J.M. Ball. Strongly continuous semigroups, weak solutions, and the variation of constants formula. *Proceedings of the American Mathematical Society*, 63:370–373, 1977.
- [2] H. T. Banks and D. J. Inman. On damping mechanisms in beams. Technical report, Institute for Computer Applications in Science and Engineering NASA Langley Research Center, September 1989.
- [3] H. T. Banks, R. C. Smith, and Y. Wang. *Smart Material Structures*. Masson and Wiley, Paris, 1996.
- [4] H.T. Banks, R.H. Fabiano, Y. Wang and D.J. Inman, and Jr. H. Cudney. Spatial hysteresis versus time hysteresis in damping mechanisms. *Proceedings of the 1988 Decision and Control Conference*, pages 1674–1677, 1988.
- [5] J.A. Burns, E.M. Cliff, Z. Liu, , and R.D. Spies. On coupled transversal and axial motions of two beams with a joint. *Mathematical Analysis and Applications*, pages 182–196, 2007.
- [6] A. Chakravarthy, K.A. Evans, and J. Evers. Sensitivities and functional gains for a flexible aircraft-inspired model. *Proceedings of the 2010 American Control Conference*, pages 4893–4898, 2010.
- [7] A. Chakravarthy, K.A. Evans, J. Evers, and L. Kuhn. Nonlinear controllers for wing morphing trajectories of a heave dynamics model. *Proceedings of the 2011 Conference on Decision and Control*, pages 2788–2793, December 2011. invited, 3 peer reviews, 59% acceptance rate.
- [8] A. Chakravarthy, K.A. Evans, J. Evers, and L. Kuhn. Target tracking strategies for a nonlinear, flexible aircraft-inspired model. *Proceedings of the 2011 American Control Conference*, pages 1783–1788, June 2011. invited, 2 peer reviews, 63% acceptance rate.
- [9] R. F. Curtain and H. J. Zwart. *An Introduction to Infinite-Dimensional Linear Systems Theory*. Springer-Verlag, New York, 1995.
- [10] M. Dickinson, F.O. Lehmann, and S. Sane. Wing rotation and the aerodynamic basis of insect flight. *Science*, pages 1954–1960, June 1999.
- [11] P. Dorato, C. Abdallah, and V. Cerone. *Linear-Quadratic Control, An Introduction*. Prentice Hall, Englewood Cliffs, 1995.

- [12] J. S. Gibson and A. Adamian. Approximation theory for linear quadratic gaussian control of flexible structures. *SIAM J. Contr. Opt.*, 29:1–37, 1991.
- [13] K. Glover and D. C. McFarlane. Robust stabilization of normalized coprime factor plant descriptions with \mathcal{H}_∞ bounded uncertainty. *IEEE Trans. AC*, 34(8):821–830, 1989.
- [14] Lisa K. James. *Modeling and Control for Heave Dynamics of a Flexible Wing Micro Aerial Vehicle Distributed Parameter System*. PhD thesis, Louisiana Tech Universty, August 2011.
- [15] M. Khamsi, B. Schröder, J. Walters, and K. Evans. A cacciopoli-type inequality to prove coercivity of a bilinear form associated with spatial hysteresis internal damping for an euler-bernoulli beam. *Mathematical Analysis and Applications*, 2014. Under Review.
- [16] B. Batten King. *Modeling and Control of Multiple Component Structures*. PhD thesis, Clemson University, December 1991.
- [17] Erwin Kreyszig. *Introductory Functional Analysis with Applications*. Wiley-Interscience, 1979.
- [18] Peter Lax. *Functional Analysis*. J. Wiley and Sons, 2002.
- [19] A. Pazy. *Semigroups of Linear Operators and Applications to Partial Differential Equations*. Springer-Verlag, New York, 1983.
- [20] David L. Russell. On mathematical models for the elastic beam with frequency-proportional damping. *Control and Estimation in Distributed Parameter Systems*, pages 125–170, 1992.
- [21] Bernd S. W. Schröder. *Mathematical Analysis A Concise Introduction*. Wiley-Interscience, 2008.
- [22] S. Skogestad and I. Postlethwaite. *Multivariable Feedback Control*. John Wiley & Sons, Chichester, 1996.
- [23] Moshen Tadi. *An Optimal Control Problem for a Timoshenko Beam*. PhD thesis, Virginia Polytechnic Institute and State University, August 1991.
- [24] X. Tian, J. Iriarte-Diaz, K. Middleton, R. Galvao, E. Israeli, A. Roemer, A. Sullivan, A. Song, S. Swartz, and K. Breuer. Direct measurements of the kinematics and dynamics of bat flight. *Bioinspiration & Biomimetics*, 1:S10–S18, 2006.
- [25] J. Walters, K.A. Evans, A. Chakravarthy, and L. Kuhn. A comparison of morphing control strategies for a flexible wing micro air vehicle model incorporating spatial hysteresis damping. *Proceedings of the 2014 Conference on Decision and Control*, December 2014. To Appear.